University of Mississippi

eGrove

Electronic Theses and Dissertations | Graduate School

1-1-2019

A mechanistic study of the teratogenic potential of 4-o-methylhonokiol (MH) on Japanese medaka (oryzias latipes)

Santu Kumar Singha

Follow this and additional works at: https://egrove.olemiss.edu/etd

 Part of the Pharmacology Commons, and the Toxicology Commons

Recommended Citation

Singha, Santu Kumar, "A mechanistic study of the teratogenic potential of 4-o-methylhonokiol (MH) on Japanese medaka (oryzias latipes)" (2019). *Electronic Theses and Dissertations*. 1786.
https://egrove.olemiss.edu/etd/1786

This Dissertation is brought to you for free and open access by the Graduate School at eGrove. It has been accepted for inclusion in Electronic Theses and Dissertations by an authorized administrator of eGrove. For more information, please contact egrove@olemiss.edu.

A MECHANISTIC STUDY OF THE TERATOGENIC POTENTIAL OF 4-*O*-METHYLHONOKIOL (MH) ON JAPANESE MEDAKA (*ORYZIAS LATIPES*)

A dissertation
Presented in partial fulfillment of requirements
For the degree of Doctor of Philosophy
In the Department of Biomolecular Sciences
Division of Pharmacology
The University of Mississippi

By

Santu Kumar Singha

August 2018

Copyright Santu Kumar Singha 2018

ALL RIGHTS RESERVED

ABSTRACT

The overall goal of this project is to characterize the teratogenic potential of 4-*O*-Methylhonokiol (MH) and to identify the underlying mechanisms of teratogenesis. Although Magnolia extracts have been reported previously for their cardioprotective effects, including anti-obesity, anti-atherosclerosis, and vascular relaxation, toxicity data are lacking. Effects of Magnolia compounds on embryonic development are not known yet. Therefore, the potential toxic effects of MH, a major bioactive constituent of *Magnolia grandiflora* seeds or *Magnolia officinalis* bark on Japanese medaka embryogenesis and on locomotion during larval stage were studied.

MH exposure caused a slow heartbeat, blood occlusion, absence of blood circulation, decreased hatching efficiency, and increased mortality in medaka embryos in a concentration- and time-dependent manner. MH might cause blood vessel occlusion by increasing the expression of FVII, FX, FXI of the blood coagulation pathway and decreasing the fold differences between the tissue plasminogen activator (tPA) and the plasminogen activator inhibitor-1 (PAI-1) of the thrombolytic system. MH might also damage the blood vessels through production of excessive pro-inflammatory mediators or reactive oxygen species, which resulted in blood vessel occlusion. Another objective of this study was to evaluate the effect of MH on locomotion in 2 days post hatch (dph) larvae. Exposed larvae showed an overall decline in the duration of movement after the first dark cycle relative to the untreated controls, however the change was not significant.

An additional goal of this project was to characterize the Wnt/β-catenin signaling pathway to unravel the adverse potential of MH on the cardiovascular system (CVS). Our study suggested

that MH-mediated cardiovascular injury may be caused due to upregulation of some major components of the Wnt/β-catenin pathway through expression of excessive pro-inflammatory mediators. Moreover, MH decreased expression of ErbB3 and NRG-2 suggesting impaired cardiac structure.

This project established the concentration-and time-dependent teratogenic potential of MH on the cardiovascular system during medaka embryogenesis. Moreover, it revealed potential mechanisms for producing these toxicities.

DEDICATION

I would like to dedicate my dissertation to everyone who helped me by providing invaluable professional and personal advice during my Ph.D. First of all, I am thankful to my parents for their love and support to fulfill my dreams. I would like to thank my advisor Dr. Ziaeddin Shariat-Madar for his invaluable guidance and constant support. Without his help I could not have made it. I would also like to thank Dr. John Matthews for his encouragement and good advice throughout my stay here at the University of Mississippi. Thank you to all my teachers, friends and family. Special thanks to my friends Dr. Taskin Karim and Dr. Ashraf Khan for always encouraging me during stressful time during my Ph.D.

LIST OF ABBREVIATIONS

AA	Arachidonic acid
AC	Arrhythmogenic cardiomyopathy
ALT	Alanine transaminase
ANOVA	Analysis of variance
APC	Adenomatous polyposis coli
APCI	Atmospheric-pressure chemical ionization
AT_1R	Angiotensin 2 type 1 receptor
ATRAP	AT II receptor associated protein
α_2-AP	α_2 Antiplasmin
BK	Bradykinin
β-ME	Beta-Mercaptoethanol
BNPA	Brain type natriuretic peptide A
BSS	Balanced salt solution
β-Trcp	Beta-transducin repeats-containing proteins
B2M	Beta 2 microglobulin
CA	California

Ca^{2+}	Calcium ions
CAT	Catalase
cDNA	Complementary deoxyribonucleic acid
CHF	Chronic heart failure
CHO	Chinese hamster ovary
CK1α	Casein kinase 1α
COX-2	Cyclooxygenase-2
CPC	Cardiac progenitor cells
cTnC	Cardiac troponin C
cTnI	Cardiac troponin I
cTnT	Cardiac troponin T
DAD	Diode-array detector
DCHFDA	2′, 7′-dichlorodihydro-fluorescein diacetate
DE	Delaware
dpf	days post fertilization
dph	days post hatching
DKK	Dickkopf proteins
DMSO	Dimethyl sulfoxide
DNA	Deoxyribonucleic acid
DOHaD	Developmental origins of health and disease

Dvl	Dishevelled
EC	Endothelial cell
ET_B	Endothelin receptor B
EGFR	Epidermal growth factor receptor
elf1α	Elongation factor 1 alpha
ErbB	Erythroblastic leukemia viral oncogene homolog
ERK	Extracellular signal regulated kinase
ESI	Electrospray ionization
EST	Expressed sequence tags
ET	Endothelin
FL	Florida
FoxO1	Forkhead box O1
Fzd	Frizzled
FVII	Stable factor
FVIII	Antihemophilic factor
FIX	Christmas factor
FX	Stuart-Prower factor
FXI	Plasma thromboplastin antecedent
FXII	Hageman factor
GABA	Gamma-Aminobutyric acid

GAPDH	Glyceraldehyde 3-phosphate dehydrogenase
GPX2	Glutathione peroxidase2
GSH	Glutathione
GSK3	Glycogen synthase kinase 3
GSTA	Glutathione S-transferase A
G6PD	Glucose-6-phosphate dehydrogenase
HED	Huma equivalent dose
HFD	High fat diet
HK	High molecular weight kininogen
HMW	High molecular weight
H_2O_2	Hydrogen peroxide
IkBα	Nuclear factor of kappa light polypeptide gene enhancer in B-cells inhibitor, alpha
IKK	IκB kinase
IL-1β	Interleukin 1beta
IL-6	Interleukin 6
iNOS	Inducible nitric oxide synthase
JNK	c-Jun N-terminal kinase
KKS	Kallikrein-kinin system
KNG	Kininogen

Krm	Kremen
LC_{50}	Lethal concentration (50%)
LDL	Low-density lipoprotein
LK	Low molecular weight kininogen
LMW	Low molecular weight
LPS	Lipopolysaccharide
LRP5/6	Low-density lipoprotein receptor-related protein 5/6
LV	Left ventricle
MD	Maryland
MEK	Mitogen-activated protein kinase kinase
MH	4-*O*-Methylhonokiol
mRNA	Messenger ribonucleic acid
mTOR	Mechanistic target of rapamycin
NC	North Carolina
NF-kB	Nuclear factor kappa-light-chain-enhancer of activated B cells
NO	Nitric oxide
NOS	Nitric oxide synthase
NRG	Neuregulin
NY	New York
PAI	Plasminogen activator inhibitor

PCP	Planar cell polarity
PDA	Persistent ductus arteriosus
PK	Prekallikrein
PLC	Phospholipase C
PPARγ	Peroxisome proliferator-activated receptor-gamma
qPCR	quantitative polymerase chain reaction
Rb	Retinoblastoma
RHOA	Ras homolog gene family, member A
RNA	Ribonucleic acid
ROS	Reactive oxygen species
RT	Reverse transcription
RT-qPCR	Reverse transcription – quantitative polymerase chain reaction
SEM	Standard error mean
SIM	Selected ion monitoring
SOD2	Superoxide dismutase2
TAFI	Thrombin activatable fibrinolysis inhibitor
TBP	TATA-binding protein
TCF/LEF	T-cell factor/lymphoid enhancer factor
TF	Tissue factor
TIC	Total ion chromatogram

TNF-α	Tumor necrosis factor-α
Tn-I	Troponin-I
t-PA	Tissue-type plasminogen activator
TXA	Thromboxane
UHPLC/MS	Ultra-high performance liquid chromatography/Mass spectrometer
u-PA	Urokinase-type plasminogen activator
UT	Utah
V	Vaccine
VA	Virginia
VEGF	Vascular endothelial growth factor
VSMC	Vascular Smooth muscle cells

ACKNOWLEDGEMENTS

First of all, I would like to thank my advisor, Dr. Ziaeddin Shariat-Madar, for accepting me into his lab and for providing me the training, materials and environment needed for the experiments. His invaluable guidance, support and encouragement has helped me to grow as a Scientist. His door was always open for any kinds of suggestions. I am grateful to him for giving me the opportunity to work with him and his contribution to my career. Special thanks to Dr. Kristie Willett, Dr. Ikhlas A. Khan and Dr. Asok Dasmahapatra for serving on my committee and for providing their valuable suggestions. I am also grateful to Dr. Willett and Dr. Nicole Ashpole for allowing me to use the equipment in their labs. I would also like to thank Cammi Thornton for helping with the maintenance of the fish facility. I am thankful to the department of the Biomolecular Sciences division of Pharmacology for accepting me as a graduate student and for providing me funding throughout my study. I would also like to thank all the fish feeders. My gratitude goes to our collaborator Dr. Muhammad Ilias for his effortless support with the analytical chemistry part and providing the compound for my project. His valuable suggestions and advice have helped to improve that part. I am also grateful to Dr. Mohamed Ali Ibrahim for helping with the isolation of the compound. Thank you to Dr. Mei Wang and Dr. Yan-Hong Wang for helping with the analytical chemistry part. I also owe my gratitude to my lab mate Cody Cissom for his friendship and continuous support.

TABLE OF CONTENTS

LIST OF TABLES

LIST OF FIGURES

CHAPTER 1: INTRODUCTION

1.1 Background of natural products

The impact of natural products on human health has been tremendous. There are diverse sources of natural products including plants, animals and microorganisms. Paleoanthropological evidence shows that Neanderthals might have known about the medicinal properties of plants more than 60,000 years ago, which was evidenced by pollen deposits found near the Zagros Mountains of Kurdistan in Iraq (Solecki, 1975). Natural products have been used as therapeutic agents in traditional Chinese medicine for years. The ancient Chinese medicinal books “Wu Shi Er Bing Fang” (Prescriptions for Fifty-Two Diseases), compiled around 350 BC, documented 247 natural agents and about 150 combinatorial drug formulae along with the efficacies, properties, and synergies of natural products (Ji et al., 2009; Jiao and Wang, 2005; Wan and Zhong, 1990). During the Eastern Han dynasty (25-220 AD), a monograph named “Shen Nong Ben Cao Jing” (Shen Nong Materia Medica) listed 252 medicinal plants and 67 medicinal animals (Gao, 2004). China published the first national Pharmacopaeia titled “Xin Xiu Ben Cao” (Newly Revised Medicinal Materials), which documented 850 agents during 659 AD (Gao, 2004). Li Shi-Zhen, a Chinese scientist, pharmacologist, and herbalist issued his work “Ben Cao Gang Mu” (Compendium of Medicinal Materials) in 1587 AD that listed 1,892 agents and about 11,000 combinatorial formulae (Gao, 2004). The introduction of structural and analytical chemistry has helped with the purification and structural elucidation of diverse compounds and is used as an important tool to know their mechanisms in the physiological system. In 1805, morphine was isolated from opium by Friedrich Wilhelm Serturner and became not only the first naturally derived medicine but also the first one to be commercialized by Merck in 1826 (Ji et al., 2009).

Although almost all civilizations show evidence of uses of natural products, they have not received popularity until the Nobel Prize winning isolation of penicillin by Sir Alexander Fleming in 1945 (Ji et al., 2009; Shen, 2015). Around 50% of all drugs approved between 1981-2014 came directly or indirectly from natural products (Table 1.1).

Table 1.1: All new drugs approved from 1981 to 2014

Sources of drugs	Number of drugs approved (%)
Unaltered natural product	67 (4%)
Natural product derivative	320 (21%)
Mimic of natural product (/NM)	172 (11%)
Botanical drug	9 (1%)
Biological macromolecule	250 (16%)
Synthetic drug	420 (27%)
Synthetic drug-NP Pharmacophore (S*)	61 (4%)
Vaccine	101 (6%)
S*/NM	162 (10%)

S*- Synthetic drug-NP Pharmacophore; /NM- Mimic of natural product (Newman and Cragg, 2016)

Unfortunately, companies reduced investments in natural product discovery because of progress towards combinatorial synthesis and high throughput screening in the early 1990s (Ji et al., 2009). However, because of the inadequacy of newly discovered drug entities, scientists decided to turn their attention back to natural product discovery. Moreover, the Nobel Prize winning work in 2015 for the discovery of a plant natural product, artemisinin, by Dr. Youyou Tu to eliminate malaria and the discovery of a microbial natural product, avermectin, by Dr. Satoshi Omura and William C. Campbell to treat lymphatic filariasis and onchocerciasis have encouraged companies to invest more in the discovery of natural products (Shen, 2015).

1.2 Magnolia constituents and their therapeutic effects

The Magnolia genus was named in 1703 by Charles Plumier after a French botanist, Pierre Magnol (Plumier, 1703). Magnolia bark has been used in traditional Chinese and Japanese medicine for years to treat diverse diseases, including asthma, allergic diseases, fever, gastrointestinal disorders, headaches, muscular pain, and neurological disorders such as, anxiety, and depression (Amdlard et al., 2007; Dharmananda, 2002; Lee et al., 2011; Li et al., 2007; Liu et al., 2007; Poivre and Duez, 2017). The Magnolia genus has at least 255 different ingredients including alkaloids, coumarins, flavonoids, lignans, neolignans, phenylpropanoids and terpinoids (Ito et al., 1982; Tachikawa et al., 2000; Lee et al., 2011). Among these, several neolignan ingredients, including 4-*O*-Methylhonokiol (MH), honokiol, magnolol, and obovatol (Fig. 1.1) have been receiving great attention because of their wide range of therapeutic potentials against various diseases. In a previous study, honokiol was able to show anti-proliferative activity by inhibiting VEGFR2/Flk/KDR auto phosphorylation in human endothelial cells at a concentration of 37.6 μM (Bai et al., 2003). Moreover, it was able to inhibit VEGF-induced Rac activation (Zeng et al., 2001). Rac is known to promote VEGF-induced endothelial migration and proliferation (Colavitti et al., 2002; Zeng et al., 2002). Magnolia constituents have shown anti-platelet activity (Lee et al., 2011). Magnolol were proven to inhibit collagen (IC_{50} =504 μM) and arachidonic acid (AA) (IC_{50}=36 μM) induced aggregation of platelet rich plasma in rabbits (Teng et al., 1990). Honokiol is more potent in inhibiting collagen (IC_{50}=90 μM) and AA (IC_{50}=3 μM) -induced platelet aggregation (Teng et al., 1990).

Both of honokiol and magnolol show anti-platelet activity by inhibiting thromboxanes (TXA) formation, an agonist of platelet activation and contributor of thrombus formation (Lee et al., 2011). Moreover, the compounds inhibit intracellular calcium mobilization, an event necessary for platelet activation and aggregation (Lee et al., 2011). Honokiol was proven to be 5-10 times more potent than magnolol to inhibit AA induced platelet aggregation in rats (Pyo et al., 2002). Another

major component of the Magnolia family, obovatol, also inhibits epinephrine and AA induced platelet aggregation (Pyo et al., 2002).

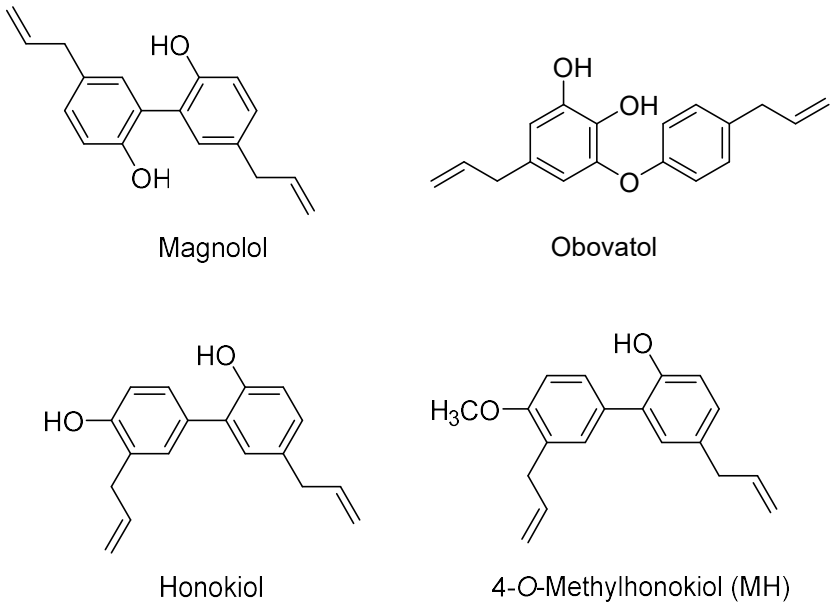

Figure 1.1: Structures of bioactive constituents of Magnolia genus

Anti-oxidant activity of both honokiol and magnolol can be exploited to treat atherosclerosis. Honokiol (2.5-20 μM) prevents oxidized LDL-mediated dysfunction by decreasing oxidized LDL-mediated adhesion molecule and improving expression of oxidized LDL-diminished NOS protein in endothelial cells (Ou et al., 2006). Magnolol inhibits proliferation of cardiac fibroblast by blocking ROS generation, thus exerting protective effect on the vascular system (Chen et al., 2006; Liou et al., 2009). Moreover, honokiol and magnolol cause p21-mediated cell cycle arrest and inhibit VSMC proliferation, which offers the possibility to treat atherosclerosis (Lee et al., 2006; Lin et al., 2009). MH reduces high fat diet (HFD) induced plasma triglycerides, cholesterol level, and prevents insulin resistance (Zhang et al., 2015). Moreover, it lowers alanine transaminase (ALT) activity, hepatic triglyceride level, liver weight, and improves hepatic steatosis (Zhang et al., 2015).

The Magnolia neolignans exert cytotoxic effects used as therapeutic agents in cancer. The Magnolia constituents can show this effect by targeting many pathological relevant pathways (Arora et al., 2012; Poivre and Duez, 2017). Honokiol and its analogs were reported to inhibit NF-kB by suppressing protein kinase B (AKT), preventing IKK activation, IkBα activation and NF-kB nuclear translocation (Poivre and Duez, 2017). MH was able to induce apoptosis in SiHa human cervical cancer cells by increasing peroxisome proliferator-activated receptor-gamma (PPARγ) activation and inhibiting PI3K/Akt pathway and intrinsic pathway induction (Hyun et al., 2015). Studies also show that neolignans are able to down regulate EGFR signaling and phosphorylation, thus inhibiting several human cancer cell lines (Fried and Arbiser, 2009; Arora et al., 2012; Kaushik et al., 2012). Neolignans, especially honokiol, can induce apoptosis by activating mTOR and its downstream signaling pathway and by inhibiting AKT and extracellular signal regulated kinases (ERK) signaling pathways (Liu et al., 2007; Fried and Arbiser, 2009; Lee et al., 2011; Arora et al., 2012; Kaushik et al., 2012; Poivre and Duez, 2017). MH decreased phosphorylation of Rb and anti-apoptotic proteins and increased the expression of cell cycle regulator p^{21} and apoptotic proteins at a concentration of 20 μM in prostate cancer cell lines (Lee et al., 2013). In addition, the compound inhibited NF-kB activity and enhanced PPARγ activity, which altogether showed therapeutic potential against prostate cancer (Lee et al., 2013).

Honokiol, magnolol and obovatol show anti-inflammatory activity by inhibiting NF-kβ pathway, important regulator of inflammation. MH (2.5-10 μM) also has anti-inflammatory effects through inhibition of LPS (1 μg/ml) induced NO generation by inhibition of NF-kB pathway in macrophage RAW 264.7 cells (Zhou et al., 2008; Oh et al., 2009). MH is also able to inhibit TPA-induced inflammatory ear edema in mice through inhibition of NF-kB, iNOS and COX-2 production (Zhou et al., 2008; Oh et al., 2009). Moreover, previous studies show that honokiol and magnolol exert anti-oxidative and anti-inflammatory activity through downregulating IFN-γ induced p-ERK1/2 and its downstream pathway for ROS and NO production (Chuang et al., 2013).

Components of Magnolia also show therapeutic potential against neuronal diseases. They show an anxiolytic effect mediated through GABA receptor/Cl^- channel activation (Lee et al., 2011). Magnolia components such as magnolol and honokiol may be involved with an anti-depressant effect by normalizing biochemical abnormalities of serotonin and its metabolite, serum corticosterone level and platelet adenylate cyclase activity (Lee et al., 2011). Several components of Magnolia, including honokiol and MH proved to have neurotrophic potential against Alzheimer's disease and nerve injuries through mitogen activated ERK kinase (MEK) (Lee et al., 2011). MH (1 μM) was found to enhance neurite outgrowth and induction of neurotrophic factors via ERK activation (Lee et al., 2009).

1.3 Toxicological effects of Magnolia family

Magnolia extracts have been used in traditional Chinese medicines without clear manifestations of safety concerns (Poivre, and Duez 2017). Few studies have been performed to evaluate the toxic potential of Magnolia bark extract. One study was designed to observe if the ethanol extract (94% magnolol and 1.5% honokiol) of Magnolia bark showed any mutagenic effect in *Salmonella typhimurium* or *Escherichia coli*. Under their experimental conditions, Magnolia bark extract did not show any mutagenic effect in *S. typhimurium* and *E. coli* (Li et al., 2007a, b, c). In another in vitro study, Magnolia bark extract did not show genotoxicity in Chinese hamster ovary (CHO) cells and Chinese hamster lung tissue (V79) cells (Zhang et al., 2008). In an in vivo study with male and female Swiss albino (CD-1) mice of 7-9 weeks old, oral administration (625-2500 mg/kg) of ethanol extract (94% magnolol and 1.5% honokiol) of Magnolia bark did not have any effect on the ratio of immature to total erythrocytes (Li et al., 2007a, b, c). Moreover, the number of micronucleated polychromatic erythrocytes did not increase significantly in the Magnolia bark extract-treated group compared to the negative control group (Li et al., 2007a, b, c; Lee et al., 2011). Previous findings did not show any effects on microscopic and macroscopic or clinical observation, urine or clinical chemistry, hematology or organ weight measurements with the

Magnolia treated group (Lee et al., 2011). Most importantly neither mortality nor significant changes in body weight were observed with the Magnolia bark extract-treated group (Liu et al., 2007). All the above findings suggest that Magnolia bark extracts have very few adverse effects and low toxicity. However, it is important to characterize the adverse effects and toxic potential of these extracts in various species at different concentrations and through various routes of administration (Lee et al., 2011).

1.4 Overview of the blood coagulation pathway

The concept of blood coagulation was introduced in 1960 when a group of scientists including Davie, Ratnoff, and Macfarlane first mentioned the “Cascade” and “Waterfall” theories, delineating the fundamental principle of a cascade of proenzymes that was activated through proteolytic cleavage leading to activation of downstream enzymes (Achneck et al., 2010; Palta et al., 2014). The coagulation cascade is divided into three pathways- the intrinsic, extrinsic, and common pathways (Fig. 1.2).

Extrinsic pathway: The extrinsic pathway is activated by tissue factor (TF) that results from damage in the endothelium and exposure in the subendothelial matrix (Lasne et al., 2006). The endothelium minimizes the interaction between the TF, and plasma procoagulants under normal physiological conditions but exposes TF to interact with the plasma protease factor (F) VII_a and calcium, forming a proteolytic complex composed of lipoproteins and phospholipids that will enzymatically activate FX to FX_a **(**Owens and Mackman, 2010; Bom and Bertina, 1990).

Intrinsic Pathway: The intrinsic pathway is a parallel pathway for blood coagulation, activated in response to vascular injury when FXII (Hageman factor) interacts with the exposed subendothelial substances. When the blood vessels are damaged, a series of proteolytic events collectively known as contact activation reactions are initiated, including the activation of FXII, prekallikrein (PK), and FXI and cleavage of high molecular weight kininogen (HK) (Kaplan and

Silberberg, 1987; Cochrane and Griffin, 1982; Kaplan et al., 1997; Colman and Schmaier, 1997). The intrinsic pathway is initiated through activation of FXI by activated FXII ($FXII_a$). FXI further activates FIX, which then forms a tenase complex with its co-factor (FVIII) on a phospholipid surface (Hall, 2010; Kumar et al., 2010; Palta et al., 2014). The resultant tenase complex will then activate FX.

Common Pathway: Both the extrinsic and intrinsic pathways coincide at the common pathway. Activated factor X (FX_a) forms a prothrombinase complex along with its co-factor (FV_a) that is attached to the surface of platelets, platelets phospholipids, tissue phospholipids, and calcium ions (Ca^{2+}), which catalyzes the conversion of prothrombin to thrombin (Roncales, 2000). Thrombin plays important role in the clot formation by two different mechanisms. Thrombin promotes proteolytic cleavage of fibrinogen to fibrin monomer that polymerizes to form fibrin fibers, and ultimately leads to the formation of the long fibers of clot reticulum (Alcott et al., 2009). Moreover, thrombin activates factor XIII ($XIII_a$), which creates covalent bonds between the fibrin fibers. This forms a fibrin network that strengthens the clot and produces a secondary hemostatic plug (Hall, 2010; Kumar et al., 2010).

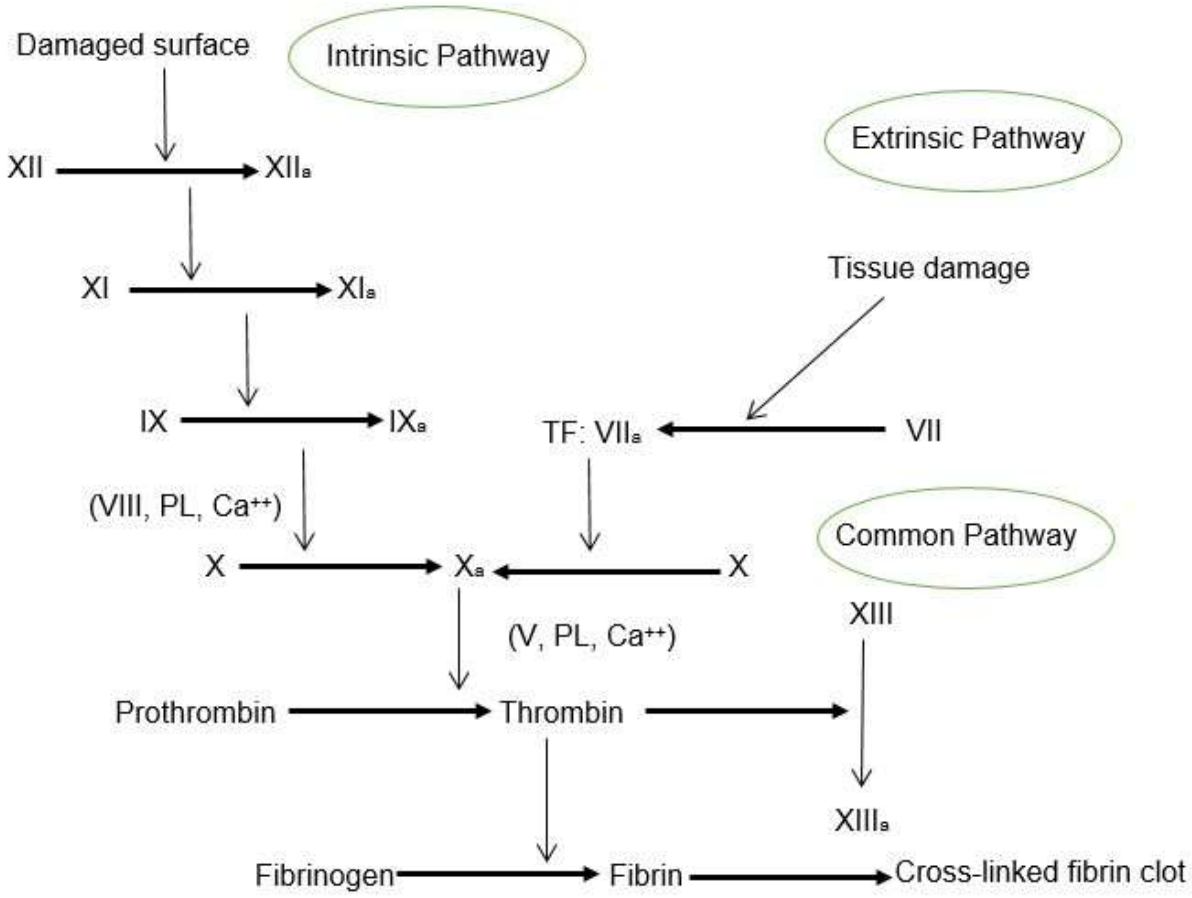

Figure 1.2: The blood coagulation pathway. The coagulation pathways are activated by a cascade of reactions in which a stable form of the protein is converted into an enzyme that will catalyze the next reaction. The intrinsic pathway is comprised of factor XII, XI, IX, and VIII. Factor VII is a unique factor of the extrinsic pathway, which is initiated by exposure of blood to tissue factor (Tavares-Dias and Oliveira, 2009). The final common pathway is activated either or both by extrinsic or intrinsic pathway that results in the conversion to thrombin. During injury to the vessels, thrombin is produced from prothrombin in the presence of factor Xa with cofactor Va. Thrombin plays important role in the conversion of fibrinogen to fibrin (Pallister and Watson, 2010).

1.4.1 Overview of the blood coagulation pathway in the teleost

Fish have delicate gills where oxygenation occurs, and the oxygenated blood is distributed throughout the body. In case of any damage in the gills, the fish will bleed to death unless it has any compensatory mechanism to control blood loss. Fish thrombocytes are biological cells equivalent to the platelets in mammals and play a role in homeostasis (Tavares-Dias and Oliveira, 2009). The presence of thrombocytes in fish was first reported in 1924 by Jordan and Speidel (Jordan and Speidel, 1924). In the teleost, thrombocytes are produced by the kidney and spleen. They first appear in the spleen during the first week of post fertilization and appear in the blood after the fourth week of fertilization (Romano et al., 1997). The half-life of thrombocytes in the circulation is up to four days, however some can survive up to 70 days (Tavares-Dias and Oliveira, 2009). The short half-life indicates the necessity of frequent substitution of these cells in order to maintain homeostasis (Fischer et al., 1998). It has been confirmed that the coagulation mechanisms in teleosts and mammals are similar in spite of their significant distance in evolution (Doolittle et al., 1962; Doolittle 1965; Cottrell and Doolittle, 1976; Doolittle et al., 1976; Doolittle and Feng, 1987; Doolittle, 1993; Wang et al., 1989). The intrinsic, extrinsic and common coagulation pathways are also present in the teleost, however, the major coagulation event is the conversion of the catalyzed thrombin to fibrinogen in blood plasma and the production of fibrin clot (Tavares-Dias and Oliveira, 2009).

Tissue factor-based coagulation in fish was first reported in 1962 (Doolittle and Surgenor, 1962; Doolittle, et al., 1962). Prothrombin, thrombin, fibrinogen, plasminogen and higher concentration of calcium are also present in teleost (Doolittle et al., 1962; Doolittle 1965; Cottrell and Doolittle, 1976; Doolittle et al., 1976; Doolittle and Feng, 1987; Wang et al., 1989). The clotting time was over one minute when the calcium concentration was 20-30 mmol/l, which was the fastest time compared to the other species (Doolittle and Surgenor, 1962). The blood coagulation time in fish is faster than mammals (Wolf, 1959; Doolittle and Surgenor, 1962; Smit and

Schoonbee, 1988), because it contains larger number of coagulation factors, which leads to the higher activity of extrinsic and intrinsic pathway in fish (Doolittle and Surgenor, 1962; Smit and Schoonbee, 1988). Fish thrombocytes, essential sources of phospholipids, lead to the activation of coagulation factors that convert prothrombin into thrombin, which catalyze the activation of fibrinogen, thus triggering thrombocyte aggregation (Tavares-Dias and Oliveira, 2009). Therefore, the number of thrombocytes plays an important role in this process, and faster clotting time indicates an increased number of thrombocytes in fish (Casilas and Smith, 1977; Ranzani-Paiva et al., 2000).

1.4.2 Teleost does not have any Plasma Kallikrein-Kinin system

The kallikrein-kinin system (KKS) has been involved in cardiovascular regulation, inflammation, immune function, pain perception, and kidney function in vertebrates (Golias et al., 2007; Petho and Reeh, 2012; Wong and Takei, 2013). KKS consists of FXII, the complex of prekallikrein (PK) and high molecular weight kininogen (HK) (Bryant and Shariat-Madar, 2009). FXIIa converts plasma to kallikrein, which, along with other stimuli, generates bradykinin (BK) and activates HK (HKa). Elevated BK is an indication of the pathogenesis of coagulopathy, endotoxemia, hypertension, and inflammation that has been implicated with KKS (Bryant and Shariat-Madar, 2009). In mammals, plasma KKS and tissue KKS are the two major cascades for kinin formation (Lalmanach et al., 2010). HK is cleaved to nonapeptide BK by plasma kallikrein (KLKB1) in the plasma KKS (Fig. 1.3). Low molecular weight kininogen (LK) is cleaved to decapeptide [Lys^0]-BK or kallidin by tissue kallikreins (KLKs) in the tissue KKS (Fig. 1.3) (Wong and Takei, 2013).

The contact activation system for Hageman factors (FXII) in thrombi formation and plasma kallikrein are not present in the teleosts (Doolittle, 2011). Moreover, the enzyme that is responsible for forming BK is also unknown (Doolittle, 2011). HK and LK are products of alternative splicing from the same gene, kininogen (KNG), in humans, and HK has two extra

domains than LK, such as D5 and D6 (Lalmanach et al., 2010). During contact activation in blood coagulation, positively charged D5 interacts with the negatively charged surface of the endothelium, and D6 interacts with the apple domain of KLKB1 that increases the binding affinity between HK and KLKB1 (Pathak et al., 2013). The KNG genes in fish do not have the D5 and D6 regions at genomic levels and D5 and D6 transcript regions in the nucleotide and expressed sequence tags (EST) databases of teleosts were also not found (Zhou et al., 2008), which confirms that the alternative splicing mechanisms of KNG1 are absent in the teleosts (Wong and Takei, 2013). In teleosts, the precursor protein, HK, the enzyme that cleaves the HK into BK, KLKB1, and the active peptide, BK, all were absent (Fig. 1.3); however, it is not known whether these genes were deleted or never evolved in those species because in the conserved synteny regions no pseudogene of KLK1 was observed (Wong and Takei, 2013). A novel immunoassay technique showing the presence of [Arg^{o}]-BK as the major circulating kinin, along with the identification of the KLK-like group in the genome of teleosts, confirm the presence of [Arg^{o}]-BK as the single effector of the KKS in teleosts (Fig. 1.3). [Arg^{o}]-BK is proven to be more potent than BK in triggering anti-dipsogenic and cardiovascular effects in eel, which suggest that [Arg^{o}]-BK has more affinity towards the endogenous BK receptors than BK (Takei et al., 2001). The retention of a single KKS in teleosts from the common ancestor play a significant role to study the original function of KKS in terms of evolutionary perspective.

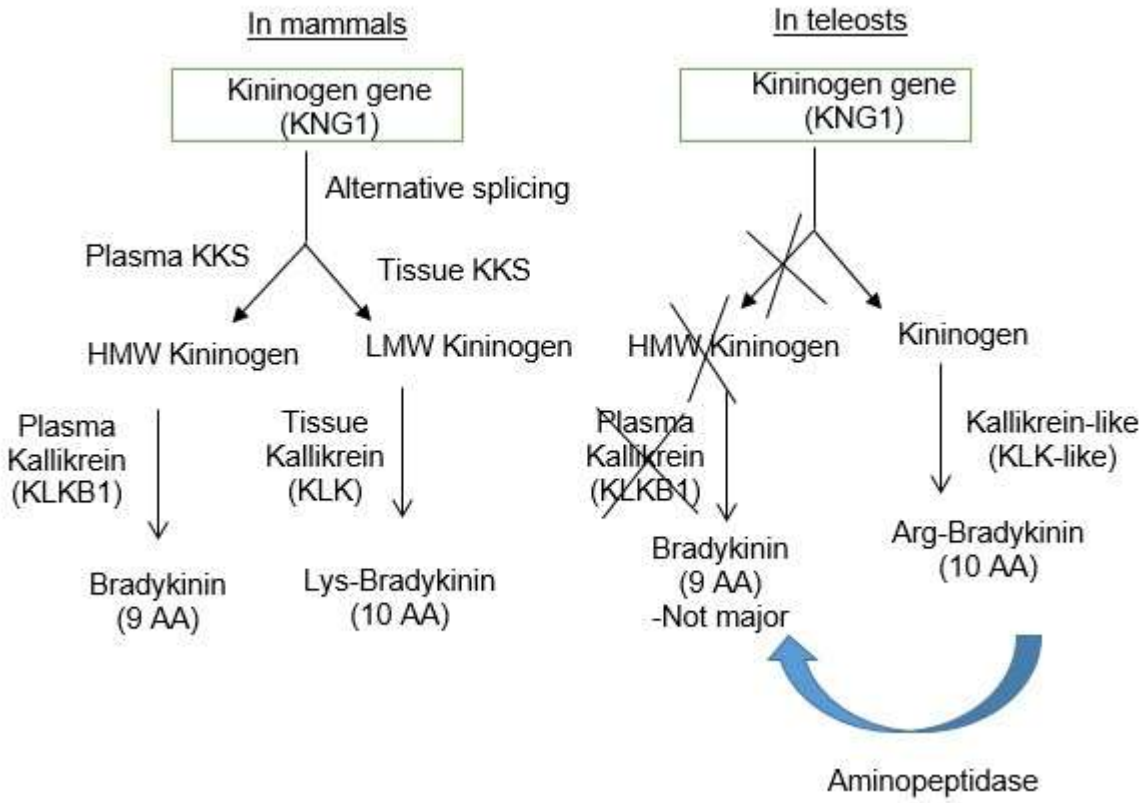

Figure 1.3: The teleost lack the Plasma Kallikrein-Kinin system (KKS). The plasma KKS system of the mammals consists of KNG, HK, KLKB1, and BK; tissue KKS system consists of KNG, LK, KLKs and decapeptide, [Lys^0]-BK. Teleosts do not have the cascade that is equivalent to the plasma KKS in mammals. The HK and KLKB1 are absent in teleost and [Arg^o]-BK is the major circulating kinin instead of BK. [Arg^o]-BK can be produced from cleavage of Kininogen, equivalent to mammals LK, by kallikrein-like enzymes. In teleosts, small amounts of BK can be produced from cleavage of [Arg^o]-BK by aminopeptidase. AA-amino acids. (Wong and Takei, 2013)

1.4.3 Fibrinolytic system

The teleost showed essential features of the thrombolytic pathway, including the activators (tissue-type plasminogen activator-t-PA; urokinase-type plasminogen activator-u-PA) and inhibitor (Plasminogen activator inhibitor-1, PAI-1) of the pathway (Hanumanthaiah et al., 2002; Lee et al., 2016; Ogiwara et al., 2015). The fibrinolytic system acts as a regulatory mechanism against the blood clots. When the injured blood vessels are healed, thrombi are lysed by plasmin. Fibrinolysis regulates the degradation of fibrin through interaction of diverse plasminogen

activators (u-PA, and t-PA) and inhibitors (PAI-1, Thrombin activatable fibrinolysis inhibitor-TAFI). Both the activators (uPA and tPA) have short half-lives (4-8 minutes) because of the presence of high concentrations of inhibitors, such as PAI-1 (Chapin and Hajjar, 2015). uPA has a lower affinity than tPA for plasminogen. Plasminogen is converted to plasmin, which is responsible for proteolysis of fibrin results in soluble fibrin degradation products (Fig. 1.4). PAI-1 is released from the endothelial cells, platelets and other cells into the circulation that inhibits tPA and uPA rapidly (Coolman et al., 2006). Elevated expression of PAI can result in excessive amount of fibrin deposition, and therefore tissue will be damaged by suppressing the fibrinolytic system.

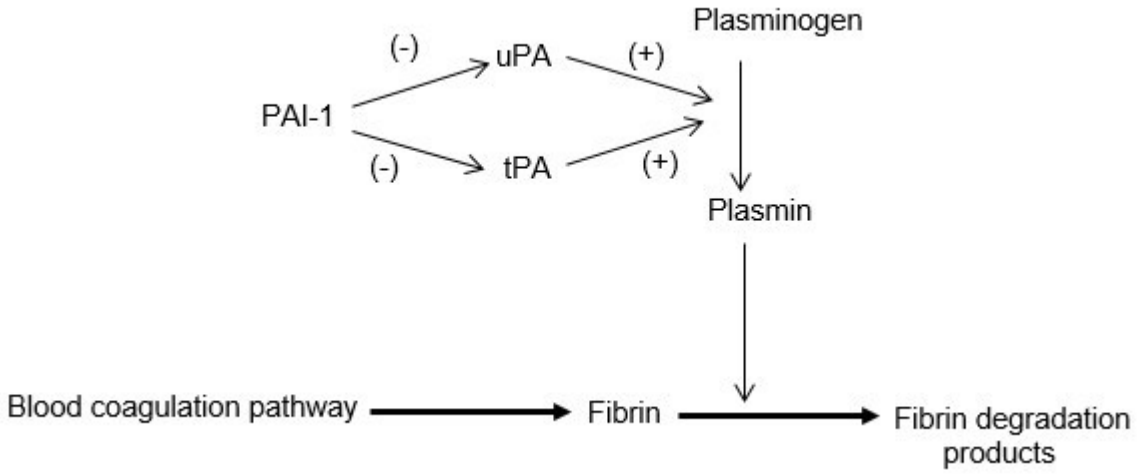

Figure 1.4: Overview of the fibrinolytic system. PAI-1 Plasminogen Activator inhibitor, t-PA tissue type plasmonigen activator, u-PA Urokinase plasminogen activator, TAFI Thrombin activatable fibrinolysis inhibitor, α_2-AP α_2 Antiplasmin. (Meltzer, 2010; Kaliappan et al., 2011)

1.5 Japanese medaka in toxicity testing

Applications of alternative species, especially small fish, are gaining popularity because of the wide range of advantages they offer. Small fish are convenient vertebrate models in all types of toxicity tests that can be used as an ecological sentinel, to identify mammalian toxicity as well as mechanisms for toxicity (Law, 2001; Shima and Mitani, 2004; Hinton el al., 2005). Acute or chronic exposure as well as multigenerational exposure of compounds can be administered either on the embryos or the adult fish (Padilla et al., 2009). Moreover, the fish offers additional advantages by providing sophisticated experimental tools such as transgenic lines (Fu et al., 2000; Wayne et al., 2005) and morpholino knock down techniques (Carl et al., 2002; Paul-Prasanth et al., 2006).

Japanese medaka is currently one of the widely used vertebrate fish models. As the name suggests Japanese medaka is native to Asian countries, primarily Japan. It is a small (2-4 cm), egg-laying fish that is hardy, and survives in wide latitudes of salinity and temperature (Padilla et al., 2009), which makes them suitable to adapt to laboratory conditions. Medaka has several advantages over mouse as an experimental model, including the production of a large number of progeny by the same two parents, the availability of a large number of embryos because of daily spawning, low cost and easy maintenance, transparent chorion, which allows high-throughput screens for developmental abnormalities during embryogenesis, and a short generation time (2 months) (Hyodo-Taguchi and Egami, 1985; Hyodo-Taguchi and Egami, 1989). Medaka plays a significant role in toxicology testing. The low cost and smaller size of medaka allow researchers to use a small amount of toxicant, more numbers per dosage group, and large treatment groups. Moreover, medaka is an excellent model for developmental toxicity because it can avoid maternal metabolism, and can be observed daily under the microscope. It is a convenient model to determine the acute and chronic toxicity and to unravel the mechanisms associated with toxicity.

1.5.1 Major developmental stages of medaka embryos

Medaka embryos are divided into 39 developmental stages based on the diagnostic features of the developing embryos (Iwamatsu, 2011). The stages related to our experiment will be discussed in this section. The heart first appears between the posterior region of the mid-brain and the anterior region of hind-brain in stage 22. In the next stage, the anterior portion of the heart continues to straighten, grow and reaches the posterior end of the eye vesicle. The cuvierian ducts (blood vessels), semicircular in shape, and the vitello-caudal vein begin to form on the yolk. A blood island appears between the 6^{th} and 11^{th} somites in the ventral region. During stage 24, the anterior portion of the heart extends to the anterior end of the forebrain and exhibits a slow heartbeat (33-64/min) (Iwamatsu, 2004). The Cuvierian ducts and vitello-caudal vein are not completed yet. The blood starts circulating in Stage 25, in which the spherical blood cells are pushed out from the blood island (located in the 7^{th} to 15^{th} somites) toward the vitello-caudal vein (Kinoshita et al 2009). The blood is pumped at a rate of 70-80/min from the heart into the anterior cardinal vein and the dorsal aorta roots (Iwamatsu, 2004). However, a blood countercurrent is observed into the aorta from the heart (Kinoshita et al 2009). Chamber differentiation of the heart also begins in this stage. Anterior and posterior portions of the heart tube differentiate into the atrium and ventricle, respectively. The differentiation of the heart cells into atrium, ventricle, sinus venosus and bulbous arteriosus occur in stage 29 (3 days and 2 hours). The chamber differentiation and correct positioning of the heart are completed by stage 36 (6 days). During stage 39, the tip of the caudal fin extends towards the base of the pectoral fin or the posterior region of the swim bladder (Kinoshita et al 2009). The internal wall of the swim bladder enlarges after hatching, and the cells in the hatching gland disappear by this time. Finally, the embryos dissolve the inner layer of egg envelope, tear the outer layer and escape from the tail of the envelope first.

1.5.2 Development of heart in Japanese medaka

The heart is the first functional organ formed in the vertebrate embryo. The embryonic heart tube is a relatively simple organ consisting of myocardium and endocardium, which form the outer and inner layer of the tube, respectively (Fishman and Chien, 1997). There are three diverse cell types in the heart including myocardiocytes, muscular cells that provide cardiac contractility; endocardiocytes, endothelial cells that provide continuity with the vascular endothelium; and additional lineage diversification, which creates subpopulation such as ventricular and atrial myocardiocytes and show distinct physiological and histological characteristics (De-Haan, 1965; Franco et al., 1998; Lyons, 1994; Satin et al., 1988; Yelon, 2001). Heart development occurs in the same manner both in Japanese medaka and zebrafish, however, the development takes place over a longer time in medaka, which allows high-resolution detailed observation of cardiac cell differentiation (Kinoshita et al., 2009). The transparent chorion of the embryos provides great advantage by permitting high-throughput screens for developmental abnormality.

Lemanski et al. (1975) reported the fine structure of the medaka heart that is located in the anterior ventral region of the abdominal cavity, immediately posterior to the gills. The primitive heart tube is composed of four chambers: (1) the sinus venosus, a thin-walled distensible sac, the posterior-most chamber that collects the returning venous blood; (2) the atrium, also thin walled, which appears smaller and angular when contracted and becomes the largest chamber when it is distended with blood during diastole; (3) the ventricle, a thick-walled major contractile part of the heart that is the largest chamber after systolic contraction; and (4) the conus arteriosus, thick but narrow tubular part of the heart, which extends from the ventricle to the truncus arteriosus (Kinoshita et al., 2009; Lemanski et al., 1975; Romer, 1956). Among the chambers, the ventricle is extensively trabeculated, and the atrium is partly trabeculated; however, no trabeculation was observed in the sinus venosus and conus arteriosus (Kinoshita et al., 2009). These trabeculae

anastomose give the whole chamber a spongy appearance (Lemanski et al., 1975). The blood enters into the sinus venosus part of the heart via the cardinal and hepatic veins, then travels into the ventricle through the atrium. The blood moves into the ventral aorta through the conus arteriosus by vigorous muscle contractions of the ventricle. From the ventral aorta, blood enters into the gills where oxygenation occurs, and then it is distributed into rest of the body.

Walls of the heart: Like humans', fish's hearts consist of three distinct layers: epicardium (outer layer), myocardium (middle layer), and endocardium (inner layer).

Epicardium: The epicardium, the outer layer of the heart, is a simple squamous epithelial layer of cells connected by desmosome that form a tight continuous sheet over the exterior part of the heart (Lemanski et al., 1975). The nuclei of the epicardial cells are oval in shape; cytoplasm are flattened if observed in cross section. However, many of the cells in cytoplasm show branching finger-like projections if they are observed in tangential sections. There are numerous rough endoplasmic reticulums. The cisternae, which are ribosome-attached, are organized in a parallel manner. Ribosomes are joined to the outer nuclear membrane in certain areas. However, there are few free ribosomes and polysomal complex present in the cytoplasm. Golgi bodies and vesicular elements are also present close to the nucleus. Moreover, there are abundant filaments in the cell cytoplasm, which are randomly arranged and have a diameter of 60Å (Lemanski et al., 1975).

Myocardium: The wall of the myocardium is a single cell layer, and each of the cells has a nucleus that is basally located. There are abundant mitochondria across the myocardium, which are centrally-located in the cells between the myofibrils, located peripherally. The large numbers of mitochondria that are associated with the myofibrils provide the actively contracting heart its increased demand of respiratory requirements. The rough endoplasmic reticulum, free ribosomes, or polysomes are rarely seen in the cells. The fewer numbers of ribosomes and rough endoplasmic reticulum indicate the paucity of activity in protein synthesis of these cells. Golgi

bodies are also seldom seen in the myocardial cells, which further support the inadequacy of protein synthesis, because this is used to collect and dispatch the protein, which are received from the endoplasmic reticulum.

Endocardium: The endocardium consists of irregularly shaped cell lines inside the heart. The nuclei look flattened to oval in cross section. The numbers of mitochondria are less, and smaller in size than in the myocardial cells, which are present along with rough endoplasmic reticulum and in close proximity. There are large numbers of ribosomes present in the cell. Golgi bodies are present in the perinuclear regions of the cells, which are well developed and, contain vesicular elements. These structures of the endocardial cells suggest that they are actively involved with protein synthesis. However, the reasons for endocardial cells being active in protein synthesis are not clear. The endocardial and myocardial cells have areas of confluent cytoplasm in certain regions, which suggests the possibility that the endocardial cells are synthesizing materials that are being used all or in part by the myocardial cells (Lemanski et al., 1975). So, the endocardium of the medaka heart serves not only as a protective layer but also as metabolically active group of cells.

1.6 Canonical Wnt/β-catenin Pathway

The Wnt1 gene, originally known as Int-1, was identified in 1982 in virally induced breast tumors activated by integration of mouse mammary tumor virus proviral DNA (Nusse and Varmus, 1982; Clevers and Nusse, 2012). Other major parameters of this signaling pathway were identified in Drosophila in 1994 including β-catenin, dishevelled (Dvl), and glycogen synthase kinase 3β (GSK3β) gene (Noordemeer et al., 1994, Peifer et al., 1994, Siegfried et al., 1992). By 2000, the Wnt receptor Frizzled (Fzd) and co-receptor lipoprotein receptor related (LRP5/6) protein and Wnt nuclear effectors T cell factor/lymphoid enhancer factor (TCF/LEF) transcription factors were discovered (Behrens et al., 1996; Bhanot et al., 1996; Molenaar et al., 1996; Wehrli et al., 2000). Since then, the Wnt/β-catenin pathway has played a significant role in unraveling many questions

in developmental biology. Signaling by the Wnt family of secreted glycoproteins plays an important role in embryonic development and homeostasis in adult tissue by cell differentiation, cell proliferation, cell migration, cell polarity, and cell fate determination (Logan and Nusse, 2004; Macdonald et al., 2009; Johnson and Rajamannan, 2006). Therefore, mutation in this pathway can cause birth defects, cardiovascular abnormality, cancer, and even mortality (Clevers, 2006; Cattelino et al., 2003). Wnt proteins signal through several pathways, of which the canonical Wnt signaling pathway is the most studied and acts by regulating the co-activator β-catenin that controls key developmental gene expression (Fig. 1.5) (Macdonald et al., 2009).

1.6.1 Role of canonical Wnt/β-catenin signaling in cardiac diseases

The canonical Wnt/β-catenin signaling pathway is involved with the regulation of embryonic development and adult homeostasis (Macdonald et al., 2009). Blocking this pathway during early differentiation is involved with inhibition of beating cardiomyocytes and early cardiac markers, and slightly later activation is involved with inhibition of cardiac differentiation (Naito et al., 2006). The Wnt/β-catenin pathway is also involved with regulation of endothelial cell (EC) development; inhibition of β-catenin in developing EC can cause embryonic mortality and loss of EC integrity (Cattelino et al., 2003). Moreover, EC specific β-catenin loss is involved with defective endocardial cushion/cardiac valve development, and loss of a frizzled receptor (Fzd5) in mice has been reported to produce defective vascular development and embryonic lethality (Cohen et al., 2007; Ishikawa et al., 2001). Cohen et al. (2007) has mentioned a resemblance between defective Wnt/β-catenin signaling pathway and human congenital heart disease. Previous studies have shown the involvement of Wnt signaling with cardiac hypertrophy (Horst et al., 2012). Blankesteijn et al. (1996) demonstrated that Fzd 2 was upregulated with cardiac hypertrophy in rat heart tissue after aortic constriction (Blankesteijn et al., 1996). Another study showed upregulation of Dvl in the case of aortic constriction in mice and rats (Van de Schans et al. 2007; Malekar et al. 2010).

Activation of the canonical Wnt pathway was reported in epicardial fibrosis of failed pediatric heart transplants (Ye et al., 2013). Deposition of fibrosis causes arrhythmias that result from cardiac diseases and cardiac repair post myocardial infarction by disrupting electrical wave propagation (Benito et al., 2011; Rohr, 2012). Wnt signaling is involved with heart failure by inhibiting apoptosis through activation of Akt and inhibition of GSK3β (Haq et al., 2001). There is conflicting evidence for the involvement of Wnt signaling in the pathogenesis of arrhythmogenic cardiomyopathy (AC). Some studies show that suppression of Wnt signaling is involved with AC. It was also demonstrated that AC can be caused by downregulation of the Wnt/β-catenin pathway due to nuclear translocation of plankoglobin, homologous with β-catenin (Garcia-Gras et al., 2006; Lombardi et al., 2009; Lombardi et al., 2011; Ben-Ze'ev et al., 2000). Due to the reduction of desmoplakin expression in mouse hearts and cultured atrial myocytes, plakoglobin is released from the cell membrane, which translocates into the nucleus, interferes with β-catenin/Tcf transcriptional activity, and produces AC phenotypes (Garcia-Gras et al., 2006; Lorenzon et al., 2017). Moreover, activation of the Hippo pathway regulates cellular differentiation and proliferation decreased activation of Wnt signaling to induce AC (Lorenzon et al., 2017). Another study showed that activation of GSK3β and suppression of AKT was able to cause exercise-mediated AC phenotypes (Martherus et al., 2016). However, some contradictory evidence shows over-activation of Wnt/β-catenin signaling due to β-catenin stabilization by AKT activation and GSK3β inhibition can induce AC pathogenesis (Li et al., 2011).

1.6.2 Overview of canonical Wnt signaling

The Wnt/β-catenin signaling pathway is well characterized in the teleost fish model (Ueno et al., 2006; Barjhoux et al., 2016). This pathway is triggered by Wnt family ligands, such as secreted lipoglycoproteins that require the Fzd family receptors and co-receptor LRP 5/6 for functional activity (Niehrs, 2012). In the absence of Wnt stimuli (resting state), β-catenin forms a complex with GSK3β, casein kinase 1α (CK1α), adenomatous polyposis coli (APC) and axin, known as the destruction complex (Fig. 1.5). The level of β-catenin is regulated by sequential

phosphorylation by Ck1α at serine 45 and then by GSK3β at threonine 41, serine 37, and serine 33 (Kimelman and Xu, 2006). The phosphorylation of β-catenin at serine 33 and 37 forms a binding site for E3 ubiquitin ligase β-Trcp, which leads to β-catenin ubiquitination and degradation (Fig. 1.5) (Macdonald et al., 2009). This causes repression of Wnt target genes by DNA-bound TCF/LEF through prevention of translocation of β-catenin into the nucleus (Fig. 1.5). Fzd is linked to the Dvl protein that is a cytoplasmic scaffolding protein directly interacting with Fzd (Macdonald et al., 2009; Wallingford and Habas, 2005; Wong et al., 2003). Dvl interacting with Axin is required during Wg signaling for Axin translocation to the plasma membrane or in case of Fzd overexpression (Cliffe at al., 2003; Zeng et al., 2008; Wallingford and Habas, 2005). A previous study showed that Fzd-Dvl recruitment of the Axin-GSK3 complex triggers GSK3 mediated LRP6 phosphorylation (Zeng et al., 2008). When Wnt ligands are present, they interact with the Fzd receptor and co-receptor LRP5/6, which results in activation of the Dvl protein (Fig. 1.5) (Billic et al., 2007). Recruitment of Dvl protein causes phosphorylation of LRP5/6 and translocation of Axin to the receptor, which inhibits degradation of β-catenin by dissociating the destruction complex (Fig. 1.5). This allows β-catenin to accumulate in the cytosol and translocate into the nucleus, which forms a complex with TCF/LEF and activate expression of Wnt responsive genes (Fig. 1.5) (Macdonald et al., 2009).

Dickkopf proteins (DKK) are inhibitors for Wnt/β-catenin signaling that bind to LRP5/6 with high affinity (Ahn et al., 2011; Bourhis et al., 2010; Niehrs, 2006). Deletion of DKK1 results in embryonic lethality and developmental abnormality such as loss of anterior head structure and fused vertebrate in mice model (Mukhopadhyay et al., 2001). DKK1 inhibits Wnt signaling by inducing LRP5/6 internalization/ degradation through binding to the cell surface receptor Kremen (Krm) (Mao et al., 2002). The probable mechanism might be disruption of the Wnt-induced Fzd-LRP5/6 complex by DKK1 with a minor modulatory role of Krm (Ellwanger et al., 2008; Semenov et al., 2001). DKK1 directly competes with Wnt for binding sites on LRP5/6, and inhibit Wnt signaling (Ahn et al., 2011).

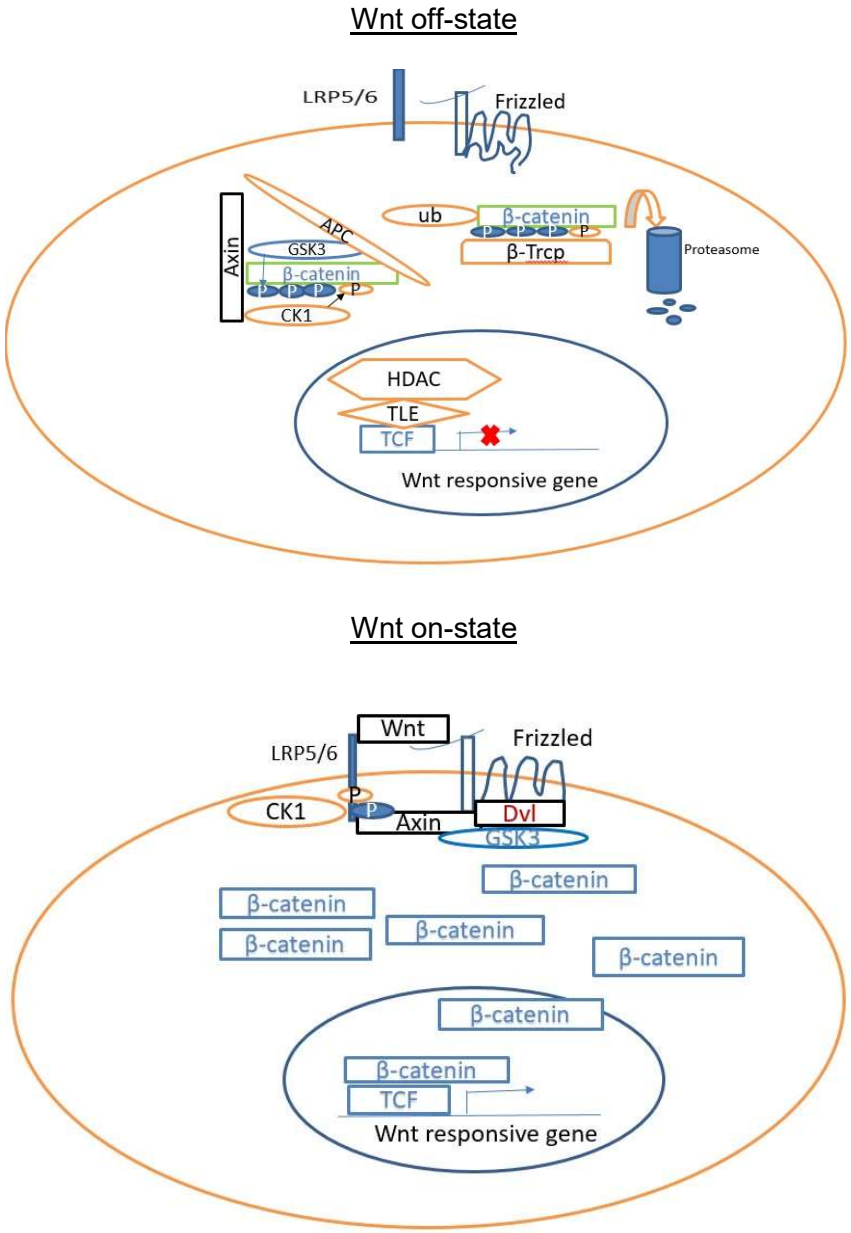

Figure 1.5: Overview of Wnt Signaling: Wnt on/ off state. Wnt off state: In the absence of Wnt, cytoplasmic β-catenin forms a complex with axin, APC, GSK3, and CK1. β-catenin is phosphorylated by CK1 and GSK3, which results in its ubiquitination by an E3 ubiquitin ligase protein β-Trcp and proteasomal degradation. This causes repression of Wnt target genes by DNA-bound TCF/LEF through prevention of translocation of β-catenin into the nucleus. **Wnt on state:** In the presence of Wnt, a complex is formed with the Fzd receptor and co-receptor, LRP5/6. Recruitment of Dvl protein causes phosphorylation of LRP5/6 and translocation of axin to the receptor that inhibits degradation of β-catenin. Therefore, β-catenin translocates to the nucleus to form a complex with TCF/LEF and activates Wnt-responsive genes. (He et al., 2004; Macdonald et al., 2009; Lorenzon et al., 2017)

1.6.3 Non-canonical Wnt pathway

The non-canonical Wnt pathway is β-catenin-independent and uses downstream components of the pathway other than β-catenin-TCF/LEF. The planar cell polarity (PCP) pathway is the best characterized non-canonical pathway in which the Fzd receptor triggers a cascade of downstream effectors, including RAC1 (small GTPase), small GTPase, Ras homolog gene family, member A (RHOA), and c-Jun N-terminal kinase (JNK), which regulate rearrangement in the cytoskeleton and gene expression (Gomez-Orte et al., 2013). This pathway controls cell polarity in morphogenetic processes including gastrulation, neural tube closure, and stereocilia orientation in the inner ear (Axelrod, 2009; Gomez-Orte et al., 2013; Kikuchi et al., 2011; Simons and Mlodzik, 2008). Another non-canonical Wnt pathway is the Wnt-Ca^{2+} signaling pathway where Wnt elicits Fzd-regulated activation of heterotrimeric G protein that results in activation of phospholipase C (PLC). Ultimately, PLC causes the release of Ca^{2+} from intracellular storage and activation of effectors that control transcription of the factors involved with regulation of cell fate and cell migration (Gomez-Orte et al., 2013). The Wnt-Ca^{2+} non-canonical pathway is involved with cancer, inflammation, and neurodegeneration (Axelrod, 2009; De, 2011; Gomez-Orte et al., 2013; Kikuchi et al., 2011; Niehrs, 2012; Macdonald et al., 2009; Simons and Mlodzik, 2008).

1.7 Specific Aims:

The objective of our study was to determine the teratogenic potential of 4-*O*-methylhonokiol (MH) on Japanese medaka and to elucidate the mechanisms which triggered this effect. MH is a major bioactive constituent of *Magnolia grandiflora* seeds or *Magnolia officinalis* bark. Magnolia genus has been widely reported to have various beneficial effects on the cardiovascular system, including anti-atherosclerosis, vascular relaxation, and antiplatelet effects (Zhao et al., 2016). MH has been proven to be successful against high-fat diet-induced cardiac pathogenic changes (Zhang et al., 2015). However, the effect of this compound on the cardiovascular system during embryogenesis hasn't been characterized yet and our preliminary study showed that the compound had produced some adverse effects by slowing heartbeat, forming thrombus, preventing vessel circulation and hatching efficiency and causing mortality during embryogenesis. Our preliminary data also showed this compound caused some birth defects and had an effect on survivability 1 month after fertilization. Therefore, it would be beneficial if the teratogenic potential of MH, a structural analog of honokiol and mechanistic study associated with it could be identified on Japanese medaka in a time- and concentration-dependent manner.

Aim 1: To determine the teratogenic potential of MH on Japanese medaka:

1a. Determination of MH effect on medaka embryogenesis:

Hypothesis: MH will cause teratogenic potential in medaka embryos in a time- and concentration-dependent manner. Approach: Embryos will be treated with different concentrations of MH throughout embryonic stage 10 to 38 (0-6 day post fertilization, dpf) and after the vessel circulation starts (stage 25-38/2-6 dpf) to observe if the compound can cause any changes in their function and survivability.

1b. Effect of MH on locomotion and survivability of medaka:

Hypothesis: MH has an effect on locomotion and survivability in larval and adult stage of the exposed embryos. Approach: Embryos will be treated with sublethal concentrations of MH from stage 10 to 38 (0-6 dpf). The 2 dph larvae will be weighed and used for locomotion study. They will be grown into 30 dpf fish to observe the effect of the compound on locomotion and survivability.

1c. Impact of MH on the components of the blood coagulation pathway and on proinflammatory mediators:

Hypothesis: MH will activate components of coagulation factors or block the fibrinolytic system to promote thrombosis. However, thrombus may be caused by other consequences, such as damaged blood vessels due to an excessive inflammatory response or oxidative stress. Approach: Effect of MH will be evaluated on some major components of the blood coagulation pathway or on the fibrinolytic pathway. The gene expression of inflammatory mediators and antioxidant enzymes will be determined by RT-qPCR. The level of reactive oxygen species (ROS) will be measured using 2′, 7′-dichlorodihydro-fluorescein diacetate (DCHFDA).

Aim 2: To characterize the Wnt/β-catenin signaling pathway as a potential mechanism of embryonic abnormality induced by MH:

Hypothesis: MH will block the Wnt/β-catenin signaling pathway to prompt embryonic abnormality because this pathway is known to control embryonic development, cardiac and endothelial cell development during embryogenesis. Moreover, blockade of this pathway is known to cause birth defects. Approach: We will analyze the expression of the major parameters of this pathway, including Wnt, β-catenin, inhibitor of Wnt (DKK1) and receptors (LRP-5, Frizzled) of Wnt in both control and treated embryos (MH treatment during stage10-38/0-6 dpf).

Upon successful completion of this study, we will be able to determine the concentration- and time-dependent teratogenic potential of MH which has been reported previously to have diverse biological activities. Moreover, the mechanistic study of inducing these effects will be helpful to unravel therapeutic strategies to prevent these consequences. This study is relevant because it will characterize for the first time effect of MH on embryogenesis, especially on the development of the cardiovascular system.

CHAPTER 2: MATERIALS AND METHODS

2.1 Animal maintenance and egg collection

Orange-red variety of Japanese medaka (*Oryzias latipes*) originally purchased from Carolina Biological (Burlington, NC) were maintained in the fish culture facility for more than 20 years. The fish were maintained with balanced salt solution (BSS, 17mM NaCl, 0.4mM KCl, 0.3mM $MgSO_4$, 0.3 mM $CaCl_2$, pH 7.4) in an Aquatic Habitats ZF0601 Zebrafish Stand-Alone system (Aquatic Habitats, Apoka, FL) at 26±1^{0}C, 16L: 8D light cycle, salinity 1.2 and pH 7.4 (Dasmahapatra et al., 2017). Fish were fed with a combination of Tetramin flakes (Tetra, Blacksburg, VA) and live brine shrimp (Brine Shrimp Direct, Ogden, UT) twice a day. Fertilized eggs were collected from the reproductively active adult female medaka fish and screened for viability.

2.2 Determination of the effect of MH on medaka embryogenesis

The objective of this study was to evaluate the effect of MH on medaka embryogenesis in a concentration- and time-dependent manner. Fertilized medaka eggs (n=5 independent exposure, each exposure had 12 embryos) (Iwamatsu stage 10) were exposed to MH (0, 1, 2, 5, 10, 20 μM) in hatching solution (17 mM NaCl, 0.4 mM KCl, 0.3 mM $MgSO_4$, 0.3 mM $CaCl_2$, with required amount of $NaHCO_3$ to maintain the pH 7.4 and 0.0002% methylene blue to reduce fungal infection) in a 48-well culture plate (one embryo/ml/well) and maintained in a high performance incubator (Thermo Fisher Scientific, Waltham, MA, USA) at 26±1°C (Dasmahapatra et al., 2017). The treatment was continued for 6 days (0-6 days post fertilization-dpf) at 0, 1, 2, 5, 10, and 20 μM concentrations and 4 days (2-6 dpf) at 0, 1, 2, 5, 10, and 20 μM concentrations; the control

embryos were maintained in 1 ml hatching solution (0.02-0.04% DMSO). After the removal of MH, the embryos were maintained in hatching solution from 6 dpf and continued until 10 dpf with 50% static media change. Heartbeats were counted for 1 minute during 3 dpf and 6 dpf under the phase contrast microscope. Vessel circulation and thrombus formation was also observed, and photographs were taken under a light microscope attached to a Cannon DC 7.4 V camera. Vessel circulation, hatching efficiency, and mortality were observed under the phase contrast microscope (AO Scientific Instruments, Buffalo, NY). The LC_{50} was calculated at 10 dpf. The photographs of the heart were taken by Eclipse Ti2 inverted microscope system (Nikon Instruments Inc., Melville, NY).

2.3 RNA extraction, cDNA synthesis, and RT-qPCR

Fertilized embryos (Iwamatsu stage 10) (n=4, 100 embryos/pool) were treated with 10 μM MH for 0-6 dpf. The control group was maintained in 50 ml of hatching solution with 0.01% of DMSO. Both groups were homogenized at 6 dpf in 1 ml of trizol (Invitrogen, Carlsbad, CA) for 6 minutes (30 seconds running and 30 seconds in ice for three times). Then they were kept in a -20˚C freezer overnight, and then thawed, and 200 μl chloroform was added. It was shaken 15 sec by hand, incubated at 15-30ºC for 2-3 min and centrifuged for 15 min at 6˚C. The upper colorless aqueous phase which contained the RNA was transferred to a fresh tube. Isopropyl alcohol (500 μl) was added, incubated at room temperature, and centrifuged for 10 min at 6˚C. The supernatant was removed and 1 ml of 75% ethanol was added, vortexed, and centrifuged for 5 min at 6˚C. Again, the supernatant was removed and the tube was air dried for 5-10 min in a way that the RNA did not dry completely. RNase free water (100 μl) and 350μl buffer RLT (QIAGEN Sciences, MD) with β-ME (9:1) were added and mixed thoroughly. Then ethanol (100%) was added, mixed thoroughly by pipetting, and 500 μl sample was transferred to a column of a collection tube. Tubes were centrifuged for 15 sec and the flow-through was poured out. The rest of the sample was

transferred to the column, centrifuged, and poured out in the same way. Then 500 µl RPE buffer (QIAGEN Sciences, MD) was added to the column and centrifuged for 2 min. The column was transferred to a new collection tube, and RNase free water was added to the column and centrifuged for 1 min. The RNA concentration was measured in a NanoDrop (Thermo Scientific, Wilmington, DE).

RNA was reverse transcribed to cDNA following manufacturer's protocol by iScript supermix (BioRad Laboratories, Hercules, CA) in a 20 µl final volume. The complete reaction was incubated in a thermal cycler for priming at 25°C for 5 min, reverse transcription at 46°C for 20 min, and RT inactivation at 95°C (BioRad Laboratories, Hercules, CA). RT-qPCR was performed with the following protocol (BioRad Laboratories, Hercules, CA): polymerase activation and DNA denaturation at 95°C for 3 min, followed by 40 cycles of denaturation at 95°C, 10 sec, and annealing at 60°C, 30 sec followed by thermal dissociation protocol for SYBR green detection. The target gene was normalized to a corresponding housekeeping gene, elf-1α. McCurley and Callard, (2008) performed an experiment with eight housekeeping genes, including bactin1, tuba1, gapdh, g6pd, tbp, b2m, elf1α, 18s rRNA to measure their variability during development, across different tissue types, and with chemical/toxicant exposure in zebrafish. The gene, elf1α showed low degree of variability compared to the other genes under all conditions (McCurley AT, Callard GV, 2008). Fold change was determined by relative quantification method ($\Delta\Delta$Ct method). The quality of the RT-qPCR product was evaluated on a 2% agarose gel containing 0.01% ethidium bromide.

Table 2.1: List of primers

Gene	Sense (5′-3′)	Antisense (3′-5′)	Product size (bp)	Reference
elf1α	GGAGGCCAGCGACAAGAT	GCGAGAAGGTGGCAGGAT	115	NM_001104662.1
FX	TGTCAAAGCCCTGTGTGAAT	AGAAATGTTCACAGCCACCA	147	XM_020710825.1
FXI	GAAGGATAATGCAGACCAGTGTC	GATGACACCCTTCAAGTAGCATC	127	XM_004074394.4
FVII	GTTCTGTCGGATAGGTGGATTT	CCTCCAGGTCATGTTTACCTAC	97	XM_004066449.3
PAI-1	ATGCCGAGGTTTTCTCTGAAC	GTTGAACATGTCTCCCAGTCC	78	XM_020711407.1
uPA	ACTGTGTTTCTGGGAAAGAGTG	GGATGATCATTTTCTCCACGGT	82	XM_004077409.4
tPA	CAGCCCCGATCCAAGC	CCCTTCCATCGCAGCC	185	XM_011478844.3
ATRAP	CATGTGGGGGAACTTCAGC	GCCCACCAGAAACATGAGG	91	XM_011475678.2
ET_B	CTGATCTTTGTGGTGGGCAT	CCCATTCCTCATGCACTTGT	78	NM_001104844.1
IL-1β	CTGTTTCTGGAGGAGGTGG	AGAAGAGGAAGCGCACATT	79	XM_011478737.2
TNF-α	AACCGAAGAGTCTGAGAGGG	AGCTGAAGAAGAGTACCGCT	105	XM_004074335.3
CAT	TGCTAGCAGTTGATTGTCTGT	CACAGATCCACTGAAACAGGA	100	XM_004069460.2
GPX2	TCAACGGAGTAAACACGCAT	GATCCTGCATGAGAGAGCTG	90	XM_004082594.3
GST A	CTGAAGGAGAGCGGCAC	CAGGAACGAGCCAGAGC	107	XM_020710769.1
SOD2	AAATGTGCGTCCTGACTATGT	TTTTGGCTATCTGAAGACGCT	83	XM_004083471.3
Wnt1	CCAGAAAACCCAGCTCACAA	TTGTGGGAGCAGAAGTTTGG	80	XM_020704658.1

FZd2	CACATGACCCCAGACTTCAC	AGAAACCAGAAGTGATGCCG	76	XM_020705151.1
LRP5	GAAGGCCCGAGCAGTTCA	AAGACATGGCTCCGTCGT	101	XM_011472833.2
Dvl	TGCTGAAACAAAGCCCAAAGT	ACCTCAAGGATCTGAGTGAGC	87	XM_011490628.3
β-catenin	CACAGAACTCCTACACAGCC	AGGCGCTTCTTGTAGTCTTG	102	XM_004077778.3
DKK1	GTGACACATGCCTGAGATCG	CACAGGCTTACAGATGCGAG	83	XM_020709512.1
GSK3β	AGCTGCAGATTATGAGGAAGTTG	TAGACGGTCTCTGGAACATAGTC	130	XM_023950884.1
ErbB3	GAGGTTGAGAAGGATGGCGT	CTACCTGGACTTCCTGTGCC	86	XM_011474665.3
NRG-2	CTCGTCACTGTGGGGGA	CTCGTCAGTGGGGTCCA	93	XM_020708867.2
BNP A	GAGCTCTGTTGATGAGGAGG	CAGTCCTGGCTCATCTTCTC	88	NM_001104685.2
cTnT	CAGAGAGGGAAAGGGAACG	GCTGATCCGGTTTCTGAGT	362	XM_004068713.4
FoxO1	GCCCATGCCAGTTCTGAGTA	ATCCTCCGTGTTGGTGGATG	102	XM_011485361.2

2.4 Effect of MH on locomotion

The aim of this method is to evaluate the role of MH on locomotion of the hatched embryo (larvae). The embryos (n=14-16) were treated with sub lethal concentration of MH (0, 5 µM) during 0-6 dpf. At 2 days post hatching (dph), the larvae were placed in a 24-well plate with a single fish per well containing 2 ml hatching solution for a locomotion assay. They were placed in the darkness of the Zebrabox for 20 min (Viewpoint, Montreal, Canada) to achieve the basal swimming activity (Bihanic et al., 2015) and monitored every 2 min for a 20 minutes cycle (10 min in the dark followed by 10 min in light). This cycle was repeated twice. The assay was performed between 1:00 pm and 4:00 pm, which is the optimal time interval for obtaining the stability of the basal activity (Chiffre et al., 2016). The duration of movements was measured at a velocity of ≥2 mm/sec. Data were analyzed by two-way ANOVA followed by a Bonferroni post-hoc test. Each value represents the mean ± SEM of 14-16 observations.

2.5 UHPLC/MS Analysis

This experiment was designed to confirm whether MH infiltrated into the embryonic tissues. It was performed on an Agilent 1290 Infinity liquid chromatograph coupled with an Agilent 6120 single quadrupole mass spectrometer. The chromatographic column was a Waters Acquity UPLC^{TM} BEH RP-C_{18} column (1.7µm, 2.1 x 150mm). The mobile phase consisted of A (water with 0.05% formic acid) and B (acetonitrile with 0.05% formic acid) at a flow rate of 0.3 mL/min. The gradient elution started with 50% A, and then it was linearly increased to 100% A in 6 min and held for 2 min. The column temperature was maintained at 30°C. A standard curve was prepared with MH in the range of 1.8 µM to 35.7 µM concentrations. Two wavelengths, 210 and 254 nm, were monitored for the DAD detector. MH was analyzed by ESI and APCI in both positive and negative modes. APCI positive mode was selected for the analysis because it produced a better ion signal for MH than other ionization modes. The drying gas flow was 10 L/min, and the nebulizer

pressure was 30 psi. The drying gas temperature and vaporizer temperature were set to 250ºC and 200ºC, respectively. The capillary voltage was 4000 V and the corona current was 4.0 µA. The MS was operated in both scan and selected ion monitoring (SIM) mode. $[M+H]^+$ 281 was selected to monitor the targeted compounds.

2.6 Statistics

Results were expressed as Mean ± SEM. Morphological data (0-6 dpf and 2-6 dpf exposure of MH at 0, 1, 2, 5, 10, 20 µM concentrations) (n=5 independent exposure, each exposure had 12 embryos) were analyzed by one way ANOVA followed by Tukey's post-hoc multiple comparison test. The LC_{50} was calculated by log transformed data using nonlinear regression (Curve-fit) (Graph pad Prism). Statistical analysis for all RT-qPCR data (0-6 dpf exposure of MH at 0, 10 µM concentrations) (n=4, 100 embryos/pool) was performed by non-parametric *t*-test followed by unpaired-t test. Data for locomotion study (0-6 dpf exposure of MH at 0, 5 µM concentrations) (14-16 observations) were analyzed by two-way ANOVA followed by Bonferroni post-hoc test. Statistical significance was defined as $p<0.05$.

CHAPTER 3: RESULTS

3.1 Effect of MH exposure throughout all of the embryonic development (0-6 dpf) on survival and function

This experiment was designed to observe whether MH exerted any effect if treated during embryogenesis (0-6 dpf). The morphological parameters, such as survivability, hatching efficiency, and cardiovascular parameters, such as heart beat, and blood circulation were evaluated.

3.1.1 Effect of MH on survivability of medaka embryos

Fertilized medaka eggs (n=5 independent exposure, each exposure had 12 embryos) of Iwamatsu stage 10 were exposed to different concentrations of MH (0, 1, 2, 5, 10, 20 μM) for 6 days (0-6 dpf). The effect of MH was evaluated on the survivability of medaka embryos, and the LC_{50} was also calculated (Fig. 3.1). MH caused an increased trend in mortality from 7 dpf until 10 dpf with 10 μM exposure. It showed about 80% mortality in 10 dpf. The highest concentration of MH (20 μM) caused 75% mortality by 4 dpf and showed 100% cumulative mortality by 10 dpf. MH, 5 μM caused 20% mortality at 10 dpf (Fig. 3.1). However, lower concentrations (1, 2 μM) did not produce significant mortality (Fig. 3.1). The calculated LC_{50} was observed to be 5.3 ± 0.1 μM (Fig. 3.1).

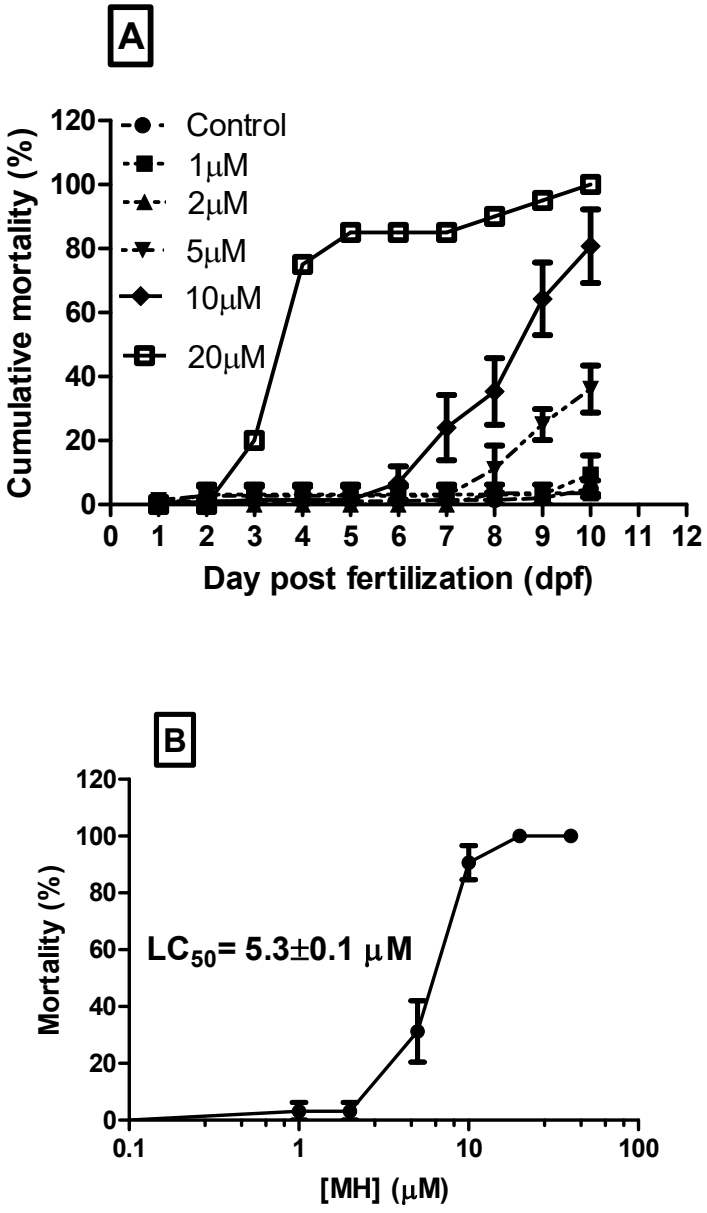

Figure 3.1: Cumulative mortality of medaka embryos. Embryos were exposed to 1, 2, 5, 10, and 20 μM of MH for 0-6 dpf. The effect on cumulative mortality (**Panel A**) was assessed until 10 dpf. Each value represents mean ± SEM. (n=5 independent exposure, each exposure had 12 embryos). The LC_{50} **(Panel B)** was calculated by log transformed data using nonlinear regression (Curve-fit) (Graph pad Prism).

3.1.2 Impact of MH on hatching efficiency of medaka embryos

Hatching efficiency was significantly decreased with 0-6 dpf 10 µM MH exposure compared to the control group at 10 dpf (Fig 3.2). Other treatment groups (1, 2, 5 µM) did not show any significant change in hatching efficiency (Fig 3.2).

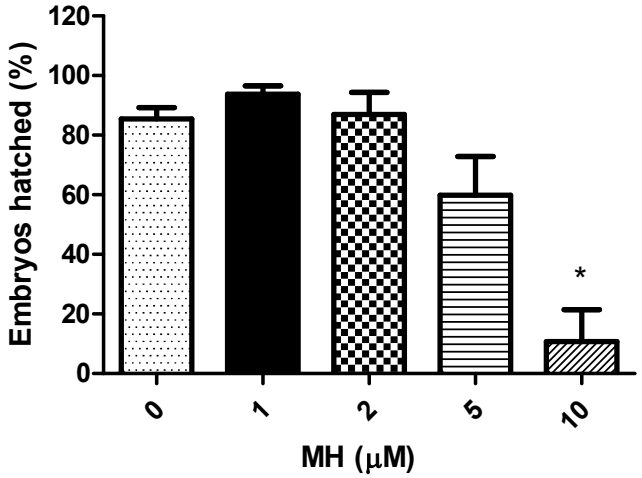

Figure 3.2: Hatching efficiency of medaka embryos. MH (10 µM) significantly prevented hatching efficiency compared to the control until 10 dpf. Each value represents the mean ± SEM (n=5 independent exposure, each exposure had 12 embryos). Statistical analysis was performed by one-way ANOVA followed by Tukey's post-hoc multiple comparison test. $p<0.05$ was considered as significant. The asterisk (*) represent the values are significantly different from control.

3.1.3 Effect of MH on homeostasis

MH also affected blood circulation in a concentration-dependent manner. In the highest concentration (10 µM), MH stopped circulation and thrombi formation was a consequence (Fig 3.3). Representative images are shown in Fig 3.4.

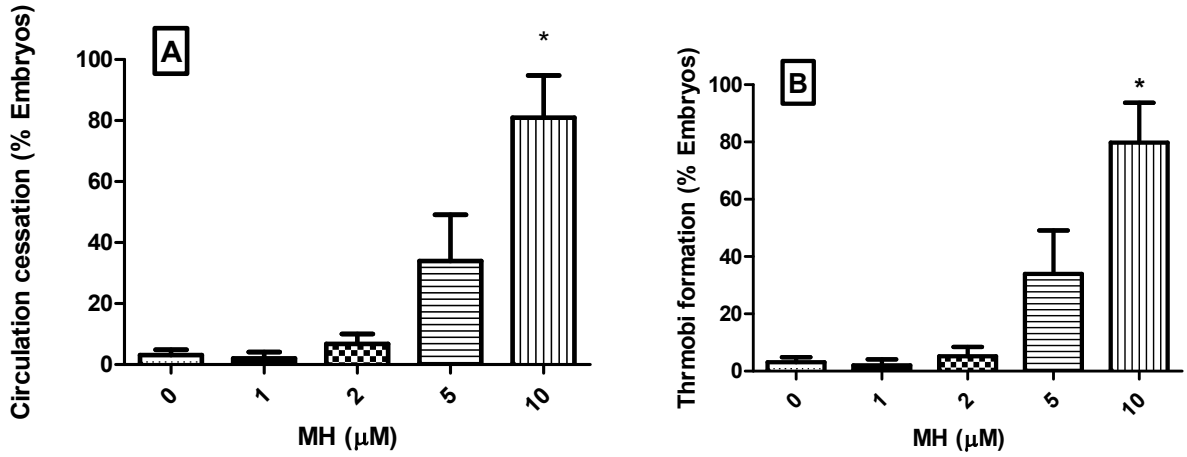

Figure 3.3: Blood circulation cessation and thrombus formation in medaka embryos. MH (10 µM) significantly ceased blood circulation (**Panel A**) and caused induction of thrombi formation (**Panel B**) until 10 dpf. Bars represent mean ± SEM (n=5 independent exposure, each exposure had 12 embryos). Analysis was performed by one-way ANOVA followed by Tukey's post-hoc multiple comparison test. $p<0.05$ was considered as significant. The asterisk (*) represents the value is significantly different from control.

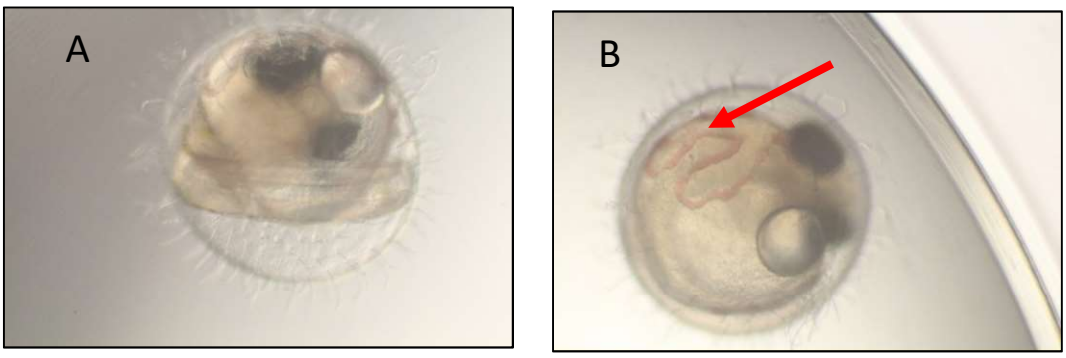

Figure 3.4: Representative thrombus generation by MH. The photographs were taken under the light microscope attached to a Cannon DC 7.4 V camera. Panel **A** represents the control group, and panel **B** represents thrombus formation (red arrow) in 10 µM treatment groups

3.1.4 Impact of MH on heart beat

Embryos were exposed to 2, 5, and 10 μM of MH for 0-6 dpf, and heartbeats were counted for 1 minute at 3 dpf and 6 dpf (Table 3.1). MH exposure was not able to cause any change in heart beat by 3 dpf. However, 10 μM MH treatment decreased the heart beat significantly at 6 dpf compared to the 6 dpf control group. The other treatment groups did not show any significant change in heartbeat (Table 3.1).

Table 3.1: Effect of MH on heartbeat of medaka embryos on both 3 dpf and 6 dpf

Treatment groups (μM)	Heartbeat/min 3 dpf (Mean ± SEM)	6 dpf (Mean ± SEM)
0	105±2	117±1
2	103±3	115±2
5	106±2	115±1
10	103±2	107±2*

Each value represents the mean ± SEM (n=3 independent exposure, each exposure had 12 embryos). The asterisk (*) represents value is significant versus the corresponding control group ($p<0.05$). Data analysis was performed by one-way ANOVA followed by Tukey's post-hoc multiple comparison test.

3.2 Effect of MH exposure on embryos following circulation (2-6 dpf) on survival and function

This study was designed to observe whether MH caused any effect on medaka embryos when they were treated after the onset of blood circulation. The same parameters were also evaluated here as the previous experiments.

3.2.1 Impact of MH on survivability of medaka embryos

When embryos were treated following onset of circulation (2-6 dpf), 10 µM MH caused 35% mortality at 9 dpf and about 50% mortality in 10 dpf (Fig 3.5). Treatment with higher concentrations (20 µM) caused 58% mortality at 8 dpf, and 100% by 10 dpf. The LC_{50} was calculated to be 9.9 ± 0.2 µM (Fig 3.5).

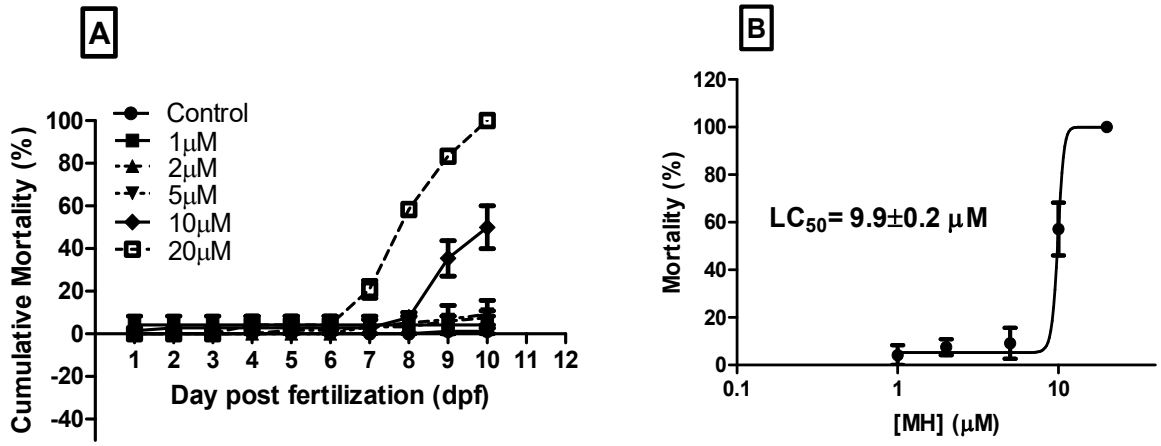

Figure 3.5: Cumulative mortality of medaka embryos. Embryos were exposed to 1, 2, 5, 10, and 20 µM of MH for 2-6 dpf. The effect on cumulative mortality (**Panel A**) was assessed until 10 dpf. Each value represents the mean ± SEM (n=5 independent exposure, each exposure had 12 embryos). The LC_{50} **(Panel B)** was calculated by log transformed data using nonlinear regression (Curve-fit) (Graph pad Prism).

3.2.2 Impact of MH on hatching efficiency of medaka embryos

Hatching efficiency was significantly decreased with 10 µM MH exposure for 4 days (2-6 dpf) compared to the control group until 10 dpf (Fig 3.6). Other treatment groups (2, 5 µM) did not show any significant change in hatching efficiency.

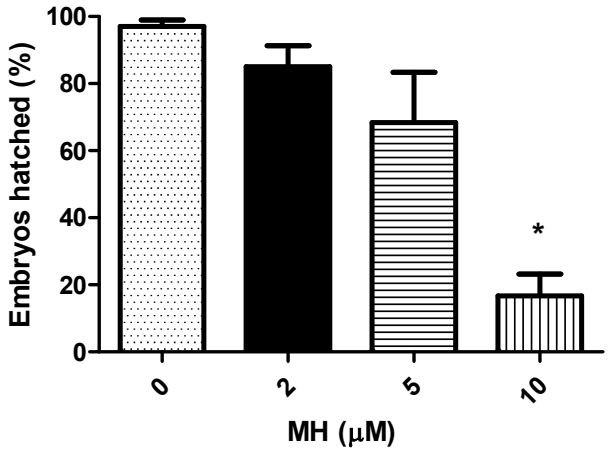

Figure 3.6: Hatching efficiency of medaka embryos. MH (10 µM) significantly prevented hatching efficiency compared to control at 10 dpf. Statistical analysis was performed by one-way ANOVA followed by Tukey's post-hoc multiple comparison test. $p<0.05$ was considered significant. The asterisk (*) represents that the values are significantly different from the control group. Bars represent mean ± SEM (n=5 independent exposure, each exposure had 12 embryos).

3.2.3 Effect of MH on homeostasis

Due to treatment with 10 µM MH for 4 days (2-6 dpf), blood circulation ceased and thrombus was generated significantly compared to the control group (Fig 3.7). The other groups (2, 5 µM) did not cause any significant change in terms of blood circulation and thrombus formation. Representative images are shown in Fig 3.8.

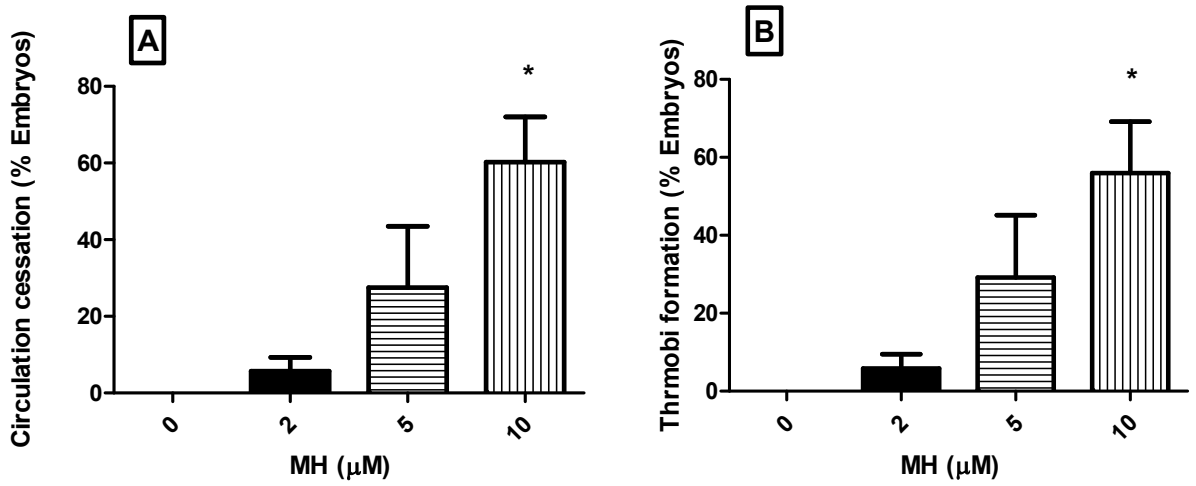

Figure 3.7: Blood circulation cessation and thrombus formation in medaka embryos. MH (10 μM) significantly ceased blood circulation (**Panel A**), and caused induction of thrombi formation (**Panel B**) until 10 dpf. Analysis was performed by one-way ANOVA followed by Tukey's post-hoc multiple comparison test. $p<0.05$ was considered significant. The asterisk (*) represents the value is significantly different from control. Bars indicates mean ± SEM (n=5 independent exposure, each exposure had 12 embryos).

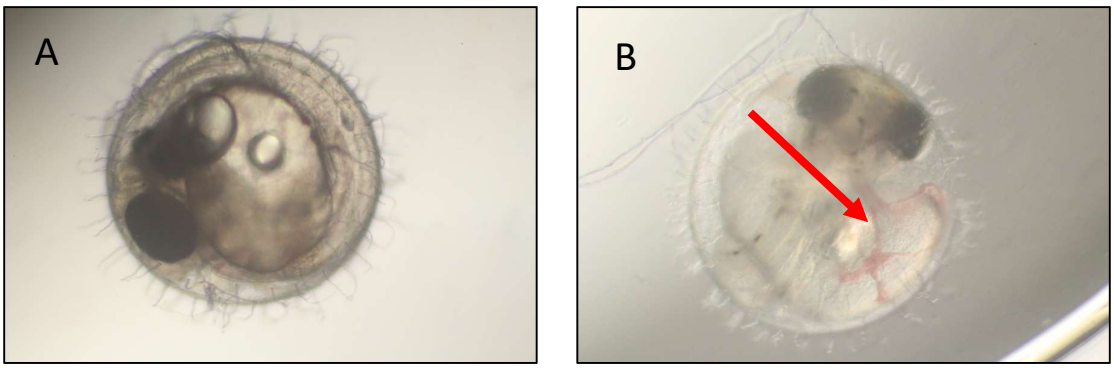

Figure 3.8: Representative thrombus formation induced by MH. Fertilized eggs were exposed to 1, 2, 5, and 10 μM of MH for 4 days (2-6 dpf), and the photographs were taken under the light microscope attached to a Cannon DC 7.4 V camera. Panel **A** represents the control group, and panel **B** represents thrombus formation (red arrow) in 10 μM treatment groups.

3.2.4 Impact of MH on heart beat

Embryos were exposed to 2, 5, and 10 μM of MH for 2-6 dpf, and heartbeats were counted for 1 minute during 3 dpf and 6 dpf (Table 3.2). MH exposure did not cause any change in heart beat in 3 dpf compared to the control group. However, 10 μM MH treatment decreased the heart beat significantly in 6 dpf compared to control group. The other treatment groups did not show any significant change in heartbeat (Table 3.2).

Table 3.2: Effect of MH on heartbeat of medaka embryos on both 3 dpf and 6 dpf

Treatment groups (μM)	Heartbeat/min 3 dpf (Mean ± SEM)	6 dpf (Mean ± SEM)
0	116±6	131±3
2	117±6	134±6
5	114±5	125±5
10	112±5	120±3*

Each value represents mean ± SEM (n=3 independent exposure, each exposure had 12 embryos). Data analysis was performed by one-way ANOVA followed by Tukey's post-hoc multiple comparison test. The asterisk (*) represents value is significant compared to the control group ($p<0.05$).

3.3 Effect of MH on major components of blood coagulation pathway

This experiment was designed to evaluate the expression of major components in the blood coagulation pathway to explore MH-induced blood vessel occlusion during medaka embryogenesis. Following exposure of MH throughout the whole embryonic period (0-6 dpf), the embryos were screened for gene expression of major components in the blood coagulation pathway (FVII, FX, FXI). Each experiment consisted of 100 embryos and experiments were repeated for 4 times. Embryos were treated for 6 days (0-6 dpf) with 0 or 10 μM of MH. Total RNA was extracted from both groups at 6 dpf, and reverse transcribed to cDNA and used for RT-qPCR analysis utilizing FX, FXI, and FVII gene-specific primers. Gene expression of FX (1.8 fold), and FXI (1.6 fold) was increased significantly due to 10 μM treatment with MH compared to the control group (Fig. 3.9). FVII is a major component of the extrinsic blood coagulation pathway. FVII was differentially up-regulated (1.5 fold) for 10 μM treatment with MH compared to the control group (Fig. 3.9).

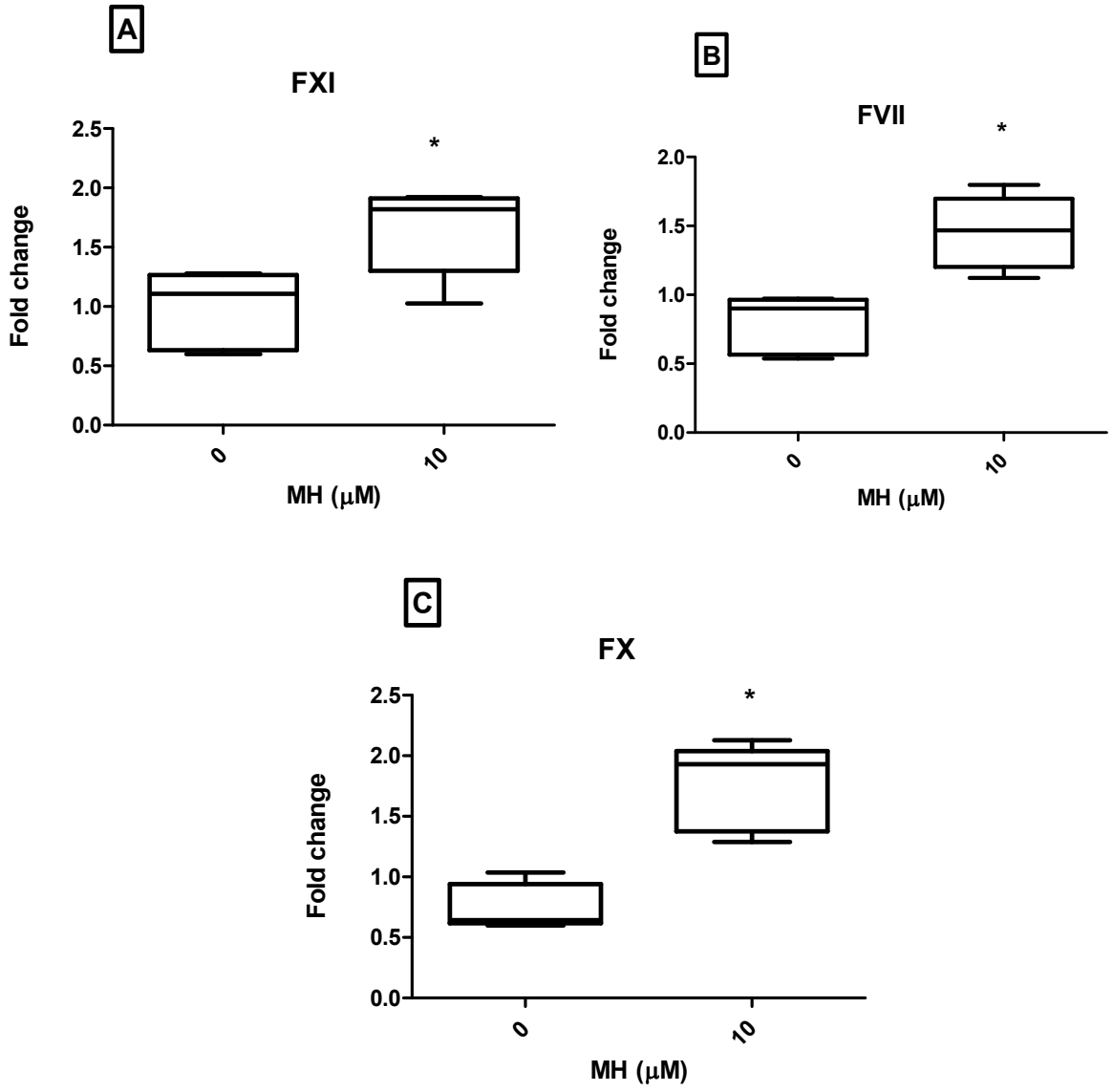

Figure 3.9: Gene expression of FXI, FVII, and FX. Differential expression by RT-qPCR normalized to elf-1α following exposure to 0 and 10 μM of MH for 0-6 dpf. The groups were analyzed using the $2^{-\Delta\Delta CT}$ method and analyzed by non-parametric *t*-test followed by unpaired-t test (n=4, 100 embryos/pool). The asterisk (*) represents that the value is significant versus the control group ($p<0.05$).

3.4 Impact of MH on the fibrinolytic system:

This study was designed to evaluate the effect of MH on the fibrinolytic system. The effect of the compound was characterized on the inhibitor of the pathway, PAI-1 that inhibits the conversion of plasminogen to plasmin and the activators (tPA, uPA), which catalyzes the conversion into plasmin. MH increased the expression of PAI-1 (1.6 fold), and uPA (1.8 fold) significantly, however it did not change the expression of tPA (Fig. 3.10). The ratio of fold differences between tPA and PAI-1 is 0.6 (Table 3.3).

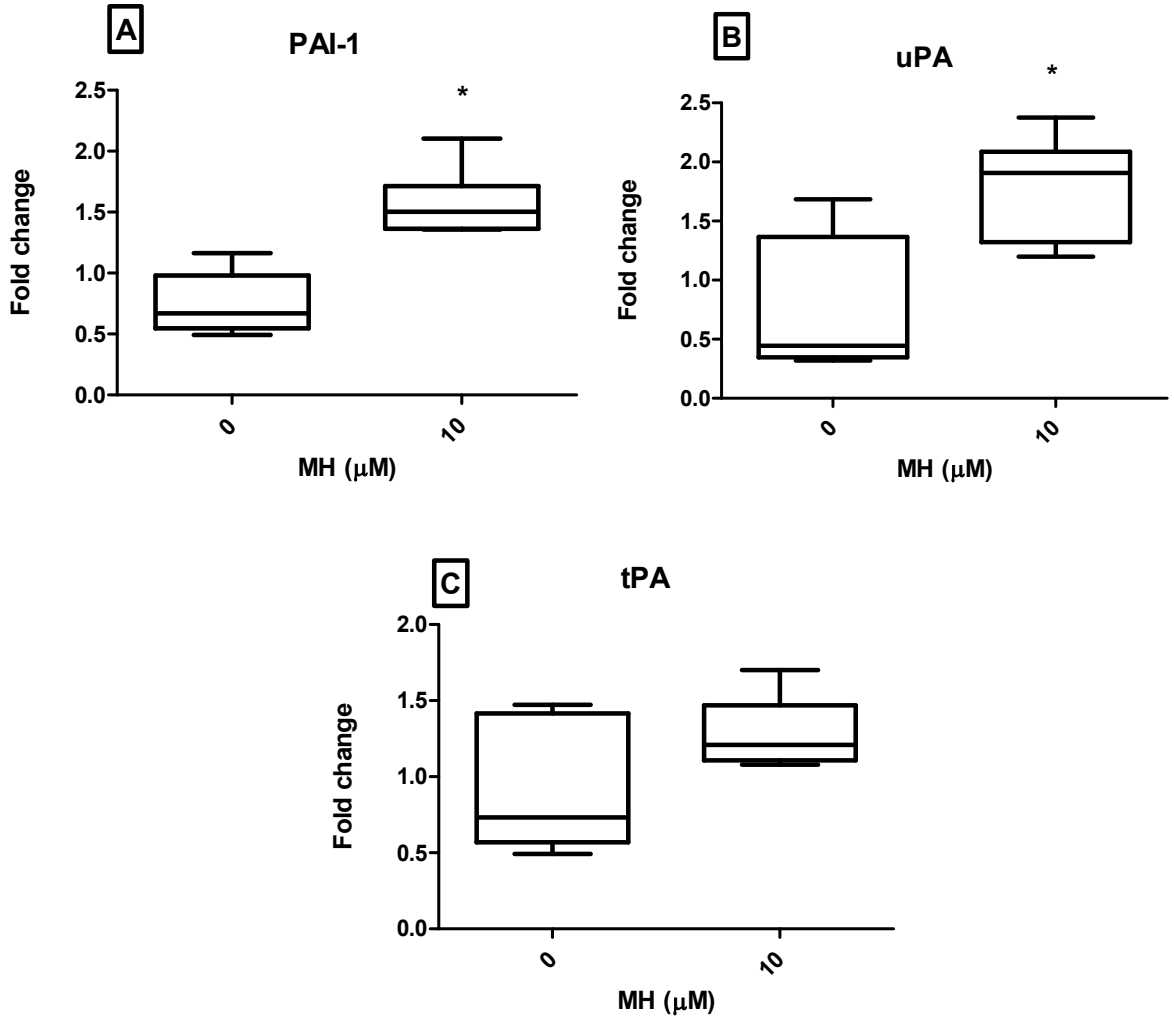

Figure 3.10: Gene expression of PAI-1, uPA, and tPA. Following MH exposure embryos were used for RT-qPCR analysis utilizing PAI-1 gene-specific primer. Each value represents mean ± SEM (n=4 pools, 100 embryos/pool). Data analysis was performed by non-parametric *t*-test followed by unpaired-t test. The asterisk (*) represents value is significant versus the control group ($p<0.05$).

Table 3.3: Ratio between the fold differences of the activators and inhibitor of the fibrinolytic system

Activator/Inhibitor	Ratio of fold differences
uPA/PAI-1	1.2
tPA/PAI-1	0.6

3.5 Impact of MH on anti-oxidant enzymes

The expression of the anti-oxidant enzymes, Catalase (CAT), Glutathione peroxidase 2 (GPX 2), Glutathione *S*-transferase A (GST A), and Super-oxide dismutase 2 (SOD 2) were evaluated in the MH (10 µM) treated embryos to evaluate the effect of the compound on oxidative stress. MH increased the expression of CAT (1.8 fold), GPX 2 (1.9 fold), GST A (1.8 fold) (Fig. 3.11). Transcription factors of the forkhead box, class O1 (FoxO1) promote cellular antioxidant defense, thus act as a regulator of the cellular stress (Klotz et al., 2015). MH increases the expression of FoxO1 (1.9 fold) (Fig. 3.12).

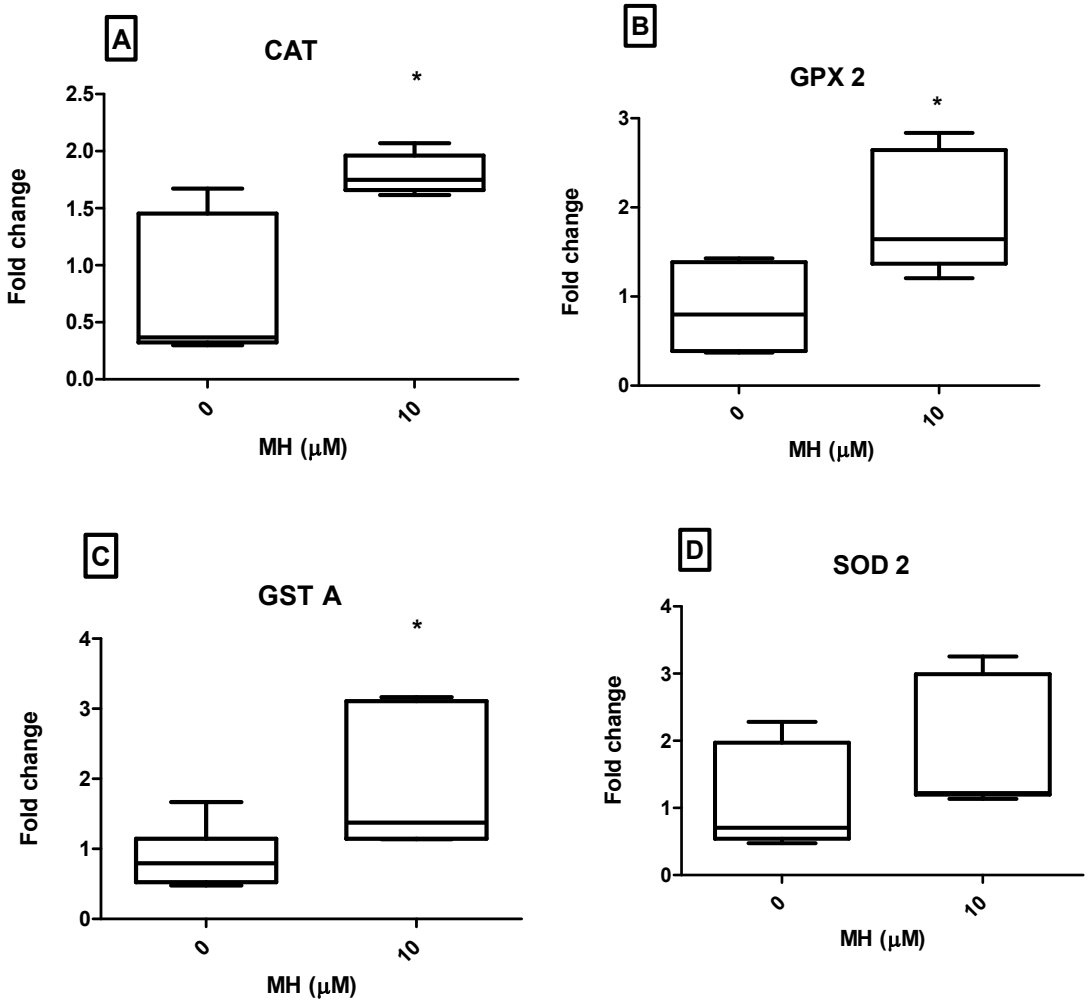

Figure 3.11: Gene expression of anti-oxidant enzymes (CAT, GPX 2, GST A, and SOD 2). Each value represents mean ± SEM (n= 4 pools, 100 embryos/pool). The groups were normalized to elf-1α and analyzed using the $2^{-\Delta\Delta CT}$ method. Data analysis was performed by non-parametric *t*-test followed by unpaired-t test. The asterisk (*) represents value is significant against the control group ($p<0.05$).

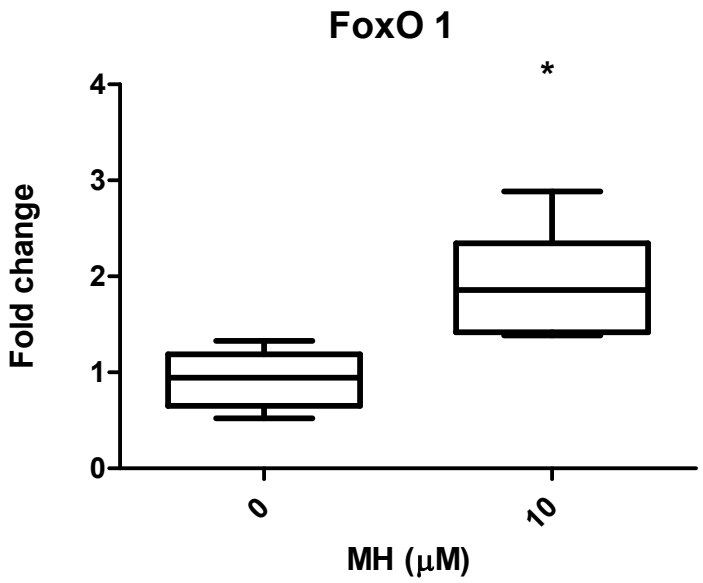

Figure 3.12: Gene expression of FoxO1. Each value represents mean ± SEM (n=4, 100 embryos/pool). The groups were normalized to elf-1α and analyzed using the $2^{-\Delta\Delta CT}$ method. Data analysis was performed by non-parametric *t*-test followed by unpaired-t test. The asterisk (*) represents value is significant compared to the control group ($p<0.05$).

3.6 Effect of MH on blood vessels

The goal of this study was to observe the effect of MH on the major receptors in the blood vessels to explain vasoconstriction, such as endothelin B (ET_B), Angiotensin 2 receptor associated protein (ATRAP). ET_B is produced in response to elevated production of ET_1. ATRAP interacts with angiotensin 2 type 1 receptor (AT_1R). MH increased expression of ET_B (1.4 fold), although did not cause any change in ATRAP expression (Fig. 3.13).

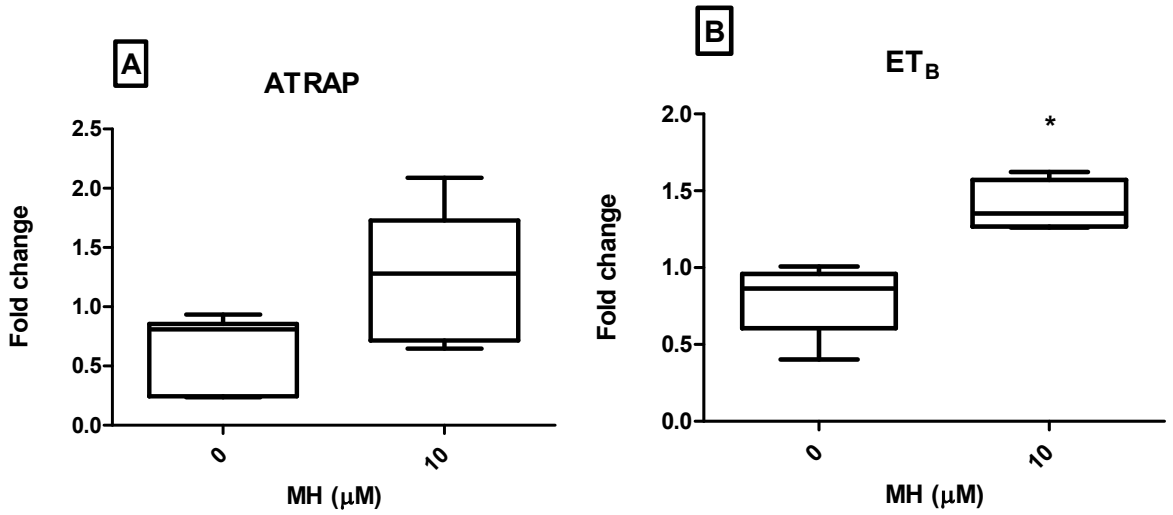

Figure 3.13: Gene expression of ATRAP and ET_B. Each value represents mean ± SEM (n=4, 100 embryos/pool). The groups were normalized to elf-1α and analyzed using the $2^{-\Delta\Delta CT}$ method. Data analysis was performed by non-parametric *t*-test followed by unpaired-t test. The asterisk (*) represents value is significant compared to the control group ($p<0.05$).

3.7 Impact of MH on cardiac development

The goal of this study was to evaluate the effect of MH on neuregulin-2 (NRG-2) and erythroblastic leukemia viral oncogene homolog (ErbB) 3 receptor tyrosine kinase to clarify the compound's role in cardiac development. ErbB3 signaling is critical for normal heart development (Britto et al., 2004). We also evaluated gene expression of NRG-2 that is also expressed in the endothelial lining of the atrium during development (Carraway et al., 1997) and NRG-2 knockout mice manifests severe growth retardation and mortality (Britto et al., 2004). MH decreased the expression of NRG-2 (0.5 fold) and ErbB3 (0.5 fold) compared to the control group (Fig. 3.14).

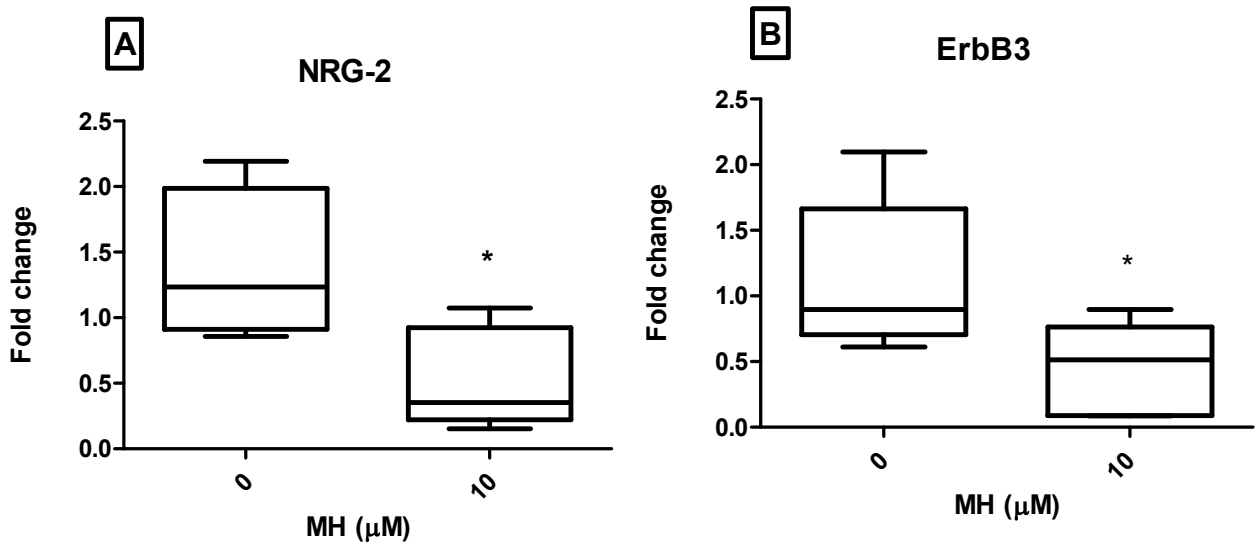

Figure 3.14: Gene expression of NRG-2, ErbB3. Each value represents mean ± SEM (n= 4 pools, 100 embryos in each pool). Data analysis was performed by non-parametric *t*-test followed by unpaired-t test. The asterisk (*) represents value is significant versus control group ($p<0.05$). The groups were normalized to elf-1α and analyzed using the $2^{-\Delta\Delta CT}$ method.

3.8 Effect of MH on cardiovascular markers

Two major cardiovascular markers, such as cardiac troponin T (cTnT), Brain natriuretic peptide A (BNP A) representative of myocardial injury were evaluated to confirm MH-induced cardiovascular abnormality. MH increased the expression of cTnT and BNP A by 2.4, and 2.5 fold, respectively (Fig 3.15).

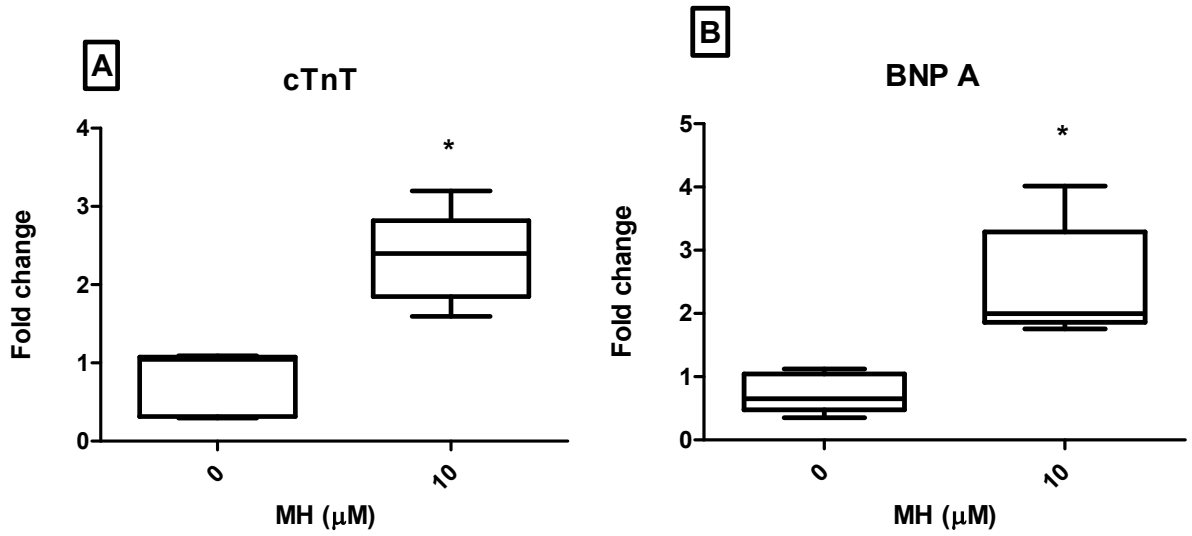

Figure 3.15: Gene expression of cTnT, and BNP A. Each value represents mean ± SEM (n= 4, 100 embryos/pool). Data analysis was done by non-parametric *t*-test followed by unpaired-t test. The asterisk (*) represents value is significant versus the control group ($p<0.05$). The groups were normalized to elf-1α and analyzed using the $2^{-\Delta\Delta CT}$ method.

3.9 Effect of MH on the major components of the Wnt/β-catenin signaling pathway

This study was performed to observe whether MH could affect the major components of the Wnt/β-catenin pathway inducing any cardiovascular abnormality. The differential expression of major upstream and downstream components of the Wnt/β-signaling pathway were evaluated following an exposure of 10 μM MH for 0-6 dpf. MH upregulated the expression of Wnt1 (2.1 fold), Fzd 2 (1.6 fold), LRP 5 (1.6 fold), Dvl (1.7 fold), β-catenin (1.9 fold), DKK1 (2 fold) (Fig. 3.16). The expression of GSK-3β was not increased due to exposure of 10 μM MH (Fig. 3.16).

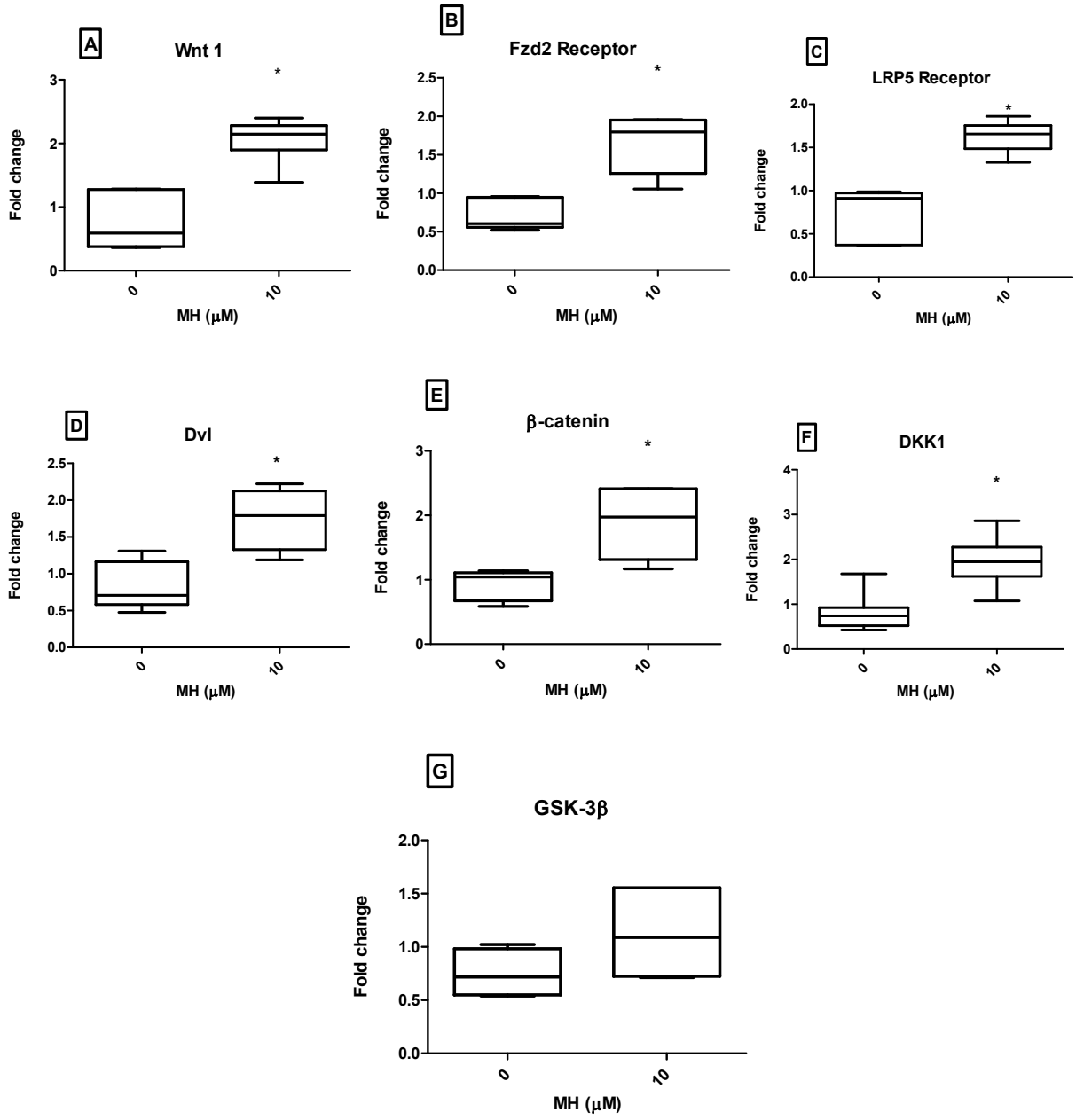

Figure 3.16: Gene expression of major components of the Wnt/β-catenin pathway. Differential expression of Wnt 1, Fzd 2, LRP5, Dvl, β-catenin, DKK1, and GSK-3β following to MH exposure via RT-qPCR. The groups were normalized to elf-1α and analyzed using the $2^{-\Delta\Delta CT}$ method. Data analysis was performed by non-parametric *t*-test followed by unpaired-t test. The asterisk (*) represents value is significant compared to the control group ($P<0.05$). Each bar represents mean ± SEM (N= 4 pools, 100 embryos/pool).

3.10 Effect of MH on inflammatory mediators

This study was designed to assess the effect of MH on the expression of the major pro-inflammatory mediators. MH treatment (10 μM) upregulated the expression of IL-1β (2.5 fold), TNF-α (1.9 fold) compared to the untreated group (Fig. 3.17).

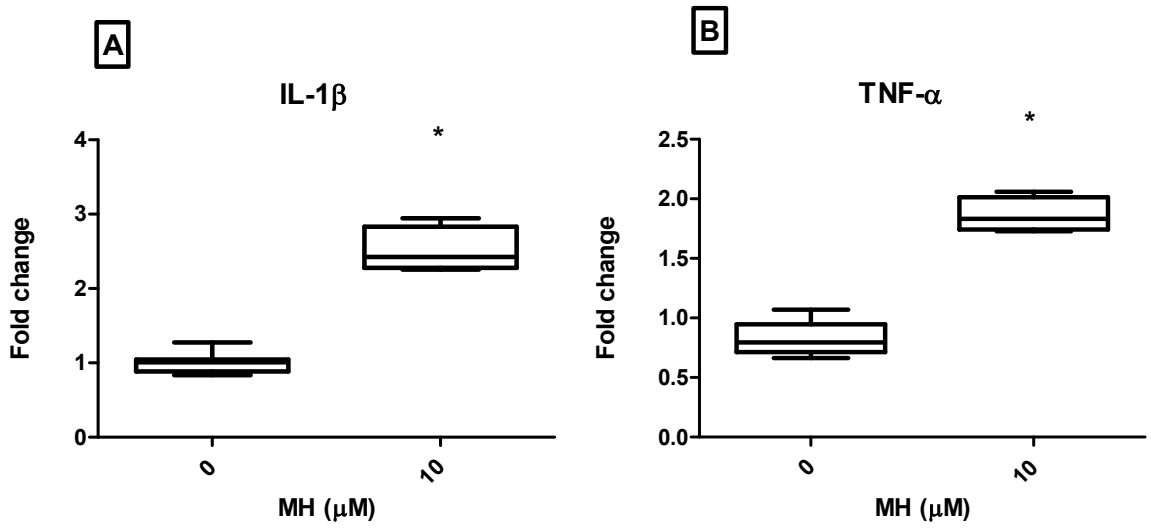

Figure 3.17: Gene expression of inflammatory mediators (IL-1β and TNF-α). The groups were normalized to elf-1α and analyzed using the $2^{-\Delta\Delta CT}$ method. Data analysis was performed by non-parametric *t*-test followed by unpaired-t test. The asterisk (*) represents value is significant versus the control group ($p<0.05$). Each value represents mean ± SEM (n=4 pools, 100 embryos/pool).

3.11 Effect of MH on the cardiovascular system

MH (10 µM) appeared to have effect on the blood flow and heart for 0-6 dpf exposure (Fig 3.18). Although the figures are in anterior and posterior position for control and treatment group, respectively (Fig. 3.18), increased expression of the markers (cTnT, BNP A) for cardiovascular abnormality (Fig. 3.15) showed the possibility of myocardial injury.

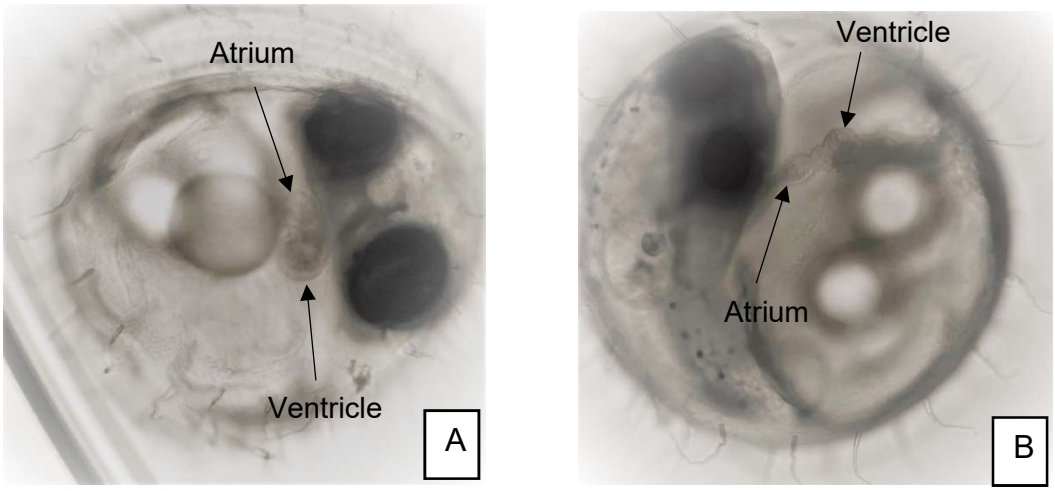

Figure 3.18: Effect of MH on the cardiovascular system. Panel **A** and **B** represents the control and MH (10 µM) treated group, respectively. The photographs were taken by Eclipse Ti2 inverted microscope system (Nikon Instruments Inc., Melville, NY).

3.12 Effect of MH on locomotion of medaka larvae:

The aim of this study was to assess the effect of MH on movement of medaka larvae. Locomotion was evaluated in both dark and light conditions. The embryos were exposed to different concentrations (0, 5 µM) of MH during the whole embryonic period (0-6 dpf) and assessed for locomotion at 2 dph. The concentration was chosen to be 5 µM, because it was a sub lethal concentration. The swimming behavior of Japanese medaka is phototactic in nature which shows activation of swimming in light and inhibition in dark (Dasmahapatra et al., 2017). Our control group shows similar pattern of locomotion activity in accordance with Dasmahapatra et al. (2017). However, exposure of 5 µM MH exhibits an overall decreased duration of movement (velocity ≥2 mm/sec), however the change was not significant with the control group (Fig. 3.20).

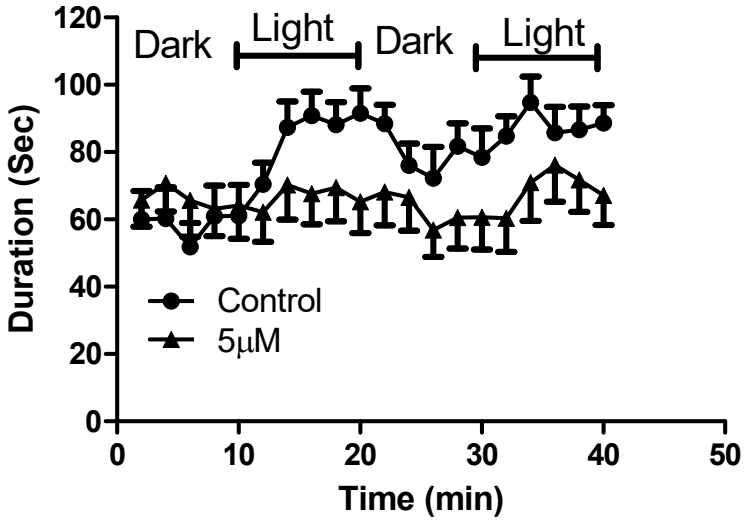

Figure 3.19: Effect of MH on the locomotion (velocity ≥2mm/sec) of medaka larvae. Medaka larvae (2 dph) were monitored for 40 min (0-10min dark, 10-20 min light, 20-30 min dark, 30-40 min light) using a ViewPoint Zebrabox. Duration of movements were measured at 2 min intervals at a velocity of ≥2 mm/sec. Data were analyzed by two-way ANOVA followed by Bonferroni post-hoc test. Each value represents mean ± SEM of 14-16 observations.

CHAPTER 4: DISCUSSION

MH is a major bioactive constituent of *Magnolia grandiflora* seeds or *Magnolia officinalis* bark. The Magnolia genus has been widely reported to have various beneficial effects on the cardiovascular system, including anti-atherosclerosis, vascular relaxation, and antiplatelet effects (Zhao et al., 2016). MH has been proven to be successful against high-fat diet-induced cardiac pathogenic changes in mice (Zhang et al., 2015). However, the effect of this compound on the cardiovascular system during embryogenesis has not been characterized yet.

This is the first study that shows the teratogenic potential of MH in a fish developmental model. Previous studies showed toxic effects of different Magnolia genus on in vitro, in vivo, and human subjects. Administration of 1 mg/ml *Magnolia officinalis* aqueous extract caused DNA damage in human intestinal epithelial cells (FHs 74 Int) (Nachtergael et al., 2015). Another study showed that 10 μM magnolol and honokiol were able to cause DNA damage in HK-2, a human proximal tubule epithelial cells (Bunel et al., 2016). In the mice model, Magnolia bark extracts did not show any toxicity and mortality; however, they showed slight fatty degeneration and sporadic focal necrosis in the liver of 11 animals out of 40 with 240 mg/kg body weight administration (Liu et al., 2007). Another study using dietary supplements containing extracts of *M. officinalis* and *Phellodendron amurense* in human subjects demonstrated that 1 out of 22 persons reported side effects including thyroid dysfunction, heartburn, perilabial numbness, shaking hands, sexual dysfunction (Garrison and Chambliss, 2006). However, no explanations were provided whether those effects were related to the treatments. A few mixtures containing Magnolia are also reported

to be hepatotoxic by Teschke et al. (2014; 2015; 2016). However, no toxicological reports of MH have been published so far.

Therefore, we have designed this experiment to determine the teratogenic potential of MH on Japanese medaka and to elucidate the mechanisms that trigger this effect. Embryos were treated with different concentrations of MH (0, 1, 2, 5, 10, 20 μM) throughout the whole embryonic period (0-6 dpf) to observe whether MH induced any teratogenicity. Treatment with 10 μM MH during the whole embryonic period showed 80% cumulative mortality at 10 dpf (Fig. 3.1). Administration of 20 μM MH causes 100% cumulative mortality in the same period of time (Fig 3.1). The LC_{50} value for treatment during 0-6 dpf was 5.3 ± 0.1 μM (Fig. 3.1). The effect of MH on hatching efficiency was also evaluated in our study, which showed significant decrease with 10 μM MH treatment (Fig 3.2), although we had not evaluated the mechanisms for this effect. Previous studies reported that delayed development and fitness in the zebrafish embryos might cause alterations in the hatching period due to decreased contractile movement (Alharty et al., 2015; Danzmann et al., 1989; Pakkasmaa and Jones, 2002).

Another objective was to observe the effect of the compound on blood homeostasis. The compound stopped blood circulation in 80% of embryos at 10 μM treatment compared to the control group (Fig 3.3, 3.4). In medaka embryos, the heart first appears in stage 22, the tubular heart forms in 23, and it becomes fully functional in stage 24 (1 day 20 hours) and starts beating. Blood circulation starts in stage 25 (2 days 2 hours). Embryos start hatching from 7 dpf. The heartbeat was counted at 3 dpf and 6 dpf. The heartbeat decreased significantly with 10 μM exposure in 6 dpf compared to the 6 dpf control group (Table 3.1). Our study of MH exposure throughout the whole embryonic period (0-6 dpf) suggested that it produced teratogenic potential in Japanese medaka in a concentration-dependent manner.

According to our observation, MH showed adverse effect on the cardiovascular system by slowing down the heartbeat, impeding blood circulation, and inducing thrombus. Therefore, we intended to see the effect of MH in case it is administered during the post circulation stage (2-6 dpf). Due to post circulation exposure with 10 μM MH, about 50% mortality was induced in 10 dpf (Fig 3.5). Higher concentration of MH (20 μM) caused 100% abnormality in medaka embryos (Fig 3.5). The LC_{50} was higher in this case (9.9±0.2 μM) compared to the 0-6 dpf exposure (Fig 3.5). The higher value of LC_{50} denotes less toxicity, which means it takes more of the compound to kill half of the test chemicals. Therefore, LC_{50} value is a good indicator of toxicity of a compound. However, treatment with 10 μM MH for 2-6 dpf also showed significant decrease in hatching efficiency (Fig. 3.6). Moreover, the same concentration stopped blood circulation in a significant number of embryos and induced blood vessel occlusion as a result (Fig. 3.7, 3.8). Furthermore heart beat was decreased significantly in 6 dpf due to treatment with 10 μM MH for 2-6 dpf (Table 3.2). Our data indicated that MH demonstrated teratogenic potential on Japanese medaka in a concentration-dependent manner regardless of the treatment period. Therefore, 10 μM MH exposure throughout the whole embryonic period (0-6 dpf) or post circulation period (2-6 dpf) produced teratogenicity in medaka embryos. Although MH has diverse therapeutic effects, described previously, the potential teratogenic effects may limit its application during pregnancy.

We intended to identify the mechanism for MH induced thrombus formation at the molecular level. Our goal was to observe if MH can induce gene expression of major components of the extrinsic, intrinsic, and common blood coagulation pathways to produce the resultant thrombus. Our data suggested that MH (10 μM) upregulated gene expression of FXI, FVII, and FX (Fig. 3.9), which suggested that thrombus might be produced in medaka embryos due to activation of major components of the blood coagulation pathway.

Moreover, we were interested to evaluate the effect of MH on the fibrinolytic system, which acts as a regulatory mechanism in order to dissolve clots. Our data suggested that MH was able to upregulate the expression of PAI-1 (Fig. 3.10) that might inhibit the conversion of plasminogen into plasmin. PAI-1 prevents the actions of u-PA and t-PA from conversion of plasminogen to plasmin (Dellas and Loskutoff, 2005). However, the expression of uPA was upregulated in our study (Fig. 3.10). uPA is an important component of the inflammatory response, which mediates leukocyte extravasation into the inflamed tissue and tPA regulates dissolution of fibrin in the circulation (Bondu et al., 2018). Inflammatory mediators, such as TNF-α, IL-1β are involved with upregulation of uPA (Kirchheimer and Remold, 1989). Therefore, MH mediated increased expression of inflammatory mediators might upregulate the expression of uPA. The ratio of fold differences between uPA and PAI-1 was calculated to be 1.2, and the ratio between tPA and PAI-1 was 0.6 (Table 3.3), which suggest that MH might exhibit prothrombotic property.

We studied MH-mediated thrombus formation from another angles by looking at the expression of the anti-oxidant enzymes and major receptors of the endothelial cells. First, we evaluated the effect of the compound on the expression of major anti-oxidant enzymes. SOD acts as a major defense system against superoxide in the vascular cells that catalyzes the dismutation of superoxide anion to molecular oxygen and hydrogen peroxide (H_2O_2) (Wassmann et al., 2004). SOD works as the first line of defense against ROS (Alscher et al., 2002). CAT is an intracellular enzyme, which is effective against high levels of oxidative stress. It is located in the cellular peroxisomes as well as in the cytosol. It catalyzes H_2O_2 to form water and molecular oxygen. It is useful when the glutathione content is limited or when the GPX activity is decreased. The GPX or GSH system is effective against low-level of oxidative stress. It is a selenium-containing antioxidant enzyme that catalyzes the conversion of H_2O_2 into water and lipid peroxides into lipid alcohols. H_2O_2 is elevated in the left ventricle after myocardial injury (Pendergrass et al., 2011). A previous study showed that H_2O_2 upregulated the mRNA transcripts of the antioxidant enzymes

such as CAT and GPX in the cardiac progenitor cells (CPC), which may protect the cells from injury and also maintain the migratory ability of CPC to provide therapeutic regenerative benefits in the damaged areas (Pendergrass et al., 2011). Another study showed that H_2O_2 addition causes increase in mRNA levels of CAT, GPX, and SOD (Mates et al., 1999). Our data confirmed that MH upregulated the mRNA transcripts of CAT, GPX 2 (Fig 3.11) suggested that it might be due to increased oxidative stress by MH-induced myocardial injury. However, the compound did not change the expression of SOD 2 (Fig 3.11). GST comprises up to 10% of cytosolic protein in some mammalian organ (Boyer, 1989; Mukanganyama et al. 2011) and catalyzes the conjugation of GSH into xenobiotic substrate for detoxification. GST A was reported in medaka fish genome database and increased in postnatal life with the advancement of age (DeKoven et al., 1992; Wu et al., 2011). GST is upregulated in response to oxidative stress (Nebert and Vasiliou, 2004). Our study demonstrated that MH increased the expression of GST A gene (Fig. 3.11). This upregulation of GST A might result from MH-induced oxidative stress. The stimulation of the major anti-oxidant enzymes might be regulated through the induction of FoxO1 that is an important regulator of the cellular stress response and promote the cellular antioxidant system (Klotz et al., 2015). Our experiment showed that MH increased the gene expression of FoxO1, which might be induced due to the increased oxidative stress produced by the compound (Fig. 3.12).

We also explored whether MH had any effect on the blood vessels to produce thrombus. Endothelin (ET) consists of three isoforms, ET_1, ET_2, and ET_3 (Yanagisawa et al., 1988; Inoue et al., 1989). ETs interact with two heptahelical G-Protein coupled receptors, ET_A and ET_B (Arai et al., 1990; Sakurai et al., 1990). All of the three isoforms interact with ET_B with similar affinity (Davenport, 2002; Davenport et al., 2006). Both of the receptors are present in the heart (Russell and Molenaar, 2000); however, ET_B predominates in the kidney (Maguire and Davenport, 2015). In chronic heart failure (CHF) patients, increased levels of ET_1 were observed due to increased production and decreased clearance of ET_1 (Parker and Thiessen, 2004). In CHF, either ET_A or

ET_B receptors, and both receptors in other cases, were elevated (Sakai et al., 1996; Tonnessen et al., 1998; Miyauchi et al., 1995; Kobayashi et al., 1999). Vascular endothelin production has been reported to be high in atherosclerosis (Schneider et al., 2007). Increased ET_B receptors mediated vasoconstriction was observed in patients with atherosclerosis in a previous study (Pernow et al., 2000). Increased expression of ET_B receptors in the intima and media was also observed in human atherosclerotic lesions (Iwasa et al., 1999). The increased expression of ET_B receptors may result in response to elevated production of ET_1 in order to clear the peptide (Schneider et al., 2007). Our experiments exhibited that MH was able to increase the gene expression of the ET_B receptor (Fig. 3.13), which suggested that the compound might exert vasoconstriction by ET_1-mediated ET_B receptor activation.

ATRAP gene product binds to the AT_1 receptor (AT_1R). ATRAP is a 18-kDa protein which was first identified in 1999 (Daviet et al., 1999), it is co-localized with AT_1R in intracellular compartments of mice and yeast, and triggers internalization and reduced signal of AT_1R (Daviet et al., 1999; Lopez-Ilasaca et al., 2003). It is also expressed in migrating hypoblast, vasculature, and in multiple embryonic epithelia in zebrafish model (Tucker et al., 2007). It is produced by many organs, including the heart, kidneys, adrenal glands and testis. Angiotensin 2 acts through ATRAP. It was noted in previous study that ATRAP knockout mice showed elevation in blood and plasma volume through vasoconstriction and by increasing sodium and water retention in the kidneys (Giani et al., 2013). Our data demonstrated that MH did not change the expression of the ATRAP (Fig. 3.13), which indicated that the compound did not have any effect on the blood vessels through AT_1R.

We intended to characterize some markers associated with impaired cardiac structure (NRG-2, ErbB3) and function (BNP A, Troponin T). First of all, the effect of MH was evaluated on two major components of the NRG/ErbB pathway, including NRG-2 and ErbB3. Zebrafish has two NRG genes, such as NRG-1, NRG-2 (Honjo et al., 2008). Both of the isoforms play important role

in cardiac development (Rasouli and Stainier, 2017; Rupert and Coulombe, 2015). Both NRG-1 and 2 are identified in the embryonic endocardium, however only NRG-1 isoform continue to be expressed in the adult heart (Carraway et al., 1997; Meyer et al., 1997; Cote et al., 2005; Zhao et al., 1998; Yamada et al., 2000). Receptors for the cardiac specific NRGs are ErbB2, ErbB3, and ErbB4 (Yarden and Sliwkowski, 2001). The NRG/ErbB interaction can activate several downstream targets, including Erk1/2, PI3K/Akt, and JAK/STAT signaling cascades (Baliga et al., 1999; Liu and Kern, 2002). Although, we did not investigate in details about the signaling cascades, we analyzed the effect of MH on two major components (NRG-2, ErbB3) to explain cardiac and developmental abnormalities. NRG-2 is required for cardiac trabeculation in zebrafish (Rasouli and Stainier, 2017). Our data demonstrated MH downregulated the expression of NRG-2 (Fig. 3.14), which might cause impairment in the cardiac structure. We also showed the effect of MH on the expression of ErbB3 receptor, which is expressed in the mesenchymal cells of the endocardial cushions of fetal heart and involved with the formation of the heart valves (Erickson et al., 1997). ErbB3 knockout mice have been reported to induce defects in the endocardial cushions and embryonic lethality (Odiete et al., 2012). Our data exhibited that MH decreased the expression of the ErbB3 receptor (Fig. 3.14), suggesting the compound might disrupt cardiac structure in medaka embryos.

We also aimed to assess the level of major markers (cTnT, BNP A) to confirm cardiovascular abnormality mediated by MH. Our study demonstrated that MH upregulated the gene expression of BNP A and cTnT that are good indicators for myocardial injury (Fig 3.15). Yousif et al. (2017) mentioned that the increased levels of circulating cardiac troponin I (Tn-I) is an indication of damaged heart muscle/ cardiovascular dysfunction in mice. Natriuretic peptide genes have been identified as markers for cardiomyocyte hypertrophy and heart failure in Zebrafish heart (Becker et al., 2012). BNP is a good example of the natriuretic peptide that has been used as a marker for cardiovascular abnormality. BNP was first detected in porcine brain

and consists of 32 amino acid. It is a polypeptide cardiac neurohormone secreted from the membrane granules of the cardiac ventricle, mostly from the left ventricle, in response to ventricular volume expansion and pressure overload (Dorothea et al., 2003). Elevated BNP is associated with diverse cardiovascular abnormalities, including acute and chronic heart failure, arrhythmias, cardiac ischemia, pulmonary disorder, and chronic renal diseases (Raizada et al., 2007).

Troponin complex consists of Troponin C (cTnC- 18 KD), Troponin I (cTnI-26 KD) and Troponin T (cTnT-39 KD), located on the thin filaments of striated muscle contractile apparatus (Frey et al., 1998). Troponin T is a myofibril protein expressed only in myocardial cells. Although 2.8-4.1% cTnI and 6-8% cTnT are cytosolic, the troponins are predominantly bound to the myofibrils (Wu and Feng, 1998). The presence of cTn in the serum is an indicator of myocardium damage (Solnica, 2004). Troponin appears in blood 2-4 hours after insult, reaches the peak in about 12 hours, and stays elevated for 7-10 days (Braunwald et al., 2001; Solnica, 2004; Tarkowska and Furmaga-Jabłońska, 2012). It is widely used in diagnostic purposes for adults as a marker for myocardial injury; however, its application in neonates has not been fully described yet (Tarkowska and Furmaga-Jabłońska, 2012). An elevated serum level of troponin is indicative of acute coronary syndrome and non-acute coronary syndrome, including chronic and acute heart failure, arrhythmias, and myocarditis (Agzew, 2009). Tarkowska and Furmaga-Jabłońska (2012) have stated the role of cTnT as a potential biomarker of congenital heart defects. Thus, increased level of cTnT can be an indication of significant heart defects in newborns. Moreover, elevated cTnT can be used as a marker for potential myocardial damage induced by persistent ductus arteriosus (PDA) (El-Khuffash, 2008). Our study demonstrated that MH increased the expression of cTnT significantly (Fig. 3.15), suggesting that the compound might cause myocardial injury.

The characterized markers showed the potential of impaired cardiac structure and function in the MH treated medaka embryos. Therefore, we intended to shed some light on the Wnt/β-

catenin pathway to elucidate MH-mediated cardiovascular abnormality. Over activation of the Wnt/β-catenin pathway at transcriptional level is involved with disruption in cardiac jogging and looping affecting left-right asymmetry of the heart in zebrafish (Lin and Xu, 2009). Overexpression of Wnt1 gene has been reported to be involved with cardiovascular injuries in medaka (Barjhoux et al., 2016). The Wnt pathway is activated during development in response to developmental cues in order to control cell differentiation and proliferation (Gomez-orte et al., 2013). The Wnt/β-catenin pathway is involved with the regulation of more than 50 mammalian genes (George, 2008). The potential of the canonical signaling of this pathway to upregulate the expression of several genes in monocytes has raised the possibility that it may also be involved with inflammation (Thiele et al., 2001). It is possible that expression of Wnts from macrophage and dendritic cells has diverse impacts on the behavior of the resident cells (such as, endothelial cells and vascular smooth muscle cells), including apoptosis (Lobov et al., 2005; Masckauchan et al., 2006), migration (Cheng et al., 2007), proliferation (Masckauchan et al., 2006; Wang et., 2002; Wang et al., 2004; Cheng et al., 2007), and invasion (Pukrop et al., 2006) through activation of canonical and non-canonical signaling (George, 2008). Activation of the Wnt/β-catenin pathway may be involved with upregulation of gene expression of inflammatory mediators, such as TNF-α, IL-1β, IL-6 (Aumiller et al., 2013; Yousif et al., 2017). In several in vivo and in vitro studies, these proinflammatory mediators have been induced in mRNA and protein levels (Aumiller et al., 2013). Further studies are needed to confirm if the inflammatory mediators represent direct targets of TCF/LEF-induced gene regulation (Aumiller et al., 2013). Previous studies showed that IL-1β acted as a potent inducer of canonical (Ma et al., 2012) as well as noncanonical (Ryu et al., 2006; Ge et al., 2009) Wnt ligands. This is why IL-1β is known as an upstream regulator of Wnt/β-catenin pathway in chondrocytes. Our study showed that MH was able to upregulate gene expression of the ligand, Wnt1 of Wnt/β-catenin signaling pathway (Fig. 3.16). The compound also increased the expression of the Fzd2 receptor and co-receptor LRP5 (Fig. 3.16). Thus MH may increase the interaction between the Wnt ligand (Wnt1) with the Fzd receptor, leading to the

formation of a cell surface complex with LRP5 by increasing their expression. This resultant complex along with recruitment of the scaffolding protein Dvl causes phosphorylation of LRP5 and activation and recruitment of Axin complex to the receptors (Macdonald et al., 2009). Our study also demonstrated that MH increased the expression of Dvl (Fig 3.16) that is an important scaffold protein**,** acts between the Fzd receptor and the destruction complex (Wang et al., 2015). Activation of the Wnt pathway triggers phosphorylation of Dvl and suppresses the downstream destruction complex, although the mechanisms need further investigation (Clevers, 2006; Wang et al., 2015). Dvl can also promote the β-catenin/TCF transcriptional complex formation, which is pivotal for Wnt/ β-catenin complex (Barry et al., 2013; Gan et al., 2008; Habas and Dawid, 2005; Torres and Nelson, 2000). Moreover, Wnt activation mediates nuclear translocation of Dvl that acts along with its cytoplasmic functions to activate the Wnt/ β-catenin signaling pathway. Increased expression of the major components of Wnt/β-catenin pathway by MH caused inhibition of Axin-induced phosphorylation and stabilization of β-catenin (Fig. 3.16) that translocated to the nucleus, and formed a complex with TCF/LEF and might activate Wnt responsive gene expression, such as TNF-α, IL-1β.

A previous study showed that honokiol and magnolol exert anti-inflammatory effects by blocking inflammatory cytokines/enzymes production, nuclear factor (NF-κB) activation, and leukocyte activation (Fried and Arbiser, 2009). However, our data suggested that MH upregulated gene expression of inflammatory cytokines, including TNF-α, IL-1β (Fig 3.17). This increased level of inflammatory mediators might be expressed through the activation of the Wnt/β-catenin signaling pathway. These inflammatory cytokines may further activate the Wnt/β-catenin pathway by inducing Wnt 1, producing a self-perpetuating effect. Expression of inflammatory mediators (TNF-α, IL-1β, IL-6) are increased following myocardial injury and sepsis (Al-Amran et al., 2011; Wang et al., 2016). Previous studies have demonstrated the correlation between inflammatory mediators and myocardial dysfunction (Yousif et al., 2011; Bravo et al., 2012; Yousif et al, 2017).

Moreover, intravenous administration of TNF-α or IL-1β in animal models caused pro-inflammatory cytokine-mediated adverse effects leading to mortality, which was ameliorated by antibodies via antagonizing their effects (Rispens et al., 2012; Yousif, 2014; Danielson et al., 2016). Our study also indicated that MH-mediated excessive production of inflammatory mediators might be involved with myocardial injury.

In previous findings, increased expression of DKK-1 of the Wnt/β-catenin pathway was observed in clinical and experimental in vivo studies and in vitro studies on endothelial cells (Ueland et al., 2009). In an ex vivo experiment, a high level of DKK-1 was produced in coronary artery disease, reflecting increased release of DKK-1 in coagulation (Ueland et al., 2009). DKK-1 induced activation of the NF-kB inflammatory pathway in the platelet-activated endothelial cell may contribute to the inflammatory interaction between platelet and endothelium (Ueland et al., 2009). Expression of DKK-1 can be induced by inflammatory cytokines, such as TNF-α, which occur within the atherosclerotic plaque (Diarra et al., 2007). DKK-1 derives from endothelium and platelet cells, increase inflammatory interaction between those cells, showing a self-propagating mechanism in the inflammatory microenvironment. Our study also demonstrated that MH increased gene expression of DKK1 (Fig. 3.16). According to our data, the inflammatory response might also be influenced by upregulation of DKK-1. The upregulation of DKK1 might result in order to slow down the Wnt/β-catenin signaling pathway by interfering the binding of the Wnt1 ligand to its receptor. However, further elucidations are needed to explain the overexpression of DKK1.

There are two isoforms of Glycogen synthase kinase 3 (GSK3) available in zebrafish, GSK3-α and GSK3-β, which are encoded by different genes (Lee et al., 2007; Woodgett, 1990). Both of the isoforms have role during zebrafish cardiogenesis (Lee et al., 2007). GSK3-α is required for cardiomyocyte survival and GSK3-β is important for left-right asymmetry and positioning of the heart (Lee et al., 2007). Deletion of the gene that encodes for GSK3-β is

embryonically lethal, and GSK3-α is unable to rescue GSK3-β-null mice (Hoeflich, 2000). GSK3 is also an important regulator of the Wnt/β-catenin pathway. The β-catenin destruction complex is composed of GSK3, axin, APC, and CK1α protein complex. GSK3 and CK1 are responsible for phosphorylating axin and APC besides phosphorylating β-catenin, enhancing association of axin and APC with β-catenin and increasing its phosphorylation and degradation (Huang and He, 2008; Kimelman and Xu, 2006). Inhibition of GSK3 activity leads to the stabilization and activation of the β-catenin and TCF-dependent gene transcription (Klein and Melton, 1996; Stambolic et al., 1996; Jope, 2003; Wu and Pan, 2009). Our data exhibited that GSK3-β expression was not changed due to MH exposure during embryogenesis (Fig 3.16), which suggested that the compound did not cause GSK-3β-mediated phosphorylation and degradation of β-catenin.

Control of cell cycle in cardiomyocytes is disrupted by diverse molecular events, including gene overexpression or silence, gene amplification, or gene mutation, which can be regulated by the Wnt/β-catenin pathway that plays a role in pathological changes in case of myocardial injury and atherosclerotic plaque (Macdonald and He, 2012). Some of the inhibitors of this pathway have been considered potential therapeutic targets of myocardial cell injury, and some are under development (Kikuchi and Yamamoto, 2007). A recent study demonstrated that Wnt/β-catenin expression was upregulated and stably expressed in myocardial injury (Yousif et al., 2017). Our study also suggested that MH-induced myocardial injury might be caused by activation of the Wnt/β-catenin pathway (Fig. 3.16) that was confirmed by the marker (Fig. 3.14, Fig 3.15) for myocardial injury.

Yousif et al. (2017) has shown that inflammatory mediators, including TNF-α, IL-1β, IL-6, were upregulated in cardiac tissue as well as in plasma of mice models for sepsis that was related with worse left ventricle (LV) function through hemodynamic measurements (heart rate and ejection fraction). Their results indicated that increased level of myocardial depressant

proinflammatory mediators in the heart reduced cardiac contractility and induced myocardial injury (Yousif et al., 2017). Our experiment also revealed that MH was able to decrease heart rate significantly (Table 3.1) when administered with 10 μM concentration for 0-6 dpf. Therefore, MH induced upregulation of pro-inflammatory mediators (Fig. 3.17) probably mediated through the Wnt/β-catenin pathway (Fig. 3.16) might cause myocardial injury (Fig. 3.18) and embryonic lethality that was characterized by decreased level of ErbB3, NRG-2 (Fig. 3.14), and increased level of cTnT, BNP A (Fig 3.15), and decrease in heartbeat (Table 3.1).

Another objective of this project was to observe whether MH had any effect on the locomotion phenotypes. As noted from our morphological data that MH prevented embryos from hatching when they were treated with 10 μM concentration, so the embryos treated with sublethal concentration of MH, 5 μM was used for the locomotion study. The swimming behavior of medaka is considered as phototactic due to its activation of swimming during the light phase and inhibition during the dark phase (Chiffre et al., 2016; Le Bihanic et al., 2015). In this study, we have observed the effect of MH on locomotion of 2 dph larvae following a 0-6 dpf developmental exposure with 5 μM concentration. Our data demonstrated that the medaka larvae did not show any change in locomotion during the first dark cycle, probably due to the acclimatization of 20 minutes in a dark environment. The treatment group (5 μM) showed an overall decline in the duration of swimming activity irrespective of the light-dark cycle after the first dark cycle, although the change was not significant compared to the control group (Fig. 3.18).

In this project, the teratogenic concentration of MH was characterized in medaka embryos. However, the human exposure dose needs to be determined. The following formula is used to determine the human equivalent dose (HED): HED (mg/kg) = Animal dose (mg/kg) X (Animal K_m/ Human K_m) (Nair and Jacob, 2016; Shin et al., 2010). The K_m is the correction factor, calculated

by dividing the average body weight (kg) of species to its body surface area (m^2) (Nair and Jacob, 2016; Shin et al., 2010).

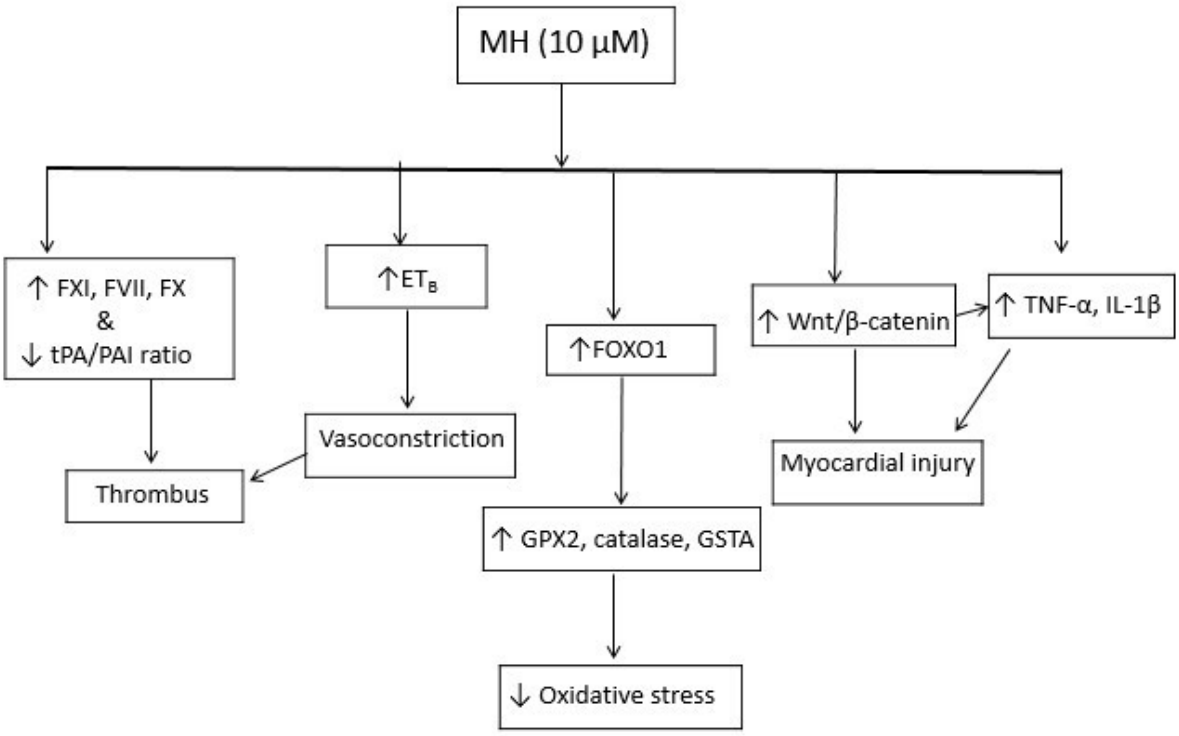

Figure 4.1: Schematic representation of the outcomes of MH (10 µM) on medaka embryos

CHAPTER 5: CONCLUSION AND FUTURE PLAN

Magnolia constituents have been used in traditional Chinese and Japanese medicine for years. MH, one of the major constituents of Magnolia, has gained lots of attention recently because of its diverse therapeutic potential. Although the biological activities for MH are well established, the toxicological studies have not yet been elucidated. So, the toxicities of MH and their associated mechanism of actions should be illustrated before they get into the clinical trials and approved as dietary supplements.

Our study was designed to evaluate the potential toxic effects of MH on medaka embryogenesis to assess its risk during pregnancy. We concluded that MH could be deleterious for the fetus in a concentration- and time-dependent manner. We characterized the mechanisms for MH toxicity by analyzing different pathways at the molecular level. Moreover, we successfully identified several markers, which can be used to evaluate cardiotoxicity in medaka.

However, there are some limitations of this study. The effect of MH on the medaka embryos were evaluated until 10 dpf. The effect had not been characterized in the later stages (30 dpf) due to some technical issues. Moreover, we could not measure the level of reactive oxygen species due to lack of a standard positive and negative control in medaka embryos.

There was a significant difference in heart beat in the control groups between the 0-6 dpf (Table 3.1) and 2-6 dpf exposure (Table 3.2) at 3 dpf and 6 dpf. These differences may be due to variations in the experimental conditions or DMSO exposure throughout the whole embryonic period for 0-6 dpf compared to the 2-6 dpf exposed embryos. Moreover, it was only visual

observations. Therefore, further experiments are needed with cutting-edge microscopic techniques to confirm the differences in heartbeat.

It is important to explore the effect of adverse events throughout life (Silveira et al., 2007). This is a relatively new division of scientific knowledge, termed as the developmental origins of health and disease (DOHaD). Future work should be performed to identify the adverse effects of MH on adult fish. Moreover, the effect of the compound should be assessed on the next generation to observe any potential cardiovascular abnormality.

Although we characterized the toxic potential of MH, we did not investigate the effect of the parent compound, honokiol. Therefore, it will be interesting to observe the effect of honokiol in medaka embryos.

To confirm the role of MH for inducing cardiovascular abnormality in medaka embryos through Wnt/β-catenin pathway, Wnt 1 knockout from the embryo heart will be produced. Then the embryos will be exposed to MH throughout the whole embryonic period and the effects will be evaluated in morphological and molecular level.

BIBLIOGRAPHY

1. Achneck HE, Sileshi B, Parikh A, Milano CA, Welsby IJ, Lawson JH, authors. Pathophysiology of bleeding and clotting in the cardiac surgery patient: from vascular endothelium to circulatory assist device surface. Circulation. 2010; 122: 2068–2077.

2. Agzew Y. Elevated serum cardiac troponin in non-acute coronary syndrome. *Clinical Cardiology*. 2009; 32:15–20.

3. Ahn VE, Chu MLH, Choi HJ, Tran D, Abo A, Weis WI. 2011. Structural basis of Wnt signaling inhibition by Dickkopf binding to LRP5/6. Dev Cell. 21: 862–873.

4. Al-Amran FG, Yousif NG, Meng X, authors. A TLR4-MCP-1-macrophage IL-18 cascade plays a major role in myocardial injury and cardiac dysfunction after permanent ischemia. J Surg Res. 2011; 165:265–6

5. Alcott C., Brockus C., Sponseller B. Homeostasis. Compendium Equine: Continuing for Veterinarians. CompendiumEquine.com. 2009

6. Alharty KM, Albaqami FF, Thornton C, Corrales J, Willett KL. Mechanistic Evaluation of Benzo[a]pyrene's Developmental Toxicities Mediated by Reduced Cyp19a1b Activity. Toxicological Sciences. 2017; 155: 135–147

7. Alscher RG, Erturk N, Heath LS. Role of superoxide dismutases (SODs) in controlling oxidative stress in plants. J Exp Bot. 2002; 53:1331-41.

8. Amblard, F., Govindarajan, B., Lefkove, B. Synthesis, cytotoxicity, and antiviral activities of new neolignans related to honokiol and magnolol. *Bioorg. Med. Chem. Lett*. 2007; 17:4428-4431

9. Arai H, Hori S, Aramori I, Ohkubo H, Nakanishi S. Cloning and expression of a cDNA encoding an endothelin receptor. Nature. 1990; 348:730-2.

10. Arora, S., Singh, S., Piazza, G.A.. Honokiol: a novel natural agent for cancer prevention and therapy. *Curr. Mol. Med*. 2012; 12:1244-1252.

11. Aumiller V, Balsara N, Wilhelm J, Gunther A, Konigshoff M. Wnt/β-catenin signaling IL-1β expression by Alveolar epithelial cells in pulmonary fibrosis. Am J Respir Cell Mol Biol. 2013; 49: 96-104

12. Axelrod, J.D. Progress and challenges in understanding planar cell polarity signaling. Semin. Cell Dev. Biol. 2009; 20: 964–971

13. Bai X, Cerimele F, Ushio-Fukai M, Waqas M, Campbell PM, Govindarajan B, Der CJ, Battle T, Frank DA, Ye K, Murad E, Dubiel W, Soff G, Arbiser JL. Honokiol, a Small Molecular Weight Natural Product, Inhibits Angiogenesis *in Vitro* and Tumor Growth *in Vivo.* The Journal of Biological Chemistry. 2003; 278: 35501-35507

14. Baliga RR, Pimental DR, Zhao YY, Simmons WW, Marchionni MA, Sawyer DB et al. NRG-1-induced cardiomyocyte hypertrophy. Role of PI-3-kinase, p70(S6K), and MEK-MAPK-RSK. Am J Physiol. 1999; 277:H2026–H2037.

15. Barjhoux I, Gonzalez P, Baudrimont M, Cachet J. Molecular and phenotypic responses of Japanese medaka (Oryzias latipes) early life stages to environmental concentrations of cadmium in sediment. Environ Sci Pollut Res. 2016; 23:17969–17981

16. Barry, E.R., Morikawa, T., Butler, B.L., Shrestha, K., de la Rosa, R., Yan, K.S., Fuchs, C.S., Magness, S.T., Smits, R., Ogino, S. Restriction of intestinal stem cell expansion and the regenerative response by YAP. Nature. 2013; 493: 106–110.

17. Becker JR, Robinson TY, Sachidanandan C, Kelly AE, Coy S, Peterson RT, Macrae CA. *In vivo* natriuretic peptide reporter assay identifies chemical modifiers of hypertrophic cardiomyopathy signaling. Cardiovasc Res. 2012; 93: 463–470.

18. Behrens, J., von Kries, J.P., Ku hl, M., Bruhn, L., Wedlich, D., Grosschedl, R., and Birchmeier, W. Functional interaction of beta-catenin with the transcription factor LEF-1. Nature. 1996; 382: 638–642.

19. Benito B, Gay-Jordi G, Serrano-Mollar A, Guasch E, Shi Y, Tardif JC, Brugada J, Nattel S, Mont L. Cardiac arrhythmogenic remodeling in a rat model of long-term intensive exercise training. Circulation. 2011; 123:13–22.

20. Ben-Ze'ev A, Shtutman M, Zhurinsky J. The integration of cell adhesion with gene expression: the role of beta-catenin. Exp Cell Res. 2000; 261:75–82.

21. Bhanot, P., Brink, M., Samos, C.H., Hsieh, J.C., Wang, Y., Macke, J.P., Andrew, D., Nathans, J., and Nusse, R. (1996). A new member of the frizzled family from Drosophila functions as a Wingless receptor. Nature. 1996; 382: 225–230.

22. Bihanic FL, Sommard V, Perrine DL, Pichon A, Grasset J, Berrada S, Budzinski H, Cousin X, Morin B, Cachot J. Environmental concentrations of benz[a]anthracene induce developmental defects and DNA damage and impair photomotor response in Japanese medaka larvae. Ecotoxicology and Environmental Safety. 2015; 113: 321–328

23. Bilic, J. et al. Wnt induces LRP6 signalosomes and promotes disheveled dependent LRP6 phosphorylation. Science. 2007;316: 1619–1622.

24. Blankesteijn WM, Essers-Janssen YP, Ulrich MM, Smits JF. Increased expression of a homologue of drosophila tissue polarity gene "*frizzled*" in left ventricular hypertrophy in the rat, as identified by subtractive hybridization. J Mol Cell Cardiol. 1996; 28:1187–1191.

25. Bom VJ, Bertina RM. The contributions of Ca2+, phospholipids and tissue-factor apoprotein to the activation of human blood-coagulation factor X by activated factor VII. *Biochem J* 1990; 265:327-336.

26. Bondu V, Bitting C, Poland VL, Hanson JA, Harkins MS, Lathrop S, Nolte KB, Lawrence DA, Buranda T. Upregulation of $P2Y_2R$, Active uPA, and PAI-1 Are Essential Components of Hantavirus Cardiopulmonary Syndrome. Front. Cell. Infect. Microbiol. 2018; 8: 169

27. Bourhis E, Tam C, Franke Y, Bazan JF, Ernst J, Hwang J, Costa M, Cochran AG, Hannoush RN. Reconstitution of a frizzled8.Wnt3a.LRP6 signaling complex reveals multiple Wnt and Dkk1 binding sites on LRP6. J Biol Chem. 2010; 285:9172–9179.

28. Boyer TD. The glutathione S-transferase: an update. Hepatology. 1989; 9: 486-96

29. Braunwald E, Fauci AS, Kasper DL. *Harrison's Principles of Internal Medicine*. 15th edition. New York, NY, USA: McGraw-Hill; 2001.

30. Bravo AA, Kumm K, Lamy C, Jeanneau J, Cuello G, Lefer J, authors. H2 therapy protects myocardial cell injury induce by sepsis via attenuated expression the level of HMGB1. Pathophysiol Cell Inj J. 2012;1:10–19

31. Britto JM, Lukehurst S, Weller R, Fraser C, Qiu Y, Hertzog P, Busfield SJ. Generation and Characterization of Neuregulin-2-Deficient Mice. Molecular and cellular biology. 2004; 24:8221-8226

32. Bryant JW, Shariat-Madar Z. Human plasma kallikrein-kinin system: Physiological and biochemical parameters. Cardiovasc Hematol Agents Med Chem. 2009; 7:234-250

33. Bunel, V., Antoine, M.H., Stévigny, C., *et al*., 2016. New in vitro insights on a cell death pathway induced by magnolol and honokiol in aristolochic acid tubulotoxicity. Food Chem. Toxicol. 2016; 87:77-87.

34. Carraway KL, Weber JL, Unger MJ, Ledesma J, Yu N, Gassmann M, Lai C. Neuregulin-2, a new ligand of ErbB3/ErbB4-receptor tyrosine kinases. Nature. 1997; 387: 512-516

35. Carl M, Loosli F, Wittbrodt J. Six3 inactivation reveals its essential role for the formation and patterning of the vertebrate eye. Development. 2002; 129:4057–4063.

36. Cassilas E, Smith LS. 1977. Effect of stress on blood coagulation and haematology in rainbow trout (*Salmo gairdneri*). *Journal of Fish Biology*. 1977; 10: 481-491.

37. Cattelino, A., Liebner, S., Gallini, R., Zanetti, A., Balconi, G., Corsi, A., Bianco, P., Wolburg, H., Moore, R., Oreda, B. The conditional inactivation of the beta-catenin gene in endothelial cells causes a defective vascular pattern and increased vascular fragility. J. Cell Biol. 2003; 162: 1111-1122.

38. Chappin JC, Hajjar KA. Fibrinolysis and the control of blood coagulation. Blood Rev. 2015; 29: 17-24

39. Cheng C-w, Yeh J-c, Fan T-P, Smith SK, Charnock-Jones DS. Wnt5amediated non-canonical Wnt signalling regulates human endothelial cell proliferation and migration. *Biochem Biophys Res Comm*. 2007; 365: 285–290.

40. Chen, Y. H., Lin, S. J., Chen, Y. L., Liu, P. L., & Chen, J. W. Anti-inflammatory effects of different drugs/agents with antioxidant property on endothelial expression of adhesion molecules. Cardiovasc Hematol Disord Drug Targets. 2006; 6: 279−304.

41. Chiffre, A., Clerandeau, C., Dwoinikoff, C., Le Bihanic, F., Budzinski, H., Geret, F., Cachot, J. Psychotrophic drugs in mixture alters swimming behavior of Japanese medaka (Oryzias latipes) larvae above environmental concentrations. Environ. Sci. Pollut. Res. 2016; 23: 4964-4977.

42. Chuang DY, Chan MH, Zong Y, Sheng W, He Y, Jiang JH, Simonyi A, Gu Z, Fritsche KL, Cui J, Lee JC, Folk WR, Lubahn DB, Sun AY, Sun GY. Magnolia polyphenols attenuate oxidative and inflammatory responses in neurons and microglial cells. Journal of Neuroinflammation. 2013; 10:15

43. Clevers H. Wnt/beta-catenin signaling in development and disease. Cell. 2006; 127:469–480.

44. Clevers H, Nusse R. Wnt/b-Catenin Signaling and Disease. Cell. 2012. 149: 1192-1205

45. Cliffe A, Hamada F, Bienz M. A role of Dishevelled in relocating Axin to the plasma membrane during wingless signaling. Curr Biol. 2003; 13:960–966.

46. Cochrane CG, Griffin JH. The biochemistry and pathophysiology of the contact system of plasma. Adv Immunol. 1982; 33: 241–59.

47. Cohen ED, Wang Z, Lepore JJ, Lu MM, Taketo MM, Epstein DJ, Morrisey EE. Wnt/beta-catenin signaling promotes expansion of Isl-1-positive cardiac progenitor cells through regulation of FGF signaling. J Clin Invest. 2007; 117:1794–1804.

48. Colman RW, Schmaier AH. Contact system: a vascular biology modulator with anticoagulant, profibrinolytic, antiadhesive, and proinflammatory attributes. Blood. 1997; 90: 3819–43.

49. Colavitti R, Pani G, Bedogni B, Anzevino R, Borrello S, Waltenbeger J, Galeotti T. (2002) J. Biol. Chem. 2002; 277: 3101-3108

50. Coolman M, de Groot CJ, Steegers EA, Geurts-Moespot A, Thomas CM, Steegers-Theunissen RP. Concentrations of plasminogen activators and their inhibitors in blood

preconceptionally, during and after pregnancy. Eur J Obstet Gynecol Reprod Biol. 2006; 128:22–29.

51. Cote GM, Miller TA, LeBrasseur NK, Kuramochi Y, Sawyer DB. Neuregulin-1a and b isoform expression in cardiac microvascular endothelial cells and function in cardiac myocytes in vitro. Exp Cell Res. 2005; 311:135–146.

52. Cottrell BA, Doolittle RF. Amino acid sequence of lamprey fibrinopeptides A and B and characterisation of the junctions split by lamprey and mammalian thrombins. Biochimica et Biophysica Acta. 1976; *453*:426-438.

53. Danielson AJ, Barnes NK, Gurantz ST, Dunne BA, Chung L, Turner J. IL-36 expression plays a potential role in acute kidney injury through down-regulation of inflammatory response. Pathophysiol Cell Inj J. 2016; 5:16–25

54. Danzmann, Ferguson & Allendorf. Genetic Variability and Components of Fitness in Hatchery Strains of Rainbow Trout. Journal of Fish Biology. 1989; 35**:** 313-319.

55. Dasmahapatra AK, Carty DR, Khan IA. Developmental ethanol exposure impairs locomotor movement in Japanese medaka (Oryzias latipes) larvae targeting epigenome. Chemosphere. 2017; 186: 901-910

56. Davenport AP. International Union of Pharmacology. XXIX. Update on endothelin receptor nomenclature. Pharmacol Rev. 2002;54:219-26.

57. Davenport AP, Maguire JJ. Endothelin. Handbk Exp Pharma- col. 2006;152:295-329.

58. Daviet L, Lehtonen JY, Tamura K, Griese DP, Horiuchi M, Dzau VJ. Cloning and characterization of ATRAP, a novel protein that interacts with the angiotensin II type 1 receptor. J Biol Chem. 1999;274: 17058–17062.

59. De, A. Wnt/Ca2+ signaling pathway: a brief overview. Acta Biochim. Biophys. Sin. (Shanghai). 2011; 43: 745–756

60. DeHaan RL. Morphogenesis of the vertebrate heart. In: DeHaan RL, Ursprung H, editors. Organogenesis. New York: Holt, Rinehart and Winston. 1965; 377–419.

61. DeKoven DL, Nunez JM, Lester SM, Conklin DE, Marty GD, Parker LM, Hinton DE. A purified diet for medaka (Oryzias latipes): refining a fish model for toxicological research. Lab Anim Sci. 1992; 42:180–189

62. Dellas, C., and Loskutoff, D. J. Historical analysis of PAI-1 from its discovery to its potential role in cell motility and disease. Thromb. Haemost. 2005; 93: 631–640.

63. Dharmananda, S. Safety Issues Affecting Chinese Herbs: Magnolia *alkaloids*. Institute for Traditional Medicine,Oregon. 2002

64. Diarra D, Stolina M, Polzer K, Zwerina J, Ominsky MS, Dwyer D. Dickkopf-1 is a master regulator of joint remodeling. Nat Med. 2007; 13: 156–163

65. Doolittle RF, Surgenor DM. Blood coagulation in fish. Americam Journal of Physiology. 1962; 203: 964-970.

66. Doolittle RF, Oncley JL, Surgenor DM. Species differences in the interaction of thrombin and fibrinogen. Journal of Biology Chemistry. 1962; 237: 3123-3127.

67. Doolittle RF. Differences in theclotting of lamprey fibrinogen by lamprey and bovine thrombins. Biochemistry Journal. 1965; 94:735-741.

68. Doolittle RF, Cottrell BA, Riley M. Amino acid composition of the subunit chains of lamprey fibrinogen: evolutionary significance of some structural anomalies. Biochimica et Biophysica Acta. 1976; 453: 439-452.

69. Doolittle RF, & Feng DF. Reconstructing the evolution of vertebrate blood coagulation from a consideration of the amino acid sequences of clotting proteins. Cold Spring Harbor Symposium on Quantitative Biology. 1987; 52: 869-874.

70. Doolittle RF. The evolution of vertebrate blood coagulation: A case of yin and yang. Thrombosis and Haemostasis, 1993; 70: 24-28.

71. Doolittle RF. Coagulation in vertebrates with a focus on evolution and inflammation. J Innate Immun. 2011; 3: 9-16.

72. Dorothea KT, Apostolos IK, Kostas GR, Aspostolos Z. Brain natriuretic peptide. Hell J card. 2003; 44:266-70.

73. Duan J, Gherghe C, Liu D, Hamlett E, Srikantha L, Rodgers L, Regan JN, Rojas M, Willis M, Leask A, Majesky M, Deb A. Wnt1/βcatenin injury response activates the epicardium and cardiac fibroblasts to promote cardiac repair. EMBO J. 2012; 31:429–42.

74. El-Khuffash AF, Molloy EJ. Serum troponin in neonatal intensive care. *Neonatology*. 2008; 94:1–7.

75. Ellwanger K, Saito H, Clement-Lacroix P, Maltry N, Niedermeyer J, Lee WK, Baron R, Rawadi G, Westphal H, Niehrs C. Targeted disruption of the Wnt regulator Kremen induces limb defects and high bone density. Molecular and cellular biology. 2008; 28:4875–4882.

76. Erickson SL, O'Shea KS, Ghaboosi N, Loverro L, Frantz G, Bauer M, Lu LH, Moore MW. ErbB3 is required for normal cerebellar and cardiac development: a comparison with ErbB2- and heregulin-deficient mice. Development. 1997; 124:4999–5011.

77. Fischer U., Ototake M., Nakanishi T. Life span of circulating blood cells in ginbuna crucian carp (*Carassius auratus langsdorfii*). Fish Shellfish Immunol. 1998; *8*: 339–349.

78. Fishman MC, Chien KR. Fashioning the vertebrate heart: Earliest embryonic decisions. Development. 1997; 124: 2099-2117.

79. Franco D, Lamers WH, Moorman AF. Patterns of expression in the developing myocardium: towards a morphologically integrated transcriptional model. Cardiovasc Res 1998; 38:25–53.

80. Frey N, Muller-Bardorff M, Katus HA. Myocardial damage: the role of troponin T. In: Kaski JC, Holt DW, eds. *Myocardial damage. Early detection by novel biochemical markers.* Location: Kluwer Academic Publishers, 1998:27–40.

81. Fried, L.E., Arbiser, J.L. Honokiol, a multifunctional antiangiogenic and antitumor agent. Antioxid. Redox Signal. 2009; 11:1139-1148.

82. Fu L, Mambrini M, Perrot E, Chourrout D. Stable and full rescue of the pigmentation in a medaka albino mutant by transfer of a 17 kb genomic clone containing the medaka tyrosinase gene. Gene. 2000; 241:205–211.

83. Gan, X.Q., Wang, J.Y., Xi, Y., Wu, Z.L., Li, Y.P., and Li, L. Nuclear Dvl, c-Jun, beta-catenin, and TCF form a complex leading to stabilization of beta-catenin- TCF interaction. J. Cell Biol. 2008; 180: 1087–1100.

84. Gao XM. Advanced traditional Chinese Medicine series/ Chinese Materia Medica. Beijing, China: People's Medical Publishing House. 2004; 1.

85. Garcia-Gras E, Lombardi R, Giocondo MJ, Willerson JT, Schneider MD, Khoury DS, Marian AJ. Suppression of canonical Wnt/beta-catenin signaling by nuclear plakoglobin recapitulates phenotype of arrhythmogenic right ventricular cardiomyopathy. J Clin Invest. 2006; 116:2012–21.

86. Garrison, R., Chambliss, W.G. Effect of a proprietary *Magnolia* and *Phellodendron* extract on weight management: a pilot, double-blind, placebo-controlled clinical trial. Altern. Ther. Health Med. 2006; 12:50-54.

87. Ge X, Ma X, Meng J, Zhang C, Ma K, Zhou C. Role of WNT-5a in interleukin-1beta–induced matrix metalloproteinase expression in rabbit temporomandibular joint condylar chondrocytes. Arthritis Rheum 2009; 60: 2714–2722.

88. George SJ. Wnt pathway: A new role in regulation of inflammation. Arterioscler Thromb Vasc Biol. 2008; 28: 400-402

89. Giani JF, Fuchs S, Gonzalez-Villalobos RA. Angiotensin II Type 1 Receptor–associated Protein A Novel Modulator of Angiotensin II Actions in the Nephron. Hypertension. 2013; 61:1150-1152.

90. Golias Ch, Charalabopoulos A, Stagikas D, Charalabopoulos K, Batistatou A. The kinin system--bradykinin: biological effects and clinical implications. Multiple Role of the Kinin System--Bradykinin. Hippokratia. 2007; 11: 124-128

91. Gomez-Orte E, Saenz-Narciso B, Moreno S, Cabello S. Multiple functions of the noncanonical Wnt pathway. Trends in Genetics. 2013; 29(9): 545-553

92. Habas, R., and Dawid, I.B. Dishevelled and Wnt signaling: is the nucleus the final frontier? J. Biol. 2005; 4: 2.

93. Hall JE. Hemostasis and blood coagulation. Guyton and Hall Textbook of Medical Physiology: Enhanced E-Book.11th ed. Philadelphia: Elsevier Health Sciences. 2010; 457–459

94. Hanumanthaiah R, Day K, Jagadeeswaran P. Comprehensive Analysis of Blood Coagulation Pathways in Teleostei: Evolution of Coagulation Factor Genes and Identification of Zebrafish Factor VIIi. Blood Cells, Molecules, and Diseases. 2002; 29: 57–68

95. Haq S, Choukroun G, Lim H, Tymitz KM, del Monte F, Gwathmey J, Grazette L, Michael A, Hajjar R, Force T, Molkentin JD. Differential activation of signal transduction pathways in human hearts with hypertrophy versus advanced heart failure. Circulation. 2001; 103:670–77.

96. He X, Semenov M, Tamai K, Zeng X. LDL receptor-related proteins 5 and 6 in Wnt/beta-catenin signaling: arrows point the way. Development (Cambridge, England). 2004;131: 1663-1677

97. Hinton DE, Kullman SW, Hardman RC, Volz DC, Chen PJ, Carney M, Bencic DC. Resolving mechanisms of toxicity while pursuing ecotoxicological relevance? Mar Pollut Bull. 2005; 51:635–648.

98. Hoeflich KP, et al. Requirement for glycogen synthase kinase-3β in cell survival and NF-κB activation. Nature 2000;406:86–90.

99. Honjo Y, Kniss J, Eisen J. Neuregulin-mediated ErbB3 signaling is required for formation of zebrafish dorsal root ganglion neurons. Development. 2008;135: 2615-2625

100. Horst PT, Smits JF, Blankesteijn WM. The Wnt/Frizzled pathway as a therapeutic target for cardiac hypertrophy: where do we stand? Acta Physiol (Oxf). 2012; 204:110–17.

101. Huang H, He X. Wnt/beta-catenin signaling: new (and old) players and new insights. Current opinion in cell biology. 2008; 20:119–125.

102. Hyodo-Taguchi Y, Egami N. Establishment of inbred strains of the medaka Oryzias latipes and the usefulness of the strains for biomedical research. Zool Sci. 1985; 2:305–316.

103. Hyodo-Taguchi Y, Egami N. Nonmammalian Animal Models for Biomedical Research, eds Woodhead AD, Vivirito K (CRC press, Boca Raton, FL). 1989; 185–214.

104. Hyun S, Kim MS, Song YS, Bak Y, Ham SY, Lee DH, Hong J, Yoon YY. Peroxisome Proliferator-Activated Receptor-Gamma Agonist 4-*O*-Methylhonokiol Induces Apoptosis by

Triggering the Intrinsic Apoptosis Pathway and Inhibiting the PI3K/Akt Survival Pathway in SiHa Human Cervical Cancer Cells. J. Microbiol. Biotechnol. 2015; 25: 334-342.

105. Inoue A, Yanagisawa M, Kimura S, Kasuya Y, Miyauchi T, Goto K, et al. The human endothelin family: three structurally and pharmacologically distinct isopeptides predicted by three separate genes. Proc Natl Acad Sci U S A. 1989; 86: 2863-7.

106. Ishikawa, T., Tamai, Y., Zorn, A. M., Yoshida, H., Seldin, M. F., Nishikawa, S. and Taketo, M. M. Mouse Wnt receptor gene Fzd5 is essential for yolk sac and placental angiogenesis. Development. 2001; 128: 25-33.

107. Ito, K., Iida, T., Ichino, K., Tsunezuka, M., Hattori, M., & Namba, T. Obovatol and obovatal, novel biphenyl ether lignans from the leaves of Magnolia obovata Thunb. Chem Pharm Bull (Tokyo). 1982; 30: 3347−3353.

108. Iwamatsu T. Stages of normal development in the medaka *Oryzias latipes*. Mechanisms of Development. 2004; 121: 605-618.

109. Iwamatsu T. Bulletin of Aichi Univ of Education. Natural Sciences. 2011; 60: 71-81

110. Iwasa S, Fan J, Shimokama T, Nagata M, Watanabe T. Increased immunoreactivity of endothelin-1 and endothelin B receptor in human atherosclerotic lesions. A possible role in atherogenesis. Atherosclerosis 1999;146: 93–100.

111. Jiao YM, and Wang F. On the usage of Astragalus membranaceus and Ampelopsis japonica in prescriptions for fifty-two diseases. Jiangxi J TCM. 2005; 36: 58-59

112. Ji HF, Li XJ, Zhang HY. Natural products and drug discovery. EMBO reports. 2009.10: 194-200

113. Johnson ML, Rajamannan N. Diseases of Wnt signaling. Rev Endocr Metab Disord. 2006; 7: 41–49.

114. Jope RS. Lithium and GSK-3: one inhibitor, two inhibitory actions, multiple outcomes. Trends Pharmacol Sci. 2003; 24:441–443.

115. Jordan HE & Speidel CC. Studies on lymphocytes. II. The origin and fate of lymphocytes in fishes. Journal of Morphology. 1924; 38: 529-546.

116. Kaliappan G, Perumal N, Raj TA, Kumar J. Effect of dietary ?? carotene on cerebral aneurysm and subarachnoid haemorrhage in the brain apo E mice. Journal of Thrombosis and Thrombolysis. 2011; 32: 343-55

117. Kaplan A, Silberberg M. The coagulation-kinin pathway of human plasma. Blood. 1987; 70: 1–15.

118. Kaplan A, Joseph K, Shibayama Y, Reddigari S, Ghebrehiwet B, Silverberg M. The intrinsic coagulation/kinin-forming cascade: assembly in plasma and cell surfaces in inflammation. Adv Immunol 1997; 66: 225–72.

119. Kaushik, G., Ramalingam, S., Subramaniam, D. Honokiol induces cytotoxic and cytostatic effects in malignant melanoma cancer cells. Am. J. Surg. 2012; 204: 868-873.

120. Kikuchi A, Yamamoto H, authors. Regulation of Wnt signalling by receptor-mediated endocytosis. J Biochem. 2007;141: 443–51.

121. Kikuchi, A. et al. (2011) New insights into the mechanism of Wnt signaling pathway activation. Int. Rev. Cell Mol. Biol. 2011; 291: 21–71

122. Kimelman D, Xu W. beta-catenin destruction complex: insights and questions from a structural perspective. Oncogene 2006; 25:7482–7491.

123. Kinoshita M, Murata K, Naruse K, Tanaka M. Medaka: biology, management, and experimental protocols. 2009

124. Kirchheimer, J. C., and Remold, H. G. (1989). Endogenous receptor-bound urokinase mediates tissue invasion of human monocytes. J. Immunol. 1989; 143: 2634–2639.

125. Klein PS, Melton DA. A molecular mechanism for the effect of lithium on development. Proc Natl Acad Sci U S A. 1996; 93:8455–8459.

126. Klotz LO, Sanchez-Ramos C, Prieto-Arroyo I, Urbanek P, Steinbrenner H, Monsalve M. Redox regulation of FoxO transcription factors. Redox Biology. 2015; 6: 51-72

127. Kobayashi T, Miyauchi T, Sakai S, Kobayashi M, Yamaguchi I, et al. Expression of endothelin-1, ETA and ETB receptors, and ECE and distribution of endothelin-1 in failing rat heart. Am J Physiol 1999; 276: H1197–H1206.

128. Kumar V, Abbas AK, Fausto N, Aster JC, authors. Hemodynamic disorders, thromboembolic disease and shock. Robbins and Cotran Pathologic Basis of Disease. 8th ed. Philadelphia, PA: Saunders Elsevier. 2010; 118–20

129. Lalmanach G, Naudin C, Lecaille F, Fritz H. Kininogens: More than cysteine protease inhibitors and kinin precursors. Biochimie. 2010; 92: 1568-1579.

130. Lasne D, Jude B, Susen S. From normal to pathological hemostasis. Can J Anesth. 2006; 53:S2–11.

131. Law JM. Mechanistic considerations in small fish carcinogenicity testing. Ilar J. 2001; 42:274–284.

132. Le Bihanic, F.L., Sommard, V., Perrine, de L., Pichon, A., Grasset, J., Berrada, S., Budzinski, H., Cousin, X., Morin, B., Cachot, J., 2015. Environmental concentrations of benz[a]anthracene induce developmental defects and DNA damage and impair photomotor response in Japanese medaka larvae. Ecotoxicol. Environ. Saf. 2015; 113: 321-328.

133. Lee, B., Kim, C. H., & Moon, S. K. (2006). Honokiol causes the p21WAF1-mediated G(1)-phase arrest of the cell cycle through inducing p38 mitogen activated protein kinase in vascular smooth muscle cells. FEBS Lett. 2006; 580: 5177−5184.

134. Lee HC, Tsai JN, Liao PY, Tsai WY, Lin KY, Chuang CC, Sun CK, Chang WC, Tsai HJ. Glycogen synthase kinase 3α and 3β have distinct functions during cardiogenesis of zebrafish embryo. BMC Dev Biol. 2007; 7: 93.

135. Lee YK, Choi IS, Kim YH, Nam SY, Yun YW, Lee MS, Oh KW, Hong JT. Neurite Outgrowth Effect of 4-*O*-methylhonokiol by Induction of Neurotrophic Factors Through ERK Activation. Neurochemical Research. 2009; 34: 2251–2260

136. Lee YJ, Lee YM, Lee CK, Jung JK, Han SB, Hong JT. Therapeutic applications of compounds in the *Magnolia* family. Pharmacology & Therapeutics. 2011; 130:157-176

137. Lee NJ, Oh JH, Ban JO, Shim JH, Lee HP, Jung JK, Ahn BW, Yoon DY, Han SB, Ham YW, Hong JT. 4-*O*-methylhonokiol, a PPARγ agonist, inhibits prostate tumor growth: p21-mediated suppression of NF-kB activity. British Journal of Pharmacology. 2013; 168: 1133-1145

138. Lee IJ, Yang YC, Chang WT, Chuang YJ, Liau I. Zebrafish model of photochemical thrombosis for translational research and thrombolytic screening in vivo. Journal of Biophotonics. 2016; 10: 494-502

139. Lemanski LF, Fitts EP, Marx BS. Fine Structure of the Heart in the Japanese Medaka *Oryzias latipes.* Journal of Ultrastructure Research. 1975; 53: 37-65

140. Li, H. B., Yi, X., Gao, J. M., Ying, X. X., Guan, H. Q., & Li, J. C.Magnolol-induced H460 cells death via autophagy but not apoptosis. Arch Pharm Res. 2007; 30: 1566−1574.

141. Li, L., Han, W., Gu, Y., Qiu, S., Lu, Q., Jin, J. Honokiol induces a necrotic cell death through the mitochondrial permeability transition pore. Cancer Res. 2007; 67:4894−4903.

142. Li, N., Song, Y., Zhang, W., Wang, W., Chen, J., Wong, A. W. Evaluation of the in vitro and in vivo genotoxicity of Magnolia bark extract. Regul Toxicol Pharmacol. 2007; 49: 154−159.

143. Li J, Swope D, Raess N, Cheng L, Muller EJ, Radice GL. Cardiac tissue-restricted deletion of plakoglobin results in progressive cardiomyopathy and activation of {beta}- catenin signaling. Mol Cell Biol. 2011; 31:1134–44.

144. Lin, Y. R., Chen, H. H., Lin, Y. C., Ko, C. H., & Chan, M. H. Antinociceptive actions of honokiol and magnolol on glutamatergic and inflammatory pain. J Biomed Sci. 2009; 16: 94.

145. Lin X, Xu X. Distinct functions of Wnt/β-catenin signaling in KV development and cardiac asymmetry. Development.2009; 136:207–217

146. Liou, J. Y., Chen, Y. L., Loh, S. H., Chen, P. Y., Hong, C. Y., Chen, J. J. Magnolol depresses urotensin-II-induced cell proliferation in rat cardiac fibroblasts. Clin Exp Pharmacol Physiol. 2009; 36: 711−716.

147. Liu J, Kern JA. Neuregulin-1 activates the JAK-STAT pathway and regulates lung epithelial cell proliferation. Am J Respir Cell Mol Biol 2002; 27:306–313.

148. Liu Z, Zhang X, Cui W, Li N, Chen J, Wong AW. Evaluation of short-term and subchronic toxicity of Magnolia bark extract in rats. Regul Toxicol Pharmacol. 2007; 49: 160-171

149. Lobov IB, Rao S, Carroll TJ, Vallance JE, Ito M, Ondr JK, Kurup S, Glass DA, Patel MS, Shu WG, Morrisey EE, McMahon AP, Karsenty G, Lang RA. WNT7b mediates macrophage-induced programmed cell death in patterning of the vasculature. Nature. 2005; 437: 417– 421.

150. Logan CY, Nusse R. The Wnt signaling pathway in development and disease. Annual review of cell and developmental biology. 2004; 20:781–810.

151. Lombardi R, Dong J, Rodriguez G, Bell A, Leung TK, Schwartz RJ, Willerson JT, Brugada R, Marian AJ. Genetic fate mapping identifies second heart field progenitor cells as a source of adipocytes in arrhythmogenic right ventricular cardiomyopathy. Circ Res. 2009; 104:1076–84.

152. Lombardi R, da Graca Cabreira-Hansen M, Bell A, Fromm RR, Willerson JT, Marian AJ. Nuclear plakoglobin is essential for differentiation of cardiac progenitor cells to adipocytes in arrhythmogenic right ventricular cardiomyopathy. Circ Res. 2011; 109:1342–53.

153. Lopez-Ilasaca M, Liu X, Tamura K, Dzau VJ. The angiotensin II type I receptor-associated protein, ATRAP, is a transmembrane protein and a modulator of angiotensin II signaling. Mol Biol Cell. 2003; 14: 5038–5050.

154. Lorenzon A, Calore M, Poloni G, De Windt LJ, Braghetta P, Rampazzo A. Wnt/β-catenin pathway in arrhythmogenic cardiomyopathy. Oncotarget. 2017; 8: 60640-60655

155. Lyons GE. In situ analysis of the cardiac muscle gene program during embryogenesis. Trends Cardiovasc Med. 1994; 3:184–190.

155. Ma B, van Blitterswijk CA, Karperien M. A WNT/beta-catenin negative feedback loop inhibits interleukin-1–induced matrix metalloproteinase expression in human articular chondrocytes. Arthritis Rheum. 2012; 64: 2589–2600.

156. McCurley AT, Callard GV. Characterization of housekeeping genes in zebrafish: male-female differences and effects of tissue type, development stage and chemical treatment. BMC Molecular Biology. 2008; 9: 102

157. MacDonald BT, He X. Frizzled and LRP5/6 receptors for Wnt/beta-catenin signaling. Cold Spring Harb Perspect Biol. 2012; 4: a007880

158. Macdonald BT, Tamai K, He X. Wnt/β-catenin signaling: components, mechanisms, and diseases. Dev Cell. 2009; 17: 9-26

159. Maguire JJ, Davenport AP. Endothelin Receptors and Their Antagonists. Seminars in Nephrology. 2015; 35:125–136.

160. Malekar, P., Hagenmueller, M., Anyanwu, A., Buss, S., Streit, M.R., Weiss, C.S., Wolf, D., Riffel, J., Bauer, A., Katus, H.A. & Hardt, S.E. Wnt signaling is critical for maladaptive cardiac hypertrophy and accelerates myocardial remodeling. Hypertension. 2010; 55: 939–945.

161. Mao B, Wu W, Davidson G, Marhold J, Li M, Mechler BM, Delius H, Hoppe D, Stannek P, Walter C, et al. Kremen proteins are Dickkopf receptors that regulate Wnt/beta-catenin signalling. Nature. 2002;417:664–667.

162. Martherus R, Jain R, Takagi K, Mendsaikhan U, Turdi S, Osinska H, James JF, Kramer K, Purevjav E, Towbin JA. Accelerated cardiac remodeling in desmoplakin transgenic mice in response to endurance exercise is associated with perturbed Wnt/β-catenin signaling. Am J Physiol Heart Circ Physiol. 2016; 310: H174–87.

163. Masckauchan TNH, Agalliu D, Vorontchikhina M, Ahn A, Parmalee NL, Li C-M, Khoo A, Tycko B, Brown AMC, Kitajewski J. Wnt5a Signaling Induces Proliferation and Survival of Endothelial Cells In Vitro and Expression of MMP-1 and Tie-2. Mol Biol Cell. 2006; 17:5163–5172.

164. Mates JM, Perez-Gomez C, Castro IND. Antioxidant Enzymes and Human Diseases. Clinical Biochemistry. 1999; 32:595–603

165. Meltzer ME. The role of the fibrinolytic system in arterial and venous thrombosis. Utrecht University Repository. Dissertation. 2010. ISBN/EAN: 978-90-393-5362-2

166. Meyer D, Yamaai T, Garratt A, Riethmacher-Sonnenberg E, Kane D, Theill LE. Isoform-specific expression and function of neuregulin. Dev Camb Engl 1997;124: 3575–3586.

167. Miyauchi T, Sakai S, Ihara M, Kasuya Y, Yamaguchi I, et al. Increased endothelin-1 binding sites in the cardiac membranes in rats with chronic heart failure. J Cardiovasc Pharmacol 1995; 26: S448–S451.

168. Molenaar, M., van de Wetering, M., Oosterwegel, M., Peterson-Maduro, J., Godsave, S., Korinek, V., Roose, J., Destre´ e, O., and Clevers, H. XTcf-3 transcription factor mediates beta-catenin-induced axis formation in Xenopus embryos. Cell. 1996; 86: 391–399.

169. Mukanganyama S, Bezabih M, Robert M, Ngadjui BT, Kapche GF, Ngandeu F, Abegaz B. "The evaluation of novel natural products as inhibitors of human glutathione transferase P1-1". Journal of Enzyme Inhibition and Medicinal Chemistry. 2011; 26: 460–7

170. Mukhopadhyay M, Shtrom S, Rodriguez-Esteban C, Chen L, Tsukui T, Gomer L, Dorward DW, Glinka A, Grinberg A, Huang SP, et al. Dickkopf1 is required for embryonic head induction and limb morphogenesis in the mouse. Dev Cell. 2001; 1:423–434.

171. Nachtergael, A., Poivre, M., Belayew, A., *et al*., 2015. In vitro genotoxicity tests point to an unexpected and harmful effect of a *Magnolia* and *Aristolochia* association. J. Ethnopharmacol. 2015; 174:178-186.

172. Nair AB, Jacob S. A simple practice guide for dose conversion between animals and human. J Basic Clin Pharm. March 2016-May 2016; 7(2): 27–31.

173. Naito AT, Shiojima I, Akazawa H, Hidaka A, Morisaki T, Kikuchi A, Komuro I. Developmental stage-specific biphasic roles of Wnt/beta-catenin signaling in cardiomyogenesis and hematopoiesis. Proc. Natl. Acad. Sci. 2006; 103; 19812-19817

174. Nebert DW, Vasiliou V. Analysis of the glutathione *S*-transferase (*GST*) gene family. Hum Genomics. 2004; 1: 460–464.

175. Newman DJ, Cragg GM. Natural Products as Sources of New Drugs from 1981 to 2014. J. Nat. Prod. 2016; 79: 629-661

176. Niehrs C. Function and biological roles of the Dickkopf family of Wnt modulators. Oncogene. 2006; 25:7469–7481.

177. Niehrs, C. The complex world of WNT receptor signalling. Nat. Rev. Mol. Cell Biol.2012; 13: 767–779.

178. Noordermeer, J., Klingensmith, J., Perrimon, N., and Nusse, R. (1994). Disheveled and armadillo act in the wingless signalling pathway in Drosophila. Nature. 1994; 367: 80–83.

179. Nusse R, Varmus HE. Many tumors induced by the mouse mammary tumor virus contain a provirus integrated in the same region of the host genome. Cell. 1982; 31: 99–109.

180. Oh JH, Kang LL, Ban JO, Kim YH, Kim KH, Han SB, Hong JT. Anti-inflammatory effect of 4-O-methylhonokiol, a novel compound isolated from *Magnolia officinalis* through inhibition of NF-kB. Chem Biol Interact. 2009; 180:506-14

181. Odiete O, Hill MF, Sawyer DB. Neuregulin in cardiovascular Development and Disease. Circ Res. 2012; 111: 1376-1385

182. Ogiwara K, Hagiwara A, Rajapakse S, Takahashi T. The Role of Urokinase Plasminogen Activator and Plasminogen Activator Inhibitor-1 in Follicle Rupture During Ovulation in the Teleost Medaka. *Biology of Reproduction*. 2015; 92:1-17

183. Ou, H. C., Chou, F. P., Lin, T. M., Yang, C. H., & Sheu, W. H. Protective effect of honokiol against oxidized LDL-induced cytotoxicity and adhesion molecule expression in endothelial cells. Chem Biol Interact. 2006; 161: 1−13.

184. Owens AP 3rd, Mackman N. Tissue factor and thrombosis: The clot starts here. Thromb Haemost. 2010; 104:432–9.

185. Padilla S., Cowden J., Hinton DE., Johnson R., Flynn K., Hardman RC., Yuen B., Law S., Kullman SW., AU DWT. Use of Medaka in Toxicity Testing. Curr Protoc Toxicol. 2009; 10: 1-49

186. Pakkasmaa S, Jones M. Individual-Level Analysis of Early Life History Traits in Hatchery-Reared Lake Trout. Journal of Fish Biology. *2002;* 60**:** 218-225.

187. Pallister CJ and Watson MS. Haematology. Scion Publishing 2010; 336–347.

188. Palta S, Saroa R, Palta A. Overview of the coagulation system. Indian J Anaesth. 2014; 58: 515-523

189. Parker JD, Thiessen JJ. Increased endothelin-1 production in patients with chronic heart failure. Am J Physiol Heart Circ Physiol. 2004; 286: H1141–H1145.

190. Pathak M, Wong SS, Dreveny I, Emsley J. Structure of plasma and tissue kallikreins. Thromb Haemost. 2013; 110: 423-433.

191. Paul-Prasanth B, Matsuda M, Lau EL, Suzuki A, Sakai F, Kobayashi T, Nagahama Y. Knock-down of DMY initiates female pathway in the genetic male medaka, *Oryzias latipes*. Biochem Biophys Res Commun. 2006; 351:815–819.

192. Peifer, M., Sweeton, D., Casey, M., and Wieschaus, E. Wingless signal and Zeste-white 3 kinase trigger opposing changes in the intracellular distribution of Armadillo. Development. 1994; 120: 369–380.

193. Pendergrass KD, Rafferty K, Davis ME. H2O2 Acutely Upregulates Glutathione Peroxidase and Catalase mRNA levels in Cardiac Progenitor Cells. Experimental Biology. 2011;25: ISSN (online): 1530-6860

194. Pernow J, Bohm F, Johansson BL, Hedin U, Ryden L. Enhanced vasoconstrictor response to endothelin-B-receptor stimulation in patients with atherosclerosis. J Cardiovasc Pharmacol. 2000;36:S418–S420.

195. Petho G, Reeh PW. Sensory and signaling mechanisms of bradykinin, eicosanoids, platelet-activating factor, and nitric oxide in peripheral nociceptors. Physiol Rev. 2012;92:1699-1775.

196. Plumier C. Nova Plantarum Americanarum genera. Paris. [New genera of American plants]. 1703; 1703-80

197. Poivre M, Duez P. Biological activity and toxicity of the Chinese herb *Magnolia officinalis* Rehder and E. Wilson (Houpo) and its constituents. J Zhejiang Univ-Sci B (Biomed & Biotechnol). 2017; 18: 194-214

198. Pukrop T, Klemm F, Hagemann T, Gradl D, Schulz M, Siemes S, Trumper L, Binder C. Wnt 5a signaling is critical for macrophageinduced invasion of breast cancer cell lines. Proc Natl Acad Sci U S A. 2006; 103: 5454 –5459

199. Pyo MY, Lee YY, Yun-Choi HS. Anti-Platelet effect of the constituents isolated from the barks and fruits of Magnolia obovate. Arch Pharm Res. 2002; 5: 325-328

200. Raizada A, Bhandari S, Khan MA, Singh HV, Thomas S, Sarabhai V, Singh N, Trehan N. Brain type natriuretic peptide (BNP)-a marker of new millennium in diagnosis of congestive heart failure. Indian Journal of Clinical Biochemistry. 2007; 22: 4-9

201. Ranzani-Paiva MJT, Silveira VR, Almeida-Dias ER, Rodrigues EL. Clotting time and hematocrit of “dourado”, *Salminus maxilosus*, and carp, *Cyprinus carpio*. Boletim Instituto Pesca. 2000 26: 113-116.

202. Rasouli SJ, Stainier DYR. Regulation of cardiomyocyte behavior in zebrafish trabeculation by Neuregulin 2a signaling. Nature Communications. 2017;8: 15281

203. Rispens E, Bron A, Lee J, Fukumoto J, authors. The pathophysiology of inflammation in cell injury. Pathophysiol Cell Inj J. 2012; 1:10–9

204. Rohr S. Arrhythmogenic implications of fibroblast-myocyte interactions. Circ Arrhythm Electrophysiol. 2012; 5:442–52.

205. Romano N, Taverine-Thiele JJ, Maanen JC, Rombout JHMW. 1997. Leucocyte subpopulations in developing carp (*Cyprinus carpio* L.): imunocytochemical studies. *Fish & Shellfish Immunology*. 1997; *7*: 439-453.

206. Romer A. The vertebrate body. Saunders, Philadelphia. 1956; 40: 164

207. Roncales FJ. Schalm's Veterinary Hematology. 5th ed. Philadelphia: Lippincott Williams & Wilkins; 2000.

208. Rupert CE, Coulombe KLK. The Roles of Neuregulin-1 in Cardiac Development, Homeostasis, and Disease. Biomarker Insights 2015;10:1–9

209. Russell FD, Molenaar P. The human heart endothelin system: ET-1 synthesis, storage, release and effect. Trends Pharmacol Sci. 2000; 21: 353–359.

210. Ryu JH, Chun JS. Opposing roles of WNT-5a and WNT-11 in interleukin-1beta regulation of Type II collagen expression in articular chondrocytes. J Biol Chem. 2006; 281:22039–22047.

211. Sakai S, Miyauchi T, Sakurai T, Kasuya Y, Ihara M, et al. Endogenous endothelin-1 participates in the maintenance of cardiac function in rats with congestive heart failure. Marked increase in endothelin-1 production in the failing heart. Circulation 1996; 93:1214–1222.

212. Sakurai T, Yanagisawa M, Takuwa Y, Miyazaki H, Kimura S, Goto K, et al. Cloning of a cDNA encoding a non-isopeptide-selective subtype of the endothelin receptor. Nature. 1990; 348:732-5.

213. Satin J, Fujii S, DeHaan RL. Development of cardiac beat rate in early chick embryos is regulated by regional cues. Dev Biol. 1988;129:103–113.

214. Schneider MP, Boesen EI, Pollock DM. Contrasting Actions of Endothelin ETA and ETB Receptors in Cardiovascular Disease. Annu Rev Pharmacol Toxicol. 2007 ; 47: 731–759.

215. Semenov MV, Tamai K, Brott BK, Kuhl M, Sokol S, He X. Head inducer Dickkopf-1 is a ligand for Wnt coreceptor LRP6. Curr Biol. 2001;11: 951–961.

216. Shen B. A New Golden Age of Natural Products Drug Discovery. Cell. 2015; 163: 1297–1300.

217. Shima A, Mitani H. Medaka as a research organism: past, present and future. Mech Dev. 2004; 121:599–604.

218. Shin JW, Seol IC, Son CG. Interpretation of Animal Dose and Human Equivalent Dose for Drug Development. 2010; 31: 1-7

219. Siegfried, E., Chou, T.B., and Perrimon, N. Wingless signaling acts through zeste-white 3, the Drosophila homolog of glycogen synthase kinase-3, to regulate engrailed and establish cell fate. Cell. 1992; 71: 1167–1179.

220. Simons, M. and Mlodzik, M. Planar cell polarity signaling: from fly development to human disease. Annu. Rev. Genet. 2008; 42: 517–540

221. Silveira PP, Portella AK, Goldani MZ, Barbieri MA. Developmental origins of health and disease (DOHaD). J Pediatr (Rio J). 2007; 83:494-504.

222. Smit GL, Schoonbee HJ. Blood coagulation factors in the freshwater fish *Oreochromis mossambicus*. Jounal of Fish Biology. 1988; 32: 673-677.

223. Solecki RS. Shanidar IV, a Neanderthal flower burial in northern Iraq. Science. 1975; 190**:** 880–881

224. Solnica B. Cardiac troponins. Medycyna Praktyczna. 2004; 10:133–136.

225. Stambolic V, et al. Lithium inhibits glycogen synthase kinase-3 activity and mimics wingless signalling in intact cells. Curr Biol. 1996;6:1664–1668.

226. Tachikawa, E., Takahashi, M., & Kashimoto, T. Effects of extract and ingredients isolated from Magnolia obovata thunberg on catecholamine secretion from bovine adrenal chromaffin cells. Biochem Pharmacol. 2000; 60: 433−440.

227. Takei Y, Tsuchida T, Li Z, Conlon JM. Antidipsogenic effects of eel bradykinins in the eel *Anguilla japonica*. Am J Physiol Regul Integr Comp Physiol. 2001; 281: R1090-R1096.

228. Tarkowska A, Furmaga-Jabłońska W. The Evaluation of Diagnostic Role of Cardiac Troponin T (cTnT) in Newborns with Heart Defects. Scientific World Journal. 2012; 2012: 682538.

229. Tavares-Dias M, Oliveira SR. A review of the blood coagulation system of fish. Brazilian journal of Biosciences. 2009; 7: 205-224

230. Teng CM, Yu SM, Chen CC, Huang YL, Huang TF. Inhibition of thrombin- and collagen-induced phosphoinositides breakdown in rabbit platelets by a PAF antagonist-denudation B, an isomer of Kadsurenone. Thromb Res. 1990. 59, 121-130

231. Teschke, R., Wolff, A., Frenzel, C. Review article: herbal hepatotoxicity—an update on traditional Chinese medicine preparations. *Aliment.* Pharmacol. Ther. 2014; 40: 32-50.

232. Teschke, R., Zhang, L., Long, H. Traditional Chinese medicine and herbal hepatotoxicity: a tabular compilation of reported cases. Ann. Hepatol. *2015;* 14:7-19.

233. Teschke, R., Larrey, D., Melchart, D., *et al*., 2016. Traditional Chinese medicine (TCM) and herbal hepatotoxicity: RUCAM and the role of novel diagnostic biomarkers such as microRNAs. *Medicines*. 2016; 3:18.

234. Thiele A, Wasner M, Muller C, Engeland K, Hauschildt S. Regulation and possible function of beta-catenin in human monocytes. J Immunol. 2001; 167: 6786–6793.

235. Tonnessen T, Lunde PK, Giaid A, Sejersted OM, Christensen G. Pulmonary and cardiac expression of preproendothelin-1 mRNA are increased in heart failure after myocardial infarction in rats. Localization of preproendothelin-1 mRNA and endothelin peptide. Cardiovasc Res. 1998; 39: 633–643.

236. Torres, M.A., and Nelson, W.J. Colocalization and redistribution of dishevelled and actin during Wnt-induced mesenchymal morphogenesis. J. Cell Biol. 2000; 149: 1433–1442.

237. Tucker B, Hepperle C, Kortschak D, Rainbird B, Wells S, Oates AC, Lardelli M. ZebraWsh Angiotensin II Receptor-like 1a (agtrl1a) is expressed in migrating hypoblast, vasculature, and in multiple embryonic epithelia. Gene Expression Patterns. 2007; 7: 258–265.

238. Ueland T, Otterdal K, Levka T, Halvorsen B, Gabrielsen A, Sandberg wj, Paulsson-Berne G, Pedersen TM, Folkersen L, Gullestad L, Oie E, Hansson GK, Aukrust P. Dickkopf-1 enhances inflammatory interaction between platelets and endothelial cells and shows increased expression in atherosclerosis. Arterioscler Thromb Vasc Biol . 2009; 29: 1228-1234.

239. Ueno S, Weidinger G, Osugi T, Kohn AD, Golob JL, Pabon L, Reinecke H, Moon RT, Murry CE. Biphasic role for Wnt/β-catenin signaling in cardiac specification in zebrafish and embryonic stem cells. PNAS. 2007. 104: 9685-9690

240. Van de Schans, V.A., van den Borne, S.W., Strzelecka, A.E., Janssen, B.J., van der Velden, J.V., Langen, R.C., Wynshaw-Boris, A., Smits, J.F. & Blankesteijn, W.M. Interruption of

Wnt signaling attenuates the onset of pressure overload-induced cardiac hypertrophy. Hypertension. 2007; 49: 473–480.

241. Wallingford JB, Habas R. The developmental biology of Dishevelled: an enigmatic protein governing cell fate and cell polarity. Development (Cambridge, England) 2005; 132:4421–4436.

242. Wan F, Zhong GS. A medication comparison between prescriptions for fifty-two diseases and ten thousands things. Acta Med Sin. 1990. 5: 55-58

243. Wang YZ, Patterson JE, Gray JE, Yu C, Cottrell, BA, Shimizu A, Graham D, Riley M & Doolittle RF. Complete sequence of the lamprey fibrinogen α chain. Biochemistry. 1989; 28: 9801-9806.

244. Wang JB, Dezube T, Kearney MM, MacLean K, authors. Pentoxifylline (PTX) attenuates LPS-induced acute liver injury via effects on ICAM-1 expression. Pathophysiol Cell Inj J. 2016; 5:26–39

245. Wang X, Xiao Y, Mou Y, Zhao Y, Blankesteijn M, Hall JL. A role for the-catenin/T-cell factor signaling cascade in vascular remodeling. *Circ Res*. 2002; 90:340 –347.

246. Wang X, Adhikari N, Li Q, Hall JL. The LDL receptor related protein LRP6 regulates proliferation and survival through the Wnt cascade in vascular smooth muscle cells. Am J Physiol Heart Circ Physiol. 2004; 287:H2376–H2383.

247. Wang W, Li X, Lee M, Jun S, Aziz KE, Feng L, Tran MK, Li N, McCrea PD, Park J, Chen J. FOXKs Promote Wnt/b-Catenin Signaling by Translocating DVL into the Nucleus. Developmental Cell. 2015; 32: 707–718.

248. Wassmann S, Wassmann K, Nickenig G. Modulation of Oxidant and Antioxidant Enzyme Expression and Function in Vascular Cells. Hypertension. 2004; 44: 381-386.

249. Wayne NL, Kuwahara K, Aida K, Nagahama Y, Okubo K. Whole-cell electrophysiology of gonadotropin-releasing hormone neurons that express green fluorescent protein in the terminal nerve of transgenic medaka (*Oryzias latipes*). Biology of reproduction. 2005; 73:1228–1234.

250. Wehrli M., Dougan S.T., Caldwell K., O'Keefe L., Schwartz S., Vaizel- Ohayon D., Schejter E., Tomlinson A., and DiNardo S. Arrow encodes an LDL-receptor-related protein essential for Wingless signalling. Nature. 2000; 407: 527–530.

251. Wolf K. Plasmoptysis and gelation of erytrocytes in coagulation of blood of freshwater bony fishes. Blood. 1959; 14: 1344.

252. Wong MKS, Takei Y. Lack of Plasma Kallikrein-Kinin System Cascade in Teleosts. PLOS ONE. 2013; 8: 1-13

253. Wong HC, Bourdelas A, Krauss A, Lee HJ, Shao Y, Wu D, Mlodzik M, Shi DL, Zheng J. Direct binding of the PDZ domain of Dishevelled to a conserved internal sequence in the C-terminal region of Frizzled. Molecular cell. 2003; 12:1251–1260.

254. Woodgett JR. Molecular cloning and expression of glycogen synthase kinase-3/factor A. EMBO J. 1990; 9:2431–2438.

255. Wu AHB, Feng YJ. Biochemical differences between cTnT and cTnI and their significance for diagnosis of acute coronary syndromes. Eur Heart J. 1998;19 (suppl N):N25–9.

256. Wu D, Pan W. GSK3: a multifaceted kinase in Wnt signaling. Trends Biochem Sci. 2009; 35: 161-168

257. Wu M, Shariat-Madar B, Haron MH, Wu M, Khan IA, Dasmahapatra AK. Ethanol induced attenuation of oxidative stress is unable to alter mRNA expression pattern of catalase, glutathione reductase, glutathione-S- transferase (GST1A), and superoxide dismutase (SOD3)

enzymes in Japanese rice fish (*Oryzias latipes*) embryogenesis. Comp Biochem Physiol C Toxicol Pharmacol. 2011; 153: 159–167.

258. Yamada K, Ichino N, Nishii K, Sawada H, Higashiyama S, Ishiguro H. Characterization of the human NTAK gene structure and distribution of the isoforms for rat NTAK mRNA. Gene. 2000; 255:15–24.

259. Yanagisawa M, Kurihara H, Kimura S, Tomobe Y, Kobayashi M, Mitsui Y. A novel potent vasoconstrictor peptide produced by vascular endothelial cells. Nature. 1988; 332: 411-5.

260. Yarden Y, Sliwkowski MX. Untangling the ErbB signalling network. Nat Rev Mol Cell Biol. 2001; 2: 127–137.

261. Ye B, Ge Y, Perens G, Hong L, Xu H, Fishbein MC, Li F. Canonical Wnt/β-catenin signaling in epicardial fibrosis of failed pediatric heart allografts with diastolic dysfunction. Cardiovasc Pathol. 2013; 22: 54–57.

262. Yelon D. Cardiac Patterning and Morphogenesis in Zebrafish. Development Dynamics. 2001; 222: 552-563

263. Yousif NG, Li J, Ao L, Reece T, Weyant MJ, Cleveland JC. Ghrelin reduces myocardial injury following global hypothermic ischemia/reperfusion via suppression of the myocardial inflammatory response. J Surg Res. 2011; 165:192–9

264. Yousif NG, author. Novel therapeutic role of siglec-E in down-regulation TLR4-mediated inflammatory response after global myocardial ischemia and reperfusion. Cardiovasc Res. 2014; 103:s90

265. Yousif NG, Hadi NR, Hassan AM. Indocyanine Green-001 (ICG-001) Attenuates Wnt/β-catenin-induces Myocardial Injury Following Sepsis. J Pharmacol Pharmacother. 2017; 8: 14-20

266. Zeng H, Dvorak HF, Mukhopadhyay D. Vascular permeability factor (VPF)/vascular endothelial growth factor (VEGF) peceptor-1 down-modulates VPF/VEGF receptor-2-mediated endothelial cell proliferation, but not migration, through phosphatidylinositol 3-kinase-dependent pathways. J Biol Chem. 2001; 276:26969–26979.

267. Zeng H, Zhao D, Mukhopadhyay D. Flt-1-mediated Down-regulation of Endothelial Cell Proliferation through Pertussis Toxin-sensitive G Proteins, βγ Subunits, Small GTPase CDC42, and Partly by Rac-1. J. Biol. Chem. 2002; 277: 4003-4009

268. Zeng X, Huang H, Tamai K, Zhang X, Harada Y, Yokota C, Almeida K, Wang J, Doble B, Woodgett J.Initiation of Wnt signaling: control of Wnt coreceptor Lrp6 phosphorylation/activation via frizzled, dishevelled and axin functions. Development (Cambridge, England). 2008; 135:367–375.

269. Zhang, B., Maniatis, T., Song, Y., Zhang, W., Zhang, X., Li, N. Evaluation of Magnolia bark extract in chromosomal aberration assays. Mutat Res. 2008; 654: 133−137.

270. Zhang Z, Chen J, Zhou S, Wang S, Cai X, Conklin DJ, Kim KS, Kim KH, Tan Y, Zheng Y, Kim YH, Cai L. *Magnolia* Bioactive Constituent 4-O-Methylhonokiol Prevents the Impairment of Cardiac Insulin Signaling and the Cardiac Pathogenesis in High-Fat Diet-Induced Obese Mice. Int J Biol Sci. 2015; 11: 879-891

271. Zhao X, Li F, Sun W, Gao L, Kim KS, Kim KT, Cai L, Zhang Z, Zheng Y. Extracts of *Magnolia* Species-Induced Prevention of Diabetic Complications: A Brief Review. Int J Mol Sci. 2016; 17: 1629.

272. Zhao YY, Sawyer DR, Baliga RR, Opel DJ, Han X, Marchionni MA et al. Neuregulins promote survival and growth of cardiac myocytes. Persistence of ErbB2 and ErbB4 expression in neonatal and adult ventricular myocytes. J Biol Chem 1998; 273:10261–10269.

273. Zhou, H. Y., Shin, E. M., Guo, L. Y., Youn, U. J., Bae, K., Kang, S. S., et al. Antiinflammatory activity of 4-methoxyhonokiol is a function of the inhibition of iNOS and COX-2 expression in RAW 264.7 macrophages via NF-kappaB, JNK and p38 MAPK inactivation. Eur J Pharmacol. 2008; 586: 340−349.

APPENDIX

APPENDIX I Analytical characterization of MH uptake into medaka embryos by UHPLC/MS analysis

A standard curve was prepared with different concentrations of MH between 1.8 μM and 35.7 μM. MH was collected in 1 dpf from the treatment media (10 μM) with embryo, which was prepared from the same stock as the standard. Both were analyzed by UHPLC/MS analysis. The method was described in chapter 2.

MH 10 µM standard

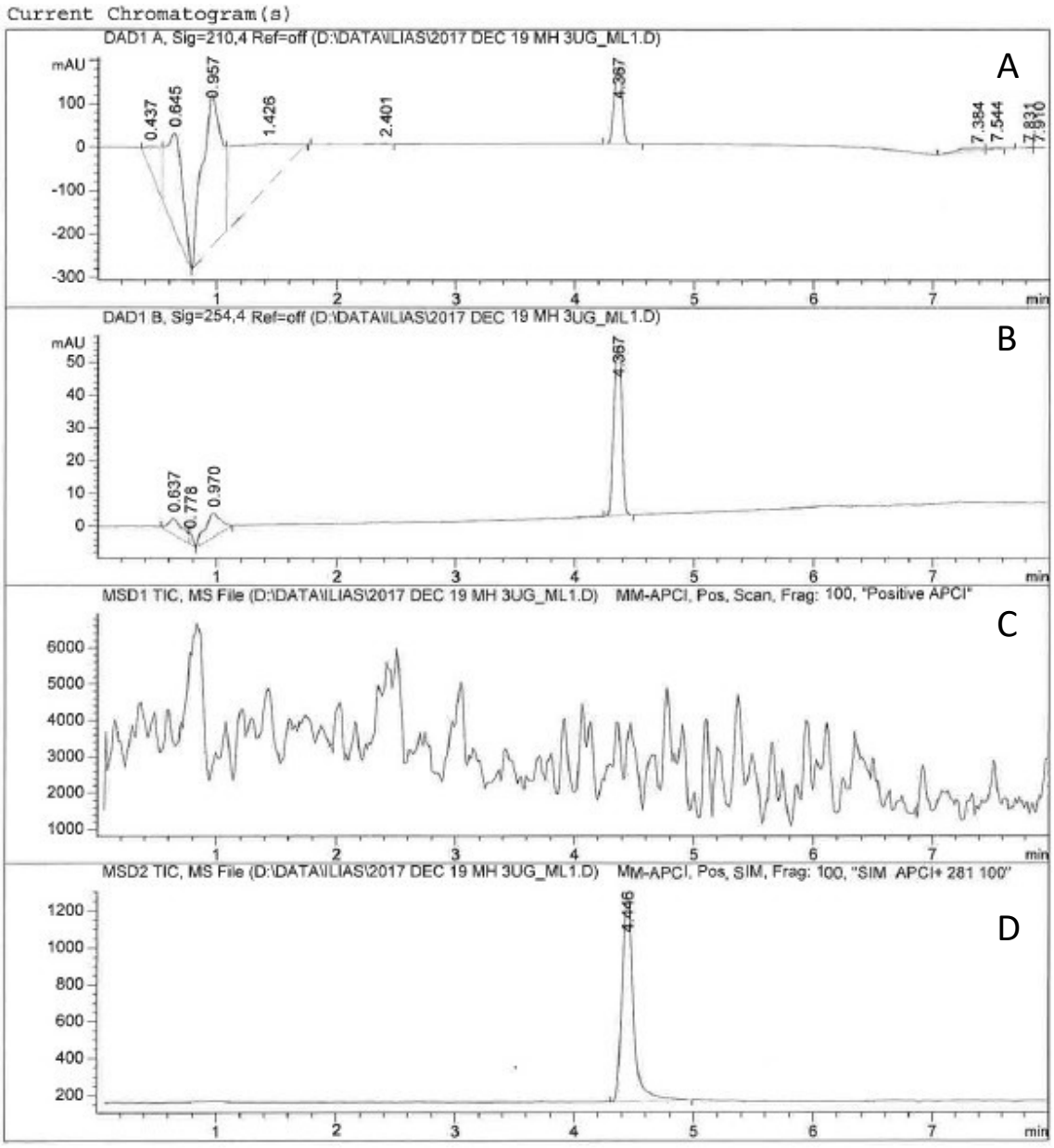

Figure A1.1: Representative UHPLC chromatogram for MH (10 µM) standard. Wavelengths of (A) 210 nm and (B) 254 nm were monitored for the DAD detector. MH was analyzed by ESI and APCI in both positive and negative modes. APCI positive mode produced a better ion signal for the tested compounds than other ionization modes. The MS was operated in (C) TIC as well as (D) SIM mode. Retention time is 4.4

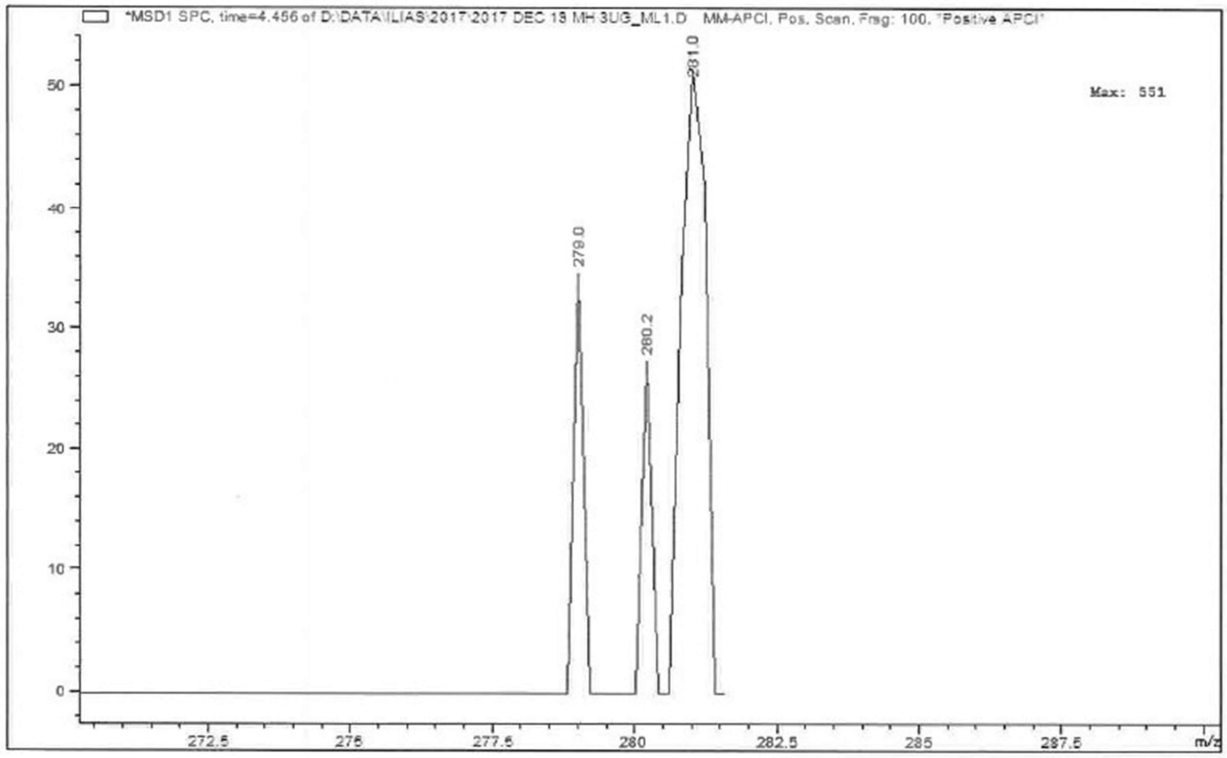

Figure A1.2: Representative LC-MS spectra of MH (10 µM) standard from TIC at the retention time 4.4 min. Quantitative ion, 281 m/z; Quantitative ion, 280.2 m/z; Quantitative ion, 279 m/z

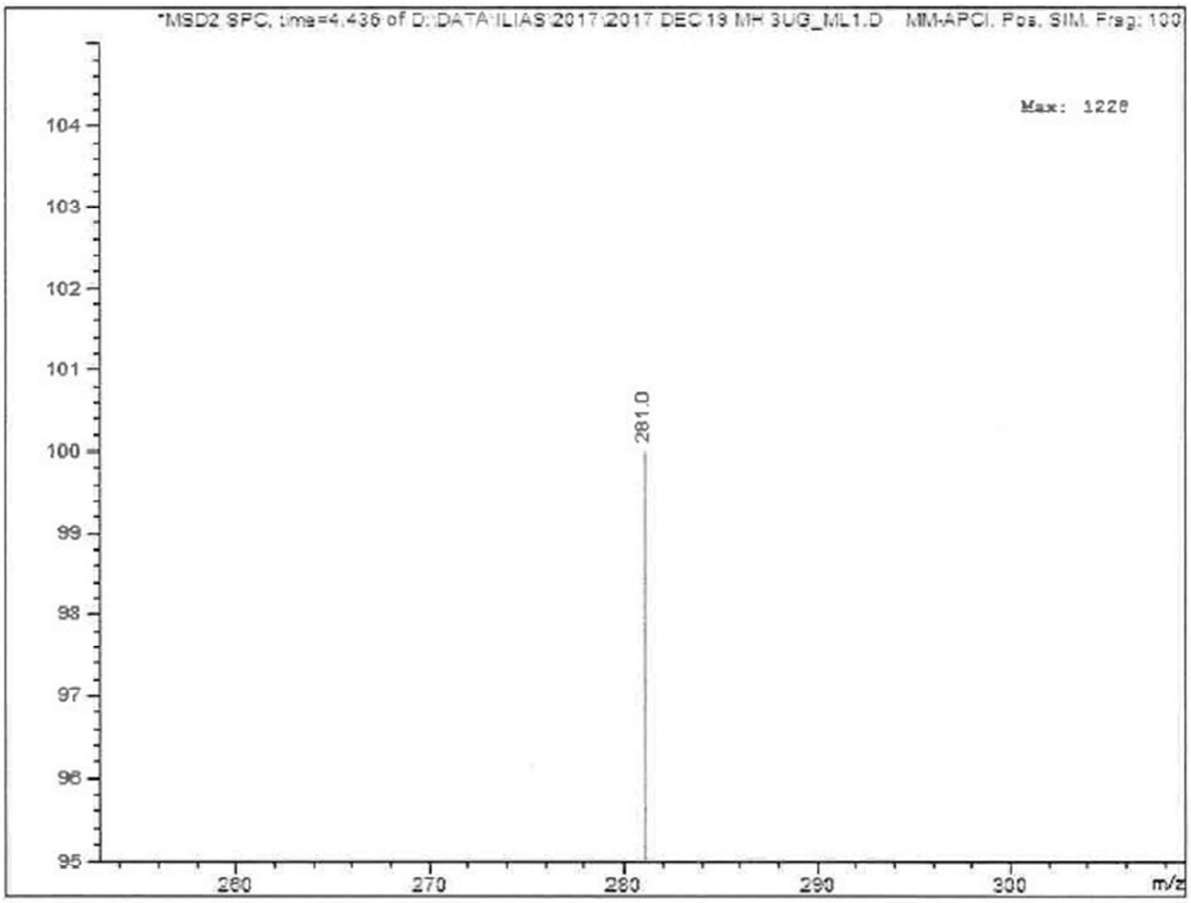

Figure A1.3: Representative LC-MS spectra of MH (10 µM) standard from SIM at the retention time 4.4 min. Quantitative ion, 281 m/z

MH 10 µM- 1dpf

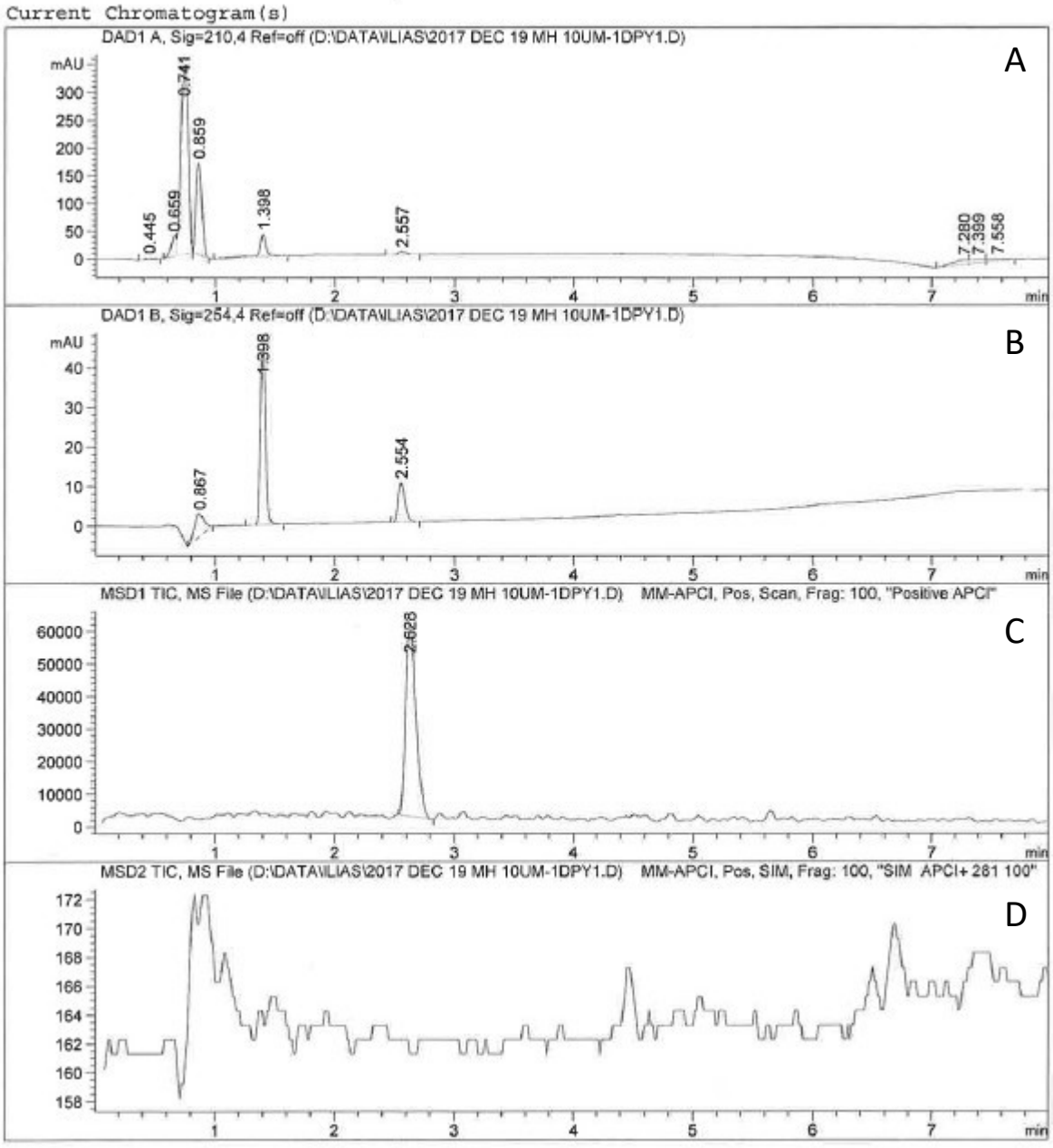

Figure A1.4: Representative chromatogram generated by MH (10 µM) in 1 dpf. Wavelengths of (A) 210 nm and (B) 254 nm were monitored for the DAD detector. MH was analyzed by ESI and APCI in both positive and negative modes. APCI positive mode produced a better ion signal for the tested compounds than other ionization modes. The MS was operated in (C) TIC as well as (D) SIM mode. Retention time is 2.6

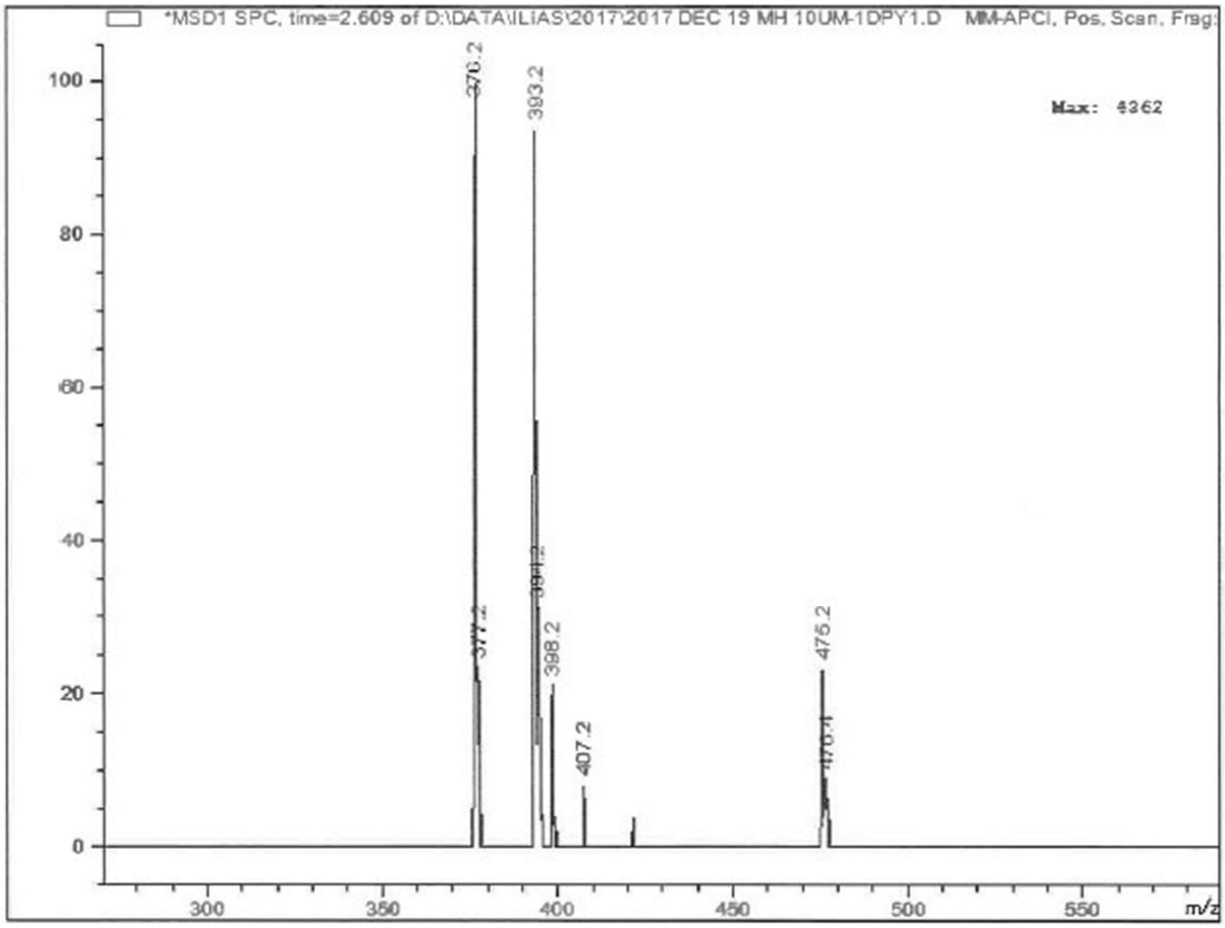

Figure A1.5: Representative LC-MS spectra of MH (10 µM) at the retention time 2.6 min. Quantitative ion, 393.2 m/z; Quantitative ion, 376.2 m/z

The retention time for the 10 μM MH standard was 4.4 min (Fig. A1.1) which corresponded *m*/*z* of 281.1 ($[M+H]^+$) (Fig. A1.2, Fig. A1.3). Therefore, the molecular weight for the compound was 280, which represented the presence of MH ($C_{19}H_{20}O_2$). By analyzing the media of 1 dpf, we observed that the HPLC peak corresponding for the standard solution disappeared and provided a new peak at a retention time of 2.6 min (Fig. A1.4). The *m/z* for the new retention time was 393.2 ($[M+H]^+$) (Fig. A1.5). Therefore, the molecular weight of the new compound was 392. However, another peak represented the *m/z* to be 376.2 ($[M+H]^+$) (Fig. A1.5) was observed, which might be due to –OH group removal from the other compound that had the *m/z* of 393.2 ($[M+H]^+$-OH). The disappearance of the peak from the 1 dpf media (Fig. A1.4) might be due to uptake of MH into the embryonic tissues. However, further studies are needed to confirm the uptake of the compound by analyzing the embryonic tissues. Moreover, further illustrations are required for identification of the compounds that were observed from 1 dpf media (Fig. A1.5).

APPENDIX II Representative agarose gel picture

The quality of the RT-qPCR product was evaluated by agarose gel electrophoresis (Fig. A2.1) on a 2% agarose gel containing 0.01% ethidium bromide.

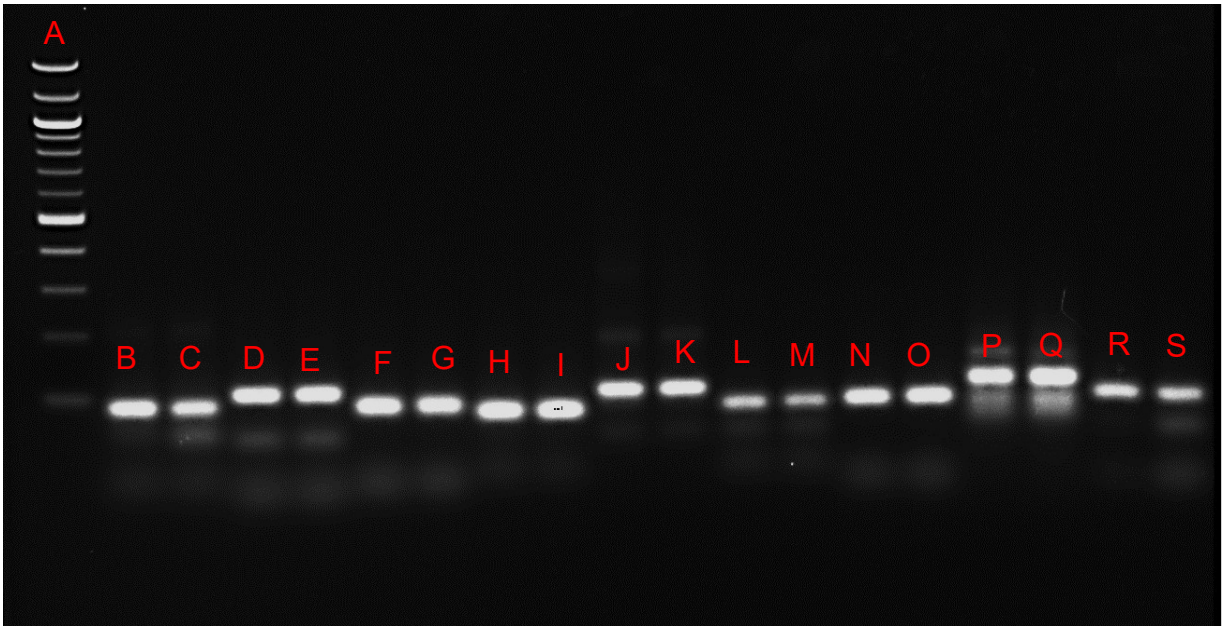

Figure A2.1 Representative gel picture of RT-qPCR analysis of ErbB3, FoxO1, NRG-2, PAI-1, tPA, uPA, Dvl, GST, GPX. The lanes are represented as (A) 100 bp ladder, (B) ErbB3-control, (C) ErbB3-treatment, (D) FoxO1-control (E) FoxO1-treatment, (F) NRG-2- control, (G) NRG-2-treatment, (H) PAI-1-control, (I) PAI-1-treatment, (J) tPA-control, (K) tPA-treatment, (L) uPA-control, (M) uPA-treatment, (N) Dvl-control, (O) Dvl-treatment, (P) GST-control, (Q) GST-treatment, (R) GPX- control, (S) GPX-treatment

VITA

EDUCATION

University of Mississippi, Oxford, MS

Ph.D. in Pharmaceutical Sciences- 2018

Research Project: A mechanistic study of the teratogenic potential of 4-*O*-Methylhonokiol (MH) on Japanese medaka (*Oryzias latipes*)

Jahangirnagar University, Dhaka, Bangladesh

MS in Pharmaceutical Science-2012

Research Project: Toxicological studies of an ayurvedic preparation Maharaj Nripatiballav (MNR) used in Sprue syndrome

Jahangirnagar University, Dhaka, Bangladesh

Bachelor of Pharmacy (Honors)-2010

Research Project: Toxicological studies of an ayurvedic medicine Dhatri Lauha (DTR) used in colicky pain

PROFESSIONAL EXPERIENCE

2013-Present Teaching Assistant, Department of Biomolecular Sciences, Division of Pharmacology, University of Mississippi

- Advanced Physiology- Phcl 662
- Human Pathophysiology I- Phcl 341

- Human Pathophysiology II- Phcl 342
- Biochemical Foundations of Therapeutics- Phcl 343
- Physiological Foundations of Therapeutics- Phcl 344

2014-Present Research Assistant, Department of Biomolecular Sciences, Division of Pharmacology, University of Mississippi

- A mechanistic study of the developmental abnormality induced by natural product derivative on Japanese medaka embryogenesis
- A Immunohistochemical and Biochemical analysis of Cannabinoid Receptors in Japanese medaka

AWARDS

2017- Summer Research Assistantship Award, Graduate School of the University of Mississippi

2017- Society of Toxicology, Graduate Student Travel Support Award

2015- Travel fellowship sponsored by the NIH Common Fund Program in Metabolomics R25 GM103798-03

2015- Society of Toxicology, South Central Chapter Student Travel Award

2015- Reproductive and Developmental Toxicology Specialty Section Travel Award Stipend

PUBLICATIONS

Jain SK, Jain J, **Singha SK**, Shariat-Madar Z. Revisiting Malaria elimination: prevention, diagnosis and treatment. EC Pharmacology and Toxicology. 2018; 6(4): 216-227

Suiter C, **Singha SK**, Khalilli R, Shariat-Madar Z. Free Fatty Acids: Circulating Contributors of Metabolic Syndrome. Cardiovasc Hematol Agents Med Chem. 2018. (Accepted)

Masuma R, Paul AK, **Singha SK**, Chowdhury IA, Kahali S, Sarker NC. An Acute Metabolic Study and Neuropharmacologic Findings of *Pleurotus ostreatus* on Rat. Bangladesh J Mushroom, 2010;4(2):35-44 (ISSN 1995- 0683).

Abstract

Singha SK, Ibrahim MA, Muhammad I, Khan IA, Dasmahapatra AK. Teratogenic potential of 4-*O*-Methylhonokiol on Japanese medaka (*Oryzias latipes*) embryogenesis. Planta Medica,2016; 82-PB44 (ISSN 0032-0943).

AFFILIATIONS

2014-Present	Graduate Student Member, Society of Toxicology (SOT)
2014-Present	Graduate Student Member, South Central Chapter, Society of Toxicology (SCC-SOT)
2015-Present	Graduate Student Member, American Association of Pharmaceutical Scientists (AAPS)

PRESENTATIONS

Podium Presentation

Singha SK, Khan IA, Dasmahapatra AK. (2015) Endocannabinoid Receptors expression in Japanese Medaka (*Oryzias latipes*) is Organ- Specific. 5th Annual Graduate Research Forum (University of Mississippi).

Singha SK, Ibrahim MA, Ilias M, Khan IA, Dasmahapatra AK. (2016) Time- and Concentration-dependent Toxicological Potential of 4-*O*-Methylhonokiol on Japanese Medaka (*Oryzias latipes*) embryogenesis. 6th Annual GSC Research Symposium (University of Mississippi).

Poster Presentation

Singha SK, Khan IA, Dasmahapatra AK. (2015) Endocannabinoid Receptor Expressions in Japanese Medaka (*Oryzias latipes*) is Organ-specific. Society of Toxicology 54th Annual Meeting and ToxExpo.

Singha SK, Khan IA, Dasmahapatra AK. (2015) Immunohistochemical and Biochemical Analysis of Cannabinoid Receptors in Japanese Medaka (*Oryzias latipes*). 42nd Annual MALTO Medicinal Chemistry-Pharmacognosy Meeting.

Singha SK, Khan IA, Ibrahim MA, Ilias M, Dasmahapatra AK. (2015) Teratogenic Potential of 4-*O*-Methylhonokiol in Japanese Medaka (*Oryzias latipes*) Embryogenesis can be mediated through Endocannabinoid Signaling. Drug Discovery and Development Colloquium 2015.

Singha SK, Ibrahim MA, Ilias M, Khan IA, Dasmahapatra AK. (2016) Cardiotoxic Potential of 4-*O*-Methylhonokiol on Japanese Medaka (*Oryzias latipes*) Embryo-larval Development. Society of Toxicology 55th Annual Meeting and ToxExpo.

Singha SK, Franklin JF, Khan IA, Dasmahapatra AK. (2016) Evaluation of Endocannabinoid System in Japanese Medaka Fish (*Oryzias latipes*) as a Potential Target of Neurobehavioral Disorders. UMMC Neuroscience Research Day.

Singha SK, Khan IA, Ibrahim MA, Ilias M, Dasmahapatra AK. (2016) Teratogenic potential of 4-*O*-Methylhonokiol on Japanese medaka (*Oryzias latipes*) embryogenesis. 16th Annual International Conference on the Science of Botanicals (ICSB) and 5th Interim American Society of Pharmacognosy (ASP).

Singha SK, Ibrahim MA, Ilias M, Khan IA, Dasmahapatra AK. (2016) Evaluation of Toxicological Potential of 4-O-Methylhonokiol on Japanese Medaka (Oryzias latipes) Embryogenesis in a Time-

and Concentration-dependent Manner. American Association of Pharmaceutical Scientists (AAPS) Annual meeting and Exposition 2016.

Singha SK, Ibrahim MA, Ilias M, Khan IA, Dasmahapatra AK. (2017). Evaluation of oxidative stress in the induction of toxicological effects caused by 4-*O*-methylhonokiol in Japanese medaka embryogenesis. Society of Toxicology 56th Annual Meeting and ToxExpo.

Singha SK, Dasmahapatra AK, Ibrahim MA, Ilias M, Shariat-Madar Z. (2018). Potential effects of 4-*O*-Methylhonokiol on Japanese medaka embryos. Society of Toxicology 57th Annual Meeting and ToxExpo.